

ANDERS SOLHEIM

THE DEPOSITIONAL ENVIRONMENT OF SURGING SUB-POLAR TIDEWATER GLACIERS

A case study of the morphology, sedimentation and sediment properties in a surge-affected marine basin outside Nordaustlandet, Northern Barents Sea



SKRIFTER NO. 194
OSLO 1991





SKRIFTER NR. 194

ANDERS SOLHEIM

The depositional environment of surging sub-polar tidewater glaciers

A case study of the morphology, sedimentation and sediment
properties in a surge affected marine basin outside
Nordaustlandet, Northern Barents Sea

Cover: Aerial photograph showing the present-day front of the grounded Bråsvellbreen glacier. The height of the front above sea level is approximately 20 metres.

ISBN 82-90307-77-2
Printed June 1991

Typeset and printed in Great Britain by
PAGE BROS¹ Page Bros, Norwich

Norsk Polarinstitutt,
Rolfstangveien 12,
N-1330 Oslo Lufthavn,
Norway

CONTENTS

Abstract	5
Introduction	5
Physical setting	8
Bedrock geology	8
Quaternary geology	8
Bathymetry and hydrography.....	10
Glaciology	10
The Bråsvellbreen surge	13
Basin 3.....	14
Material and methods	14
Coring and acoustic data acquisition	14
Sediment analyses	18
Sea floor morphology	19
The surge moraines	19
The surge zone	23
The surge-distal zone	25
Distribution and acoustic stratigraphy of unlithified sediments.....	31
Sediment composition and physical properties.....	35
Lithology	35
Physical properties.....	36
Relation to the acoustic stratigraphy	49
Parameter correlation.....	53
Sedimentation, sediment dynamics and formation of the sea floor morphology	54
Derivation of sediments for the surge moraines	54
Subglacial debris	55
Meltwater	57
Surge moraine formation	58
The rhombohedral ridge pattern.....	58
Post surge preservation of the morphology	59
The discontinuous, arcuate ridges	60
The intermediate region	61
The surge-distal regions (non surge-related features)	62
Mineralogy and carbon content	63
Mineralogy of the surge zone and surge moraine	63
Mineralogy of the surge-distal zone.....	64
Conclusion	65
Carbon content.....	66
Sedimentation rates	66
Consolidation	71
Post-surge deposition	73
Increased iceberg production	75
Erosion by the latest Bråsvellbreen surge	75
Ice volumes and surge frequencies	76
Summary and conclusions; facies distribution off marine, surging glaciers.....	78
Acknowledgements	81
References	81
Appendices	85
Appendix 1. Sediment samples in the study area	85
Appendix 2. Grain size distributions	88
Appendix 3. Physical properties	91
Appendix 4. Mineralogy from XRD.....	96

The depositional environment of surging sub-polar tidewater glaciers: a case study of the morphology, sedimentation and sediment properties in a surge affected marine basin outside Nordaustlandet, the Northern Barents Sea

ANDERS SOLHEIM



Solheim, A. 1991: The depositional environment of surging sub-polar tidewater glaciers: a case study of the morphology, sedimentation and sediment properties in a surge affected marine basin outside Nordaustlandet, the Northern Barents Sea. *Norsk Polarinstitutt Skrifter* 194. 97pp.

The present study addresses the importance of glacier surges in the marine environment. Glacier surges are common in Svalbard, as well as in other Arctic and sub-Arctic regions, and the surging of tidewater glaciers may have been an important process during past glaciations when extensive continental shelf areas were covered by grounded ice.

An area outside Austfonna ice cap, Nordaustlandet, Svalbard, has been extensively studied by means of shallow seismic profiling, side-scan sonar, and core sampling over a period of several years. Austfonna has several well-defined drainage basins, some of which are known to surge. Bråsvellbreen, the second largest drainage basin, had the largest surge ever documented when it advanced 12–15 km along a 30 km wide front between 1936 and 1938. The glacier has, since then, retreated as much as 5 km. Most of the data base is located outside Bråsvellbreen, but results from this glacier are also applied to show that an adjacent drainage basin also has experienced a surge of comparable size. Using present-day climatic parameters and volumetric estimates from the study area, the surge interval of Bråsvellbreen may be as much as 500 years, whereas the adjacent, larger basin has at least three times shorter period, due to difference in the ratio of accumulation area to ablation area, which is greater for the latter basin.

Important aspects of the shallow geology discussed include sea floor morphology, sediment distribution and sediment types, sediment physical properties and sedimentation processes and rates. One objective is to discover whether surges leave diagnostic features that can be used to identify surges in other areas or in older sequences. A suite of sea floor morphological patterns, including a terminal moraine (here termed surge moraine) and sub-glacial squeeze-up ridges in the zone previously covered by surging ice (here termed the surge zone), is the most characteristic feature. This zone contrasts strongly to the area outside the surge moraine (here termed the surge-distal zone), which is characterized by normal marine processes and iceberg ploughing. Sediments are mainly gravel and pebble rich diamictons, but patches of pre-surge, more fine grained glaciomarine mud are preserved, embedded in the diamicton, and compacted by loading of the surging glacier. Sediment physical properties vary greatly as a function of variable lithology and differences in compaction. The greatest amount of directly surge-related deposition takes place within few kilometers of the ice front, with emplacement of the surge moraine being the most important event. However, surges apparently affect depositional rates also some tens of kilometers out into the surge-distal zone through increased output of suspended material. Chronostratigraphical control is sparse, but there seem to be large variations in depositional rates, reflecting surges or periods of increased surge frequency.

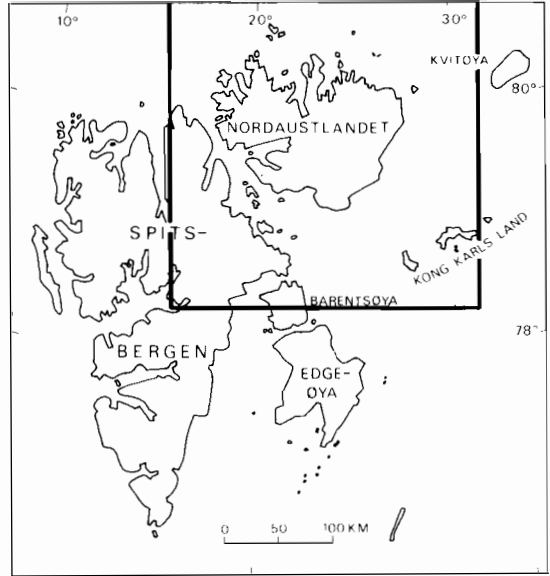
Surging glaciers are not found to produce sediments unique to this environment, but taken together, the combination and variations in sediment types, physical properties, sedimentation rates, and morphology can be diagnostic and used in the interpretation of older sequences and areas where surges are not documented.

Anders Solheim, Norsk Polarinstitutt, P.O. Box 158, N-1330 Oslo Lufthavn, Norway

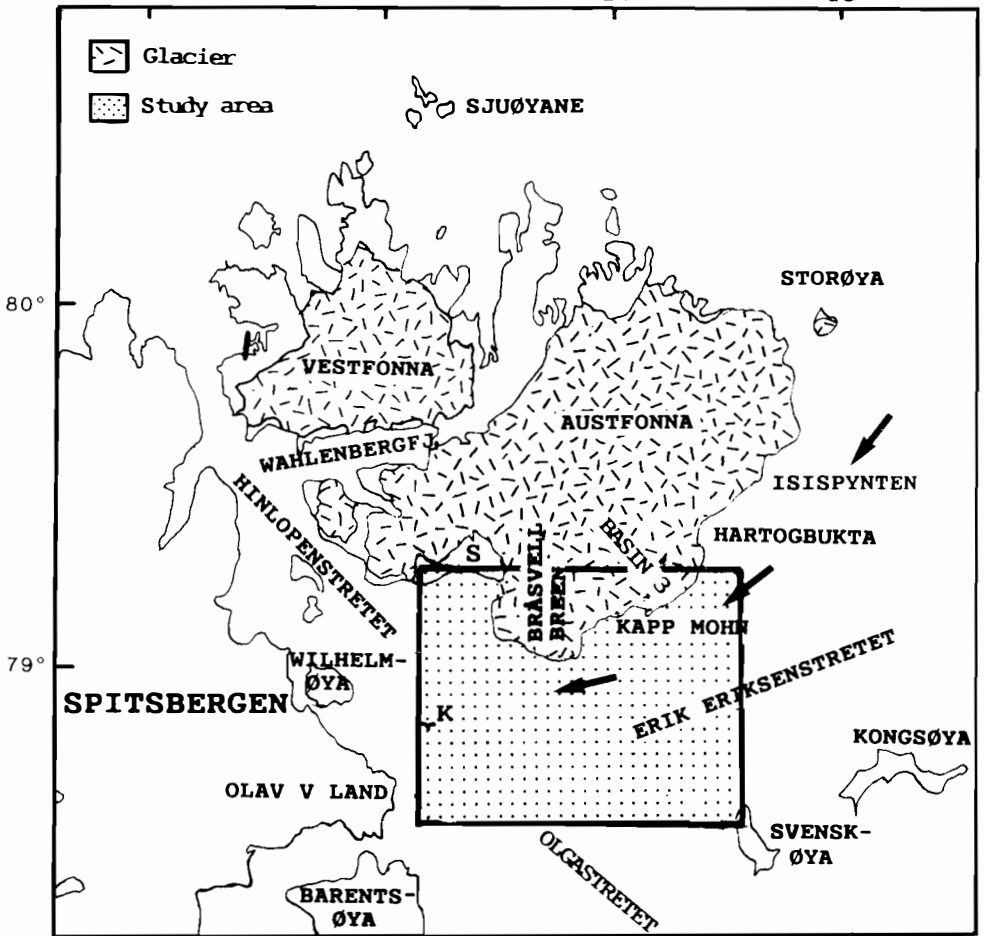
Introduction

Glacier surges are an important aspect of the dynamics of many Svalbard glaciers (Liestøl 1969) and are relatively common in other Arctic and sub-Arctic regions, for example Alaska, Iceland, and the Soviet Union (Horvath & Field 1969; Thorarinsson 1969; Dolgushin & Osipova 1974; Clarke et al. 1986). Surges have been quite extensively studied from a glaciological viewpoint (e.g.

Can. J. Earth Sci., Vol. 6, 1969: various refs.; Hagen 1987) and surge mechanisms have been much debated (Robin & Weertman 1973; Budd 1975; Clarke 1976). Recent glaciological work on surging glaciers has greatly improved the understanding of the surge process (Clarke et al. 1984; Kamb et al. 1985; Kamb 1987; Raymond 1987). However, the majority of studied surges are from on-shore areas, whereas surges of marine based glaciers have been much ignored. Furthermore,



16° 20° 24° 28°



A

reports on possible effects of surges on sediments and sedimentation are essentially lacking, in particular from the marine environment.

Surges have been proposed as a mechanism for the thinning and disintegration of large ice sheets. Hence, ice marginal features may result from past surges, as, for example, is suggested for several readvances during the retreat of the Laurentide ice sheet (Prest 1969; Dyke & Prest 1987), rather than being of climatic significance. Major surges of ice streams have likewise been suggested as a probable mechanism for the disintegration of ice domes, in particular marine ones (Budd 1975; Stuiver et al. 1981; Denton & Hughes 1981). These surges are somewhat different from presently observed surges. The disappearance of buttressing ice shelves leads to surging of marine-based ice streams. The ice stream surges proceed from the margin to the centre of marine ice domes (Hughes 1974), whereas "traditional" ice sheet surges proceed from central parts towards the margin (Budd 1975; Weertman 1976). Large ice stream surges would lead to drawdown and finally the collapse of marine ice domes. Denton & Hughes (1981) claim that disintegration of large parts of the Northern Hemisphere Late Weichselian/Wisconsin ice sheets can be accounted for by this drawdown mechanism. Paleontological and stable isotope data which indicate an early phase of rapid deglaciation from 16 to 13 ka give further support to the marine drawdown mechanism (Ruddiman & McIntyre 1981; Ruddiman & Duplessy 1985). Likewise it is also proposed as a possible mechanism for the West Antarctic ice sheet (Stuiver et al. 1981). Drawdown through ice stream surges would also partly resolve the problem of derivation of sufficient energy to waste major ice sheets, as put forward by Andrews (1973) and Hare (1976).

Recent studies of Ice Stream B in the Ross Sea area of Antarctica indicate, however, that this fast-flowing ice stream maintains its velocity through deformation of the subglacial till layer. This may provide a negative feedback mechanism that will prevent drawdown through increased ice stream flow and hence prevent ice sheet collapse (Alley et al. 1989).

Although the above theories may be disputed and involve different mechanisms and scales, the

discussion shows that glacier surge is important and may have had immense geologic and climatic consequences.

In 1936–38 Bråsvellbreen, a well-defined drainage basin of the Austfonna ice cap, Nordaustlandet, Svalbard (Fig. 1A), had the largest surge documented in historical times on the Northern Hemisphere, when an approximately 30 km wide front advanced possibly as much as 15–20 km into the Barents Sea in less than two years (Schytt 1969). The glacier has retreated up to 4–5 km since the surge and the present situation is that of a grounded, apparently quite stationary ice front with a subaerial cliff approximately 20 m in height and a submarine draft varying from 20 to 110 m. This situation offers a unique opportunity to study the effects of a glacier surge on the ice proximal glaciomarine environment. Important questions regarding this type of event are

1. What happens to the substratum over which the surging glacier advances, in terms of morphology, erosion/deposition and changes in the physical properties of the sediments?
2. How does a surge affect sedimentation and sedimentary processes at various distances from the surging glacier?
3. Are former glacier surges identifiable and, if so, what are the diagnostic features?
4. Can the sedimentary features give any indications of surge mechanisms and mode of advance and retreat?
5. Can surge frequency and timing be predicted?

The Antarctic is widely used as a model for description of glaciomarine sedimentation and interpretation of ancient glaciomarine deposits (Molnia 1983). However, the Antarctic may be atypical compared with Northern Hemisphere glaciated areas, both present and past, for several reasons, for example the apparent lack of meltwater outflows, the generally very deep continental shelf with a slope towards the continent, and the importance of extensive ice shelves. Studies of glaciomarine sediments and sedimentation in the Northern Hemisphere have, on the other hand, mostly been carried out on temperate glaciers in fjord settings. This may likewise be an inadequate model for past glaciations, as

Fig. 1A. Location of Svalbard, Nordaustlandet and the study area, with place names used in the text. S = Svartknausfya. K = Kiepertøya. Glacial coverage of Nordaustlandet is indicated, and the coastal current is marked by arrows.

extensive marine based ice sheets probably covered several continental shelf areas.

A more applicable model for Northern Hemisphere glaciomarine sedimentation is probably presented by the modern Austfonna ice cap with its dynamically distinctive drainage basins, several of which are known to surge (Liestøl 1969; Schytt 1969; Dowdeswell 1984), and the adjacent parts of the Barents Sea. Austfonna has the most extensive marine, grounded ice front (approximately 200 km long) in the present day Northern Hemisphere, and the entire front is situated in open, marine conditions. Furthermore, the regional glaciology of the ice cap has recently been mapped using radio-echo sounding methods (Dowdeswell 1984; Dowdeswell et al. 1986) providing important background information for studies of the sedimentary environment outside the glacier.

In this paper, questions 1–5 (above) are addressed through a study of the region off the southern portion of the Austfonna ice cap, Erik Eriksonstredet (Fig. 1A). Answers are sought through the interpretation of high frequency acoustic data (side scan sonar, 3.5 kHz echo sounder and sparker) and sedimentological/geotechnical analyses of sediment cores. The data were collected to cover the entire region, from the present ice front of Austfonna to the more distal regions, in order to establish a model for sedimentation and sedimentary processes in a surge-affected, open marine environment. A preliminary paper (Solheim & Pirman 1985) reported on the morphological features in the northern, most glacier proximal part of the study area using some of the acoustic data. This paper presents a synthesis of all the acoustic and sedimentological/geotechnical data.

Physical setting

Bedrock geology

Lithology of the glacial sediments may be used to trace different source areas and their relative importance, provided sufficient lateral bedrock variation exists. Based on relatively few exposures, a rough division can be made for Nordaustlandet along a line through Wahlenbergfjorden and towards east-southeast (Fig. 1B), between post Caledonian rocks to the south and older rocks mainly of the Hecla Hoek complex (Late Riphean to early Paleozoic sediments (partly metamorphosed), granites, gneisses and

gabbroic intrusives) to the north (Lauritzen & Ohta 1984).

The Hecla Hoek complex differs markedly from the overlying younger sedimentary rocks found in the southern part of Nordaustlandet. The latter range from middle Carboniferous to Lower Jurassic in age. The main part of the outcrops, including those along the southwestern periphery of Austfonna, consists of Carboniferous and Permian rocks (Lauritzen & Ohta 1984). Although a few sandstone exposures are found, the majority of these rocks are limestones and dolomitic limestones, characterized by a high chert content and silicified sediments, which renders the formation highly resistant to weathering. A few exposures show Triassic to Lower Jurassic siltstones and shales overlaying the limestones, and to be cut by Late Jurassic to Early Cretaceous dolerites.

To the south of Erik Eriksonstredet, the islands of Kong Karls Land consist of late Triassic early Cretaceous sediments (mostly clastics, with some limestones and coal beds) with interbedded lavas. The location of the boundary between these rocks and the upper Paleozoic carbonates on southern Nordaustlandet is tentatively placed along the central part of Erik Eriksonstredet and cannot be mapped more accurately from the present shallow seismic data.

Southwest of the study area, Triassic and Lower Jurassic clastic rocks outcrop in Olav V Land and on Wilhelmøya (Fig. 1B). Mesozoic doleritic intrusions form small islands and skerries, for example Kiepertøya in the southern part of Hinlopenstredet (Fig. 1A).

Quaternary geology

Generally, the Quaternary sediments found on land next to the study area consist of a relatively thin (less than 5 m) cover of till, reworked by wave action below the upper marine limit (Blake 1962). In the outer part of Hinlopenstredet (Salvigen 1978), Holocene-raised beaches indicate, through isostatic depression by ice loading, a considerably wider extension of the ice cover during the Late Weichselian maximum (probably at about 18 kA), and striae and erratics point towards ice flow from southeast to northwest through Hinlopenstredet (Blake 1962). However, while the Early Weichselian glaciation probably reached Sjuøyane to the north (Fig. 1A), the Late Weichselian glaciation most likely did not reach

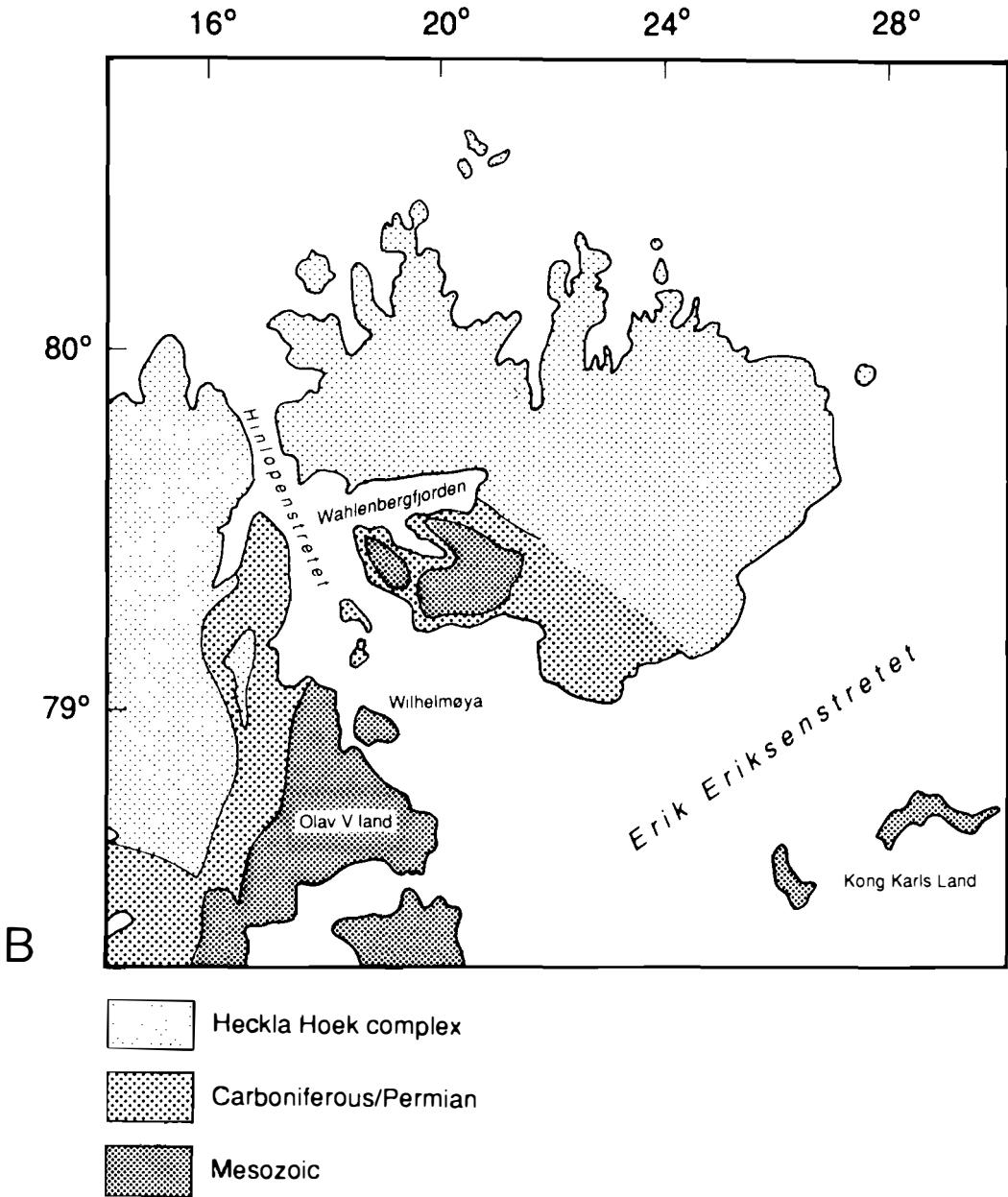


Fig. 1B. Simplified bedrock geology of the land areas surrounding the study area (modified from Worsley & Aga (1986)).

much beyond the northern coast of Nordaustlandet (Salvigsen & Nydal 1981). The pattern of ice movement from the southeast is in accordance with data which show Kong Karls Land to have the highest raised beaches, with a maximum of 110 m, in the Svalbard archipelago (Salvigsen

1981). This again supports the idea of an extensive glaciation of the Barents Sea shelf, which also is strongly indicated by the sediment distribution, sea floor morphology, and seismic stratigraphy of the Barents Sea (Elverhøi & Solheim 1983; Solheim & Kristoffersen 1984; Vorren & Kri-

stoffersen 1986; Solheim et al. 1990). Based on these lines of evidence, the entire study area was probably covered by grounded ice that flowed from southeast towards the northwest during most of the Late Weichselian. It should be mentioned, however, that various views have been presented on the existence and size of a Barents Sea ice sheet. Elverhøi and Solheim (1983) give a review of this discussion.

Deglaciation of Nordaustlandet began sometime before 10 kA (Blake 1962; Østerholm 1978). The emergence curves from Svartknausflya and Kong Karls Land (Fig. 1A) (Salvigsen 1978, 1981), indicate that the relative water depth was between 80 and 110 m deeper than at present for the first 1,000 years after deglaciation, while the shallowing during the last 5,000 years has been approximately 20–30 m.

The general Quaternary succession of the northern Barents Sea (Elverhøi & Solheim 1983) consists of an overconsolidated basal till (less than 10 m thick) with a cover of soft, Late Weichselian glaciomarine sediments (usually 1–5 m thick). The upper part of the till is often relatively soft, although geotechnically clearly different from the glaciomarine sediments, and is interpreted as a deformation till (Elverhøi et al. 1990; Russwurm 1990; Nyland Berg 1991). Mainly in water depths in excess of 300 m and in local depressions, this sequence is covered by a thin (<1 m) layer of Holocene, fine-grained mud which mostly results from reworking in shallower regions (Forsberg 1983) and sediment transport by sea ice (Elverhøi et al. 1989). However, the distinction between the Late Weichselian glaciomarine sediments and the top Holocene mud becomes less apparent northwards in the Barents Sea (Wensaas 1986) towards the heavily glaciated regions of eastern Svalbard. At present, sedimentation in the study area is dominated by deposition from turbid meltwater plumes (Pfirman 1985).

Bathymetry and hydrography

The study area covers the southwestern, shallowest part of Erik Eriksenstredet. This strait is part of a trough which continues north-northeastwards between Nordaustlandet and Kvitøya (Fig. 1A), and forms one of the three deep passages from the Barents Sea to the Arctic Ocean. Trough depths in the study area range from 260 m in the eastern part to 180 m in the central part (Map 1, Bathymetry of the study area, enclosed

in back pocket). A sill at 120 m waterdepth separates Erik Eriksenstredet from the Olgastredet trough between Kong Karls Land and Barentsøya.

Below approximately 100 m depth in the north and 150 m in the south, Erik Eriksenstredet has a gentle, rather smooth topography. The northern slope is slightly steeper than the southern slope and in the northeastern part the upper 30 m is steeper than the lower part of the slope. While the contours of the southern slope appear straight, the northern slope forms a major embayment with its apex towards Bråsvellbreen. The rather gentle deep trough contrasts distinctly with both shoulders, where the topography is highly irregular on a 10 m scale, with numerous smaller shoals and troughs. To the west, the sea floor rises to depths less than 50 m on the sill in the southern part of Hinlopenstredet.

The current pattern in this part of Erik Eriksenstredet is dominated by the approximately 20 km wide Nordaustlandet coastal current flowing in a southwesterly direction (Fig. 1A). Calculated relative geostrophic shear between station pairs varies from 4 cm/sec in the east to more than 16 cm/sec near the western border of Bråsvellbreen (Pfirman 1985). The water mass is vertically stratified into a 25–30 m thick layer of fresher surface water, a core of cold Arctic water down to 125 m, and a bottom layer of warmer Atlantic water (Pfirman 1985). No long-term current measurements exist from this part of Erik Eriksenstredet. Further northeast, between Nordaustlandet and Kvitøya, one-year measurements at 75 and 220 m levels (Aagaard et al. 1983) reveal a dominant tidal component with velocities up to 15 cm/sec and 5 cm/sec in the upper and lower levels respectively (tidal range in the area is in the order of 0.5–1.0 m (T. Eiken pers. commun. 1987)). Net velocity, however, is less than 2 cm/sec in a northward direction.

Due to the shallow sill (<60 m) in the southern part of Hinlopenstredet, there is no deep water exchange through this strait. However, a relatively strong tidal current component can be expected in this area and thus also in the western part of Erik Eriksenstredet.

Glaciology

Glaciers are usually classified as polar, temperate or sub-polar (Lagally 1932; Ahlmann 1933). Polar glaciers are entirely below the pressure melting

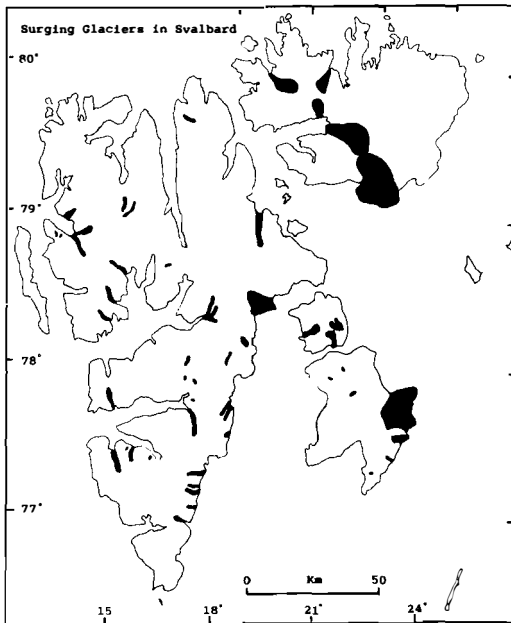


Fig. 2. Major Svalbard glaciers that have been observed to surge. More than 80 glaciers are known to show surging behaviour. Map from Dowdeswell (1984), based on data from Liestøl (1985).

point. Temperate glaciers are at the pressure melting point below the penetration depth of the winter cold wave. Sub-polar glaciers form an intermediate category between the two extremes. The overall glacier coverage of Svalbard is approximately 60%, with a general increase towards the north and east (Dowdeswell 1984). More than 75% of Nordaustlandet and 99% of Kvitøya are glacierized. Despite the high latitude, most Svalbard glaciers are of sub-polar type (Baranowski 1977). In general, the glaciers have been slowly retreating for approximately the last 100 years, after a period of advance mainly between the 17th to the late 19th century (Baranowski 1977) known as the Little Ice Age (Lamb 1977).

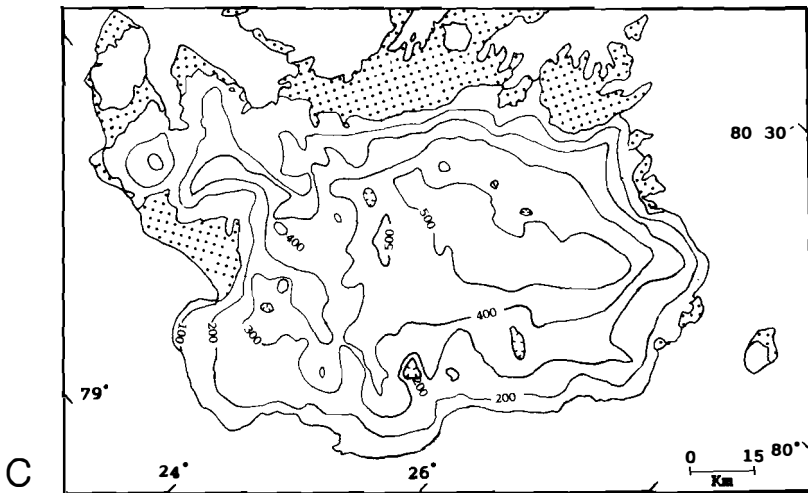
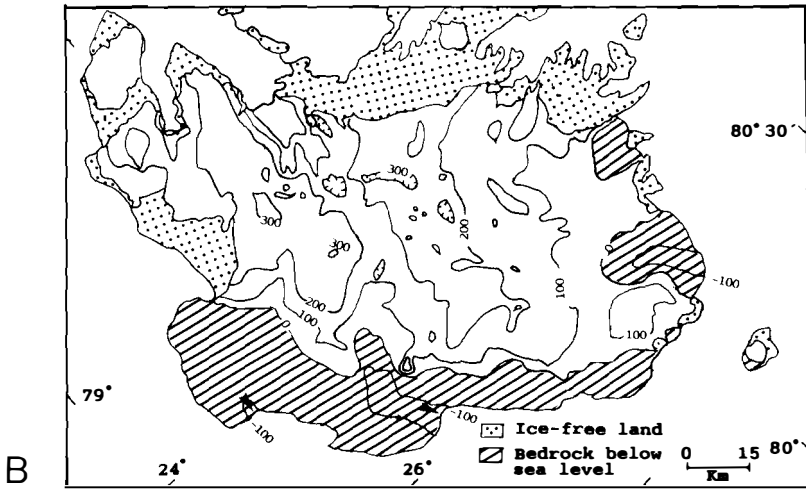
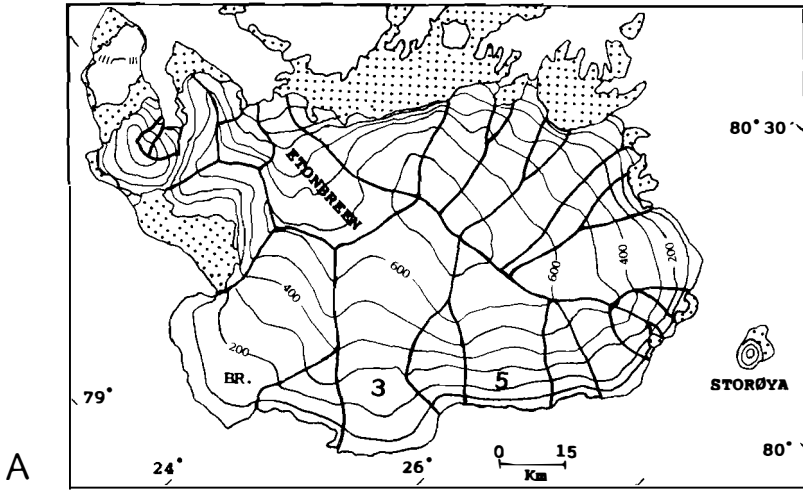
A number of Svalbard glaciers have short-term fluctuations due to surging behaviour (Fig. 2). Glacier surges in general have been extensively discussed, and a detailed discussion of surge theories is beyond the scope of this paper, but it is important to note that most of them involve build-up and activation of large amounts of pressurized water at the bed or in permeable sediments below the glacier (Clarke et al. 1984). Field observations also verify that increased amounts of meltwater

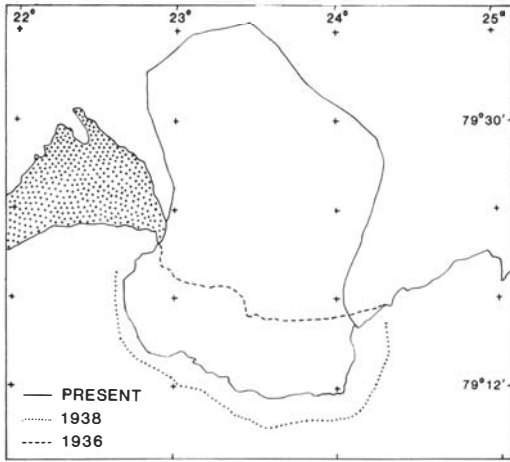
are involved in surges (Thorarinsson 1969; Kamb et al. 1985).

Most of Nordaustlandet is covered by the two ice caps Vestfonna (2,511 km²) and Austfonna (8,120 km²). The geography and glaciology of Austfonna has been investigated by several expeditions during the last 115 years (Nordenskiöld 1875; Ahlmann 1933; Glen 1937, 1941; Dege 1948, 1949; Hartog 1950; Harland & Hollin 1953; Thompson 1953; Hollin 1956; Palosuo & Schytt 1960; Schytt 1964; Ekman 1971). However, a detailed picture of the entire ice cap was not obtained until the Scott Polar Research Institute (SPRI) and the Norwegian Polar Research Institute (NP) carried out extensive airborne radio-echo sounding operations over Nordaustlandet in 1983 (Dowdeswell 1984; Dowdeswell 1986a,b; Dowdeswell et al. 1984a,b; Dowdeswell & Drewry 1985; Drewry & Liestøl 1985). The ice distribution and glaciology is thoroughly described by Dowdeswell (1984), and only a brief review will be given here, with emphasis on the south-eastern part of the ice cap, including Bråsvellbreen.

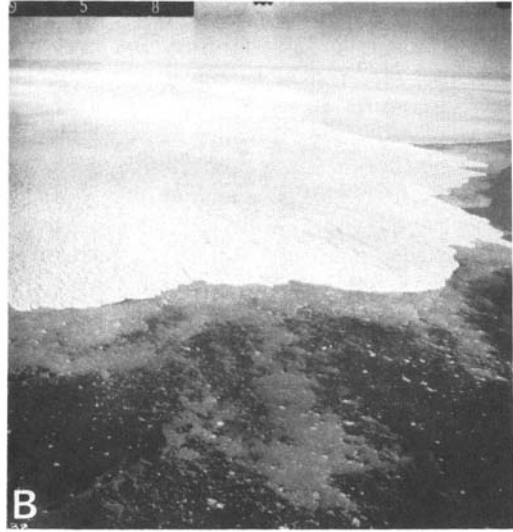
Based on surface topography, the ice cap is divided into 19 drainage basins (Fig. 3A) the largest of which are also reflected in the mapped subglacial bedrock topography (Fig. 3B). The two largest drainage basins are Bråsvellbreen and Basin 3 (1,109 km² and 1,251 km² respectively). The maximum surface elevation of the ice cap is 790 m (Fig. 3A), and the ice thickness reaches almost 600 m (Fig. 3C). The southern and eastern limits of Austfonna constitute the longest tidewater ice front on the Northern Hemisphere with its ca. 200 km of grounded glacier terminus. 28% of the total ice cap is based below sea level, and the major part of this is in the southeastern region, including 57% of Bråsvellbreen. Depths below sea level reach 157 m, but no part of the glacier is afloat. Information on the thermal regime in the ice cap is presently sparse, but a few shallow temperature measurements have indicated that the ice cap is frozen to the bed in its outer parts and at the pressure melting point under its central parts, and hence can be classified as a sub-polar glacier (Schytt 1969).

There are presently two major meltwater outlets draining Austfonna (and numerous smaller ones); one is just to the east of Bråsvellbreen, and the other is in Hartogbukta, just to the east of Basin 3 (Figs. 1 and 3B). The former of these has a sea floor valley outside the outlet, while

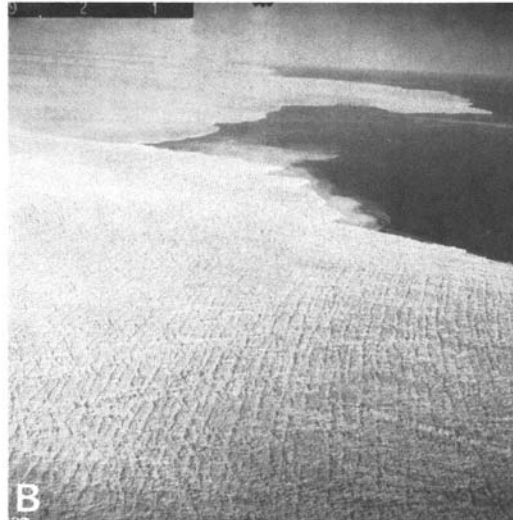




A



B



B

Fig. 4. A. The coastline of Bråsvellbreen before 1936 (very approximate, modified after Glen (1937)), in 1938 (taken from the morphologically defined maximum surge extent described by Solheim & Pfirman (1985) and later in this paper) and at present. B. Two aerial photographs taken during the surge in 1938 (Norsk Polarinstitut archive photo). Note high concentrations of icebergs outside the surging glacier.

little detail is known on the bathymetry of Har-togbukta. Both these areas, however, have bed-rock depressions continuing underneath the ice (Fig. 3B). This may indicate that meltwater outlets are at the base of the glacier, with a location most likely determined by the bedrock topography. The fact that there appears to be only sparse meltwater activity during the winter indicates that

most of the water results from surface summer melting.

The Bråsvellbreen surge

The Bråsvellbreen surge occurred sometime after 1936, when an undisturbed glacier surface was reported (Glen 1937), and before 1938, when

Fig. 3. Regional characteristics of Austfonna ice cap (from Dowdeswell et al. 1986). A. Surface elevation (m) and drainage basins. BR. 3 and 5 mark Bråsvellbreen and basins 3 and 5, respectively. B. Bedrock topography (m). Main meltwater outlets are marked with arrows. C. Ice thickness (m).

aerial photography revealed a heavily crevassed glacier tongue protruding from the pre-surge coastline (Fig. 4). The surging glacier probably advanced up to 15 km along a 30 km long front. 15 km is a somewhat tentative figure as the pre-surge coastline was not precisely mapped. Previous articles have reported up to 20 km advance (e.g. Schytt 1969), but this is most likely based on published maps that suffer from inadequate navigation. A continuous submarine ridge was considered by Solheim and Pfirman (1985) to define the maximum surge extent, but its position differs by several km from the 1938 coast on the published map (Norsk Polarinstittutt Chart 507, 1957 edition).

After an advance, the terminal regions of the surging glacier tend to stagnate (Meier & Post 1969). In the case of a marine ice mass, relatively rapid retreat of the glacier through calving from the heavily crevassed glacier ice most likely takes place (Solheim & Pfirman 1985). Sealers reported the number of icebergs in 1938 to be an order of magnitude higher than during the non-surge situation (Vinje 1985). Solheim and Pfirman (1985) estimated a retreat of up to 5 km from the maximum 1938 position of the Bråsvellbreen front as defined by the terminal ridge. Dege (1948, 1949) reported much calving from the Bråsvellbreen terminus during 1944, while Hartog and Thompson (1950) reported little calving and few open crevasses during 1948. Thus, crevasses on the fractured glacier surface may have closed during the period between 1944 and 1948, and a large part of the retreat from the maximum position may have occurred before 1948. Satellite images since 1976 indicate little ice front movement and modification during the last decade, and studies of aerial photographs taken between 1969 and 1977 show a retreat of 180 m for the western 5 km of Bråsvellbreen during this period (Dowdeswell 1986b).

Ice surface profiles based on the 1983 radio echo soundings (Dowdeswell 1984) clearly fall below the theoretically calculated surface profile, and calculated basal shear stress is low. This is

typical for glaciers in the quiescent phase between surges (Paterson 1981).

Basin 3

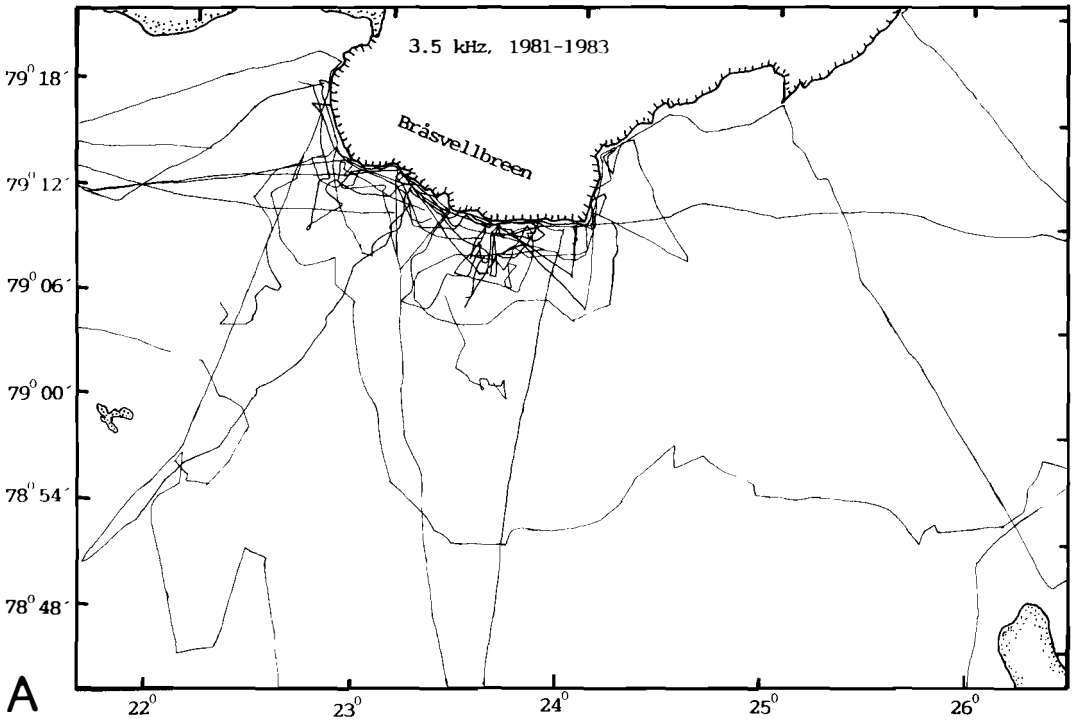
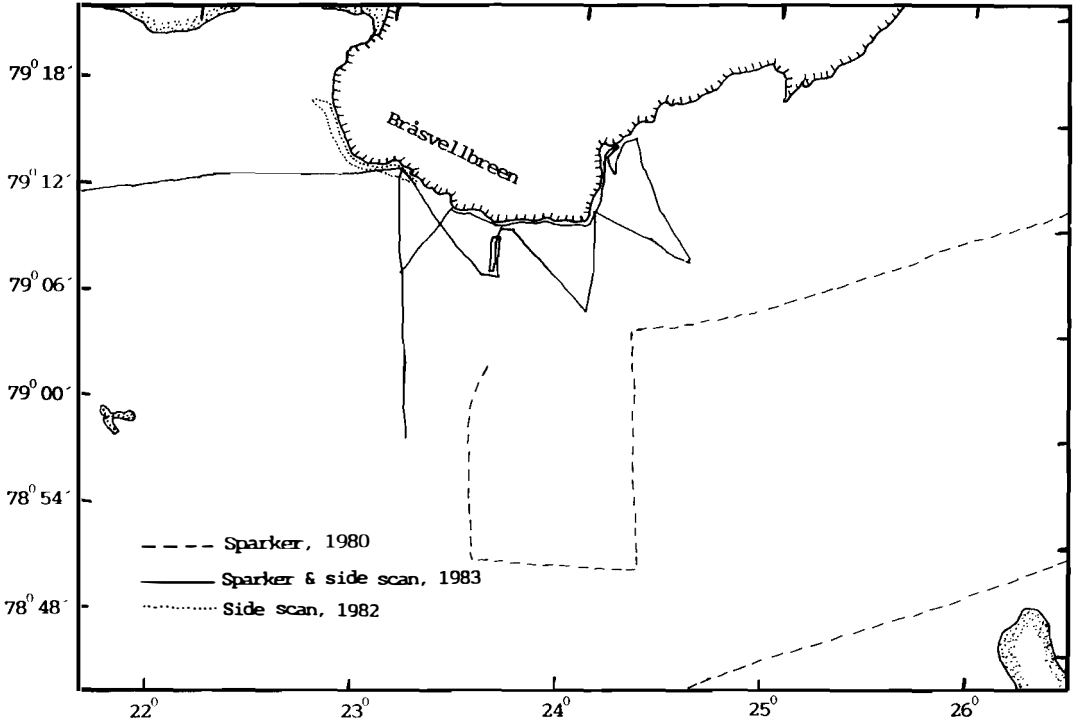
Basin 3 (Fig. 3A) is the largest drainage basin on Austfonna. Glaciologically, it shows several similarities with Bråsvellbreen. The coastline between Kapp Mohn and Hartogbukta (Fig. 1A) protrudes from the rest of the ice cap margin, the basin is well-defined by the subglacial bedrock topography, the surface profile also falls below the theoretical profile, and basal shear stress is low (Dowdeswell 1984, 1986a). Furthermore, a Swedish expedition that crossed the ice cap in 1873 reported badly crevassed ice (Nordenskiöld 1875) in a location that corresponds with the inner parts of Basin 3. Taken together, there are both historical and glaciological indications that Basin 3 is also a surging glacier.

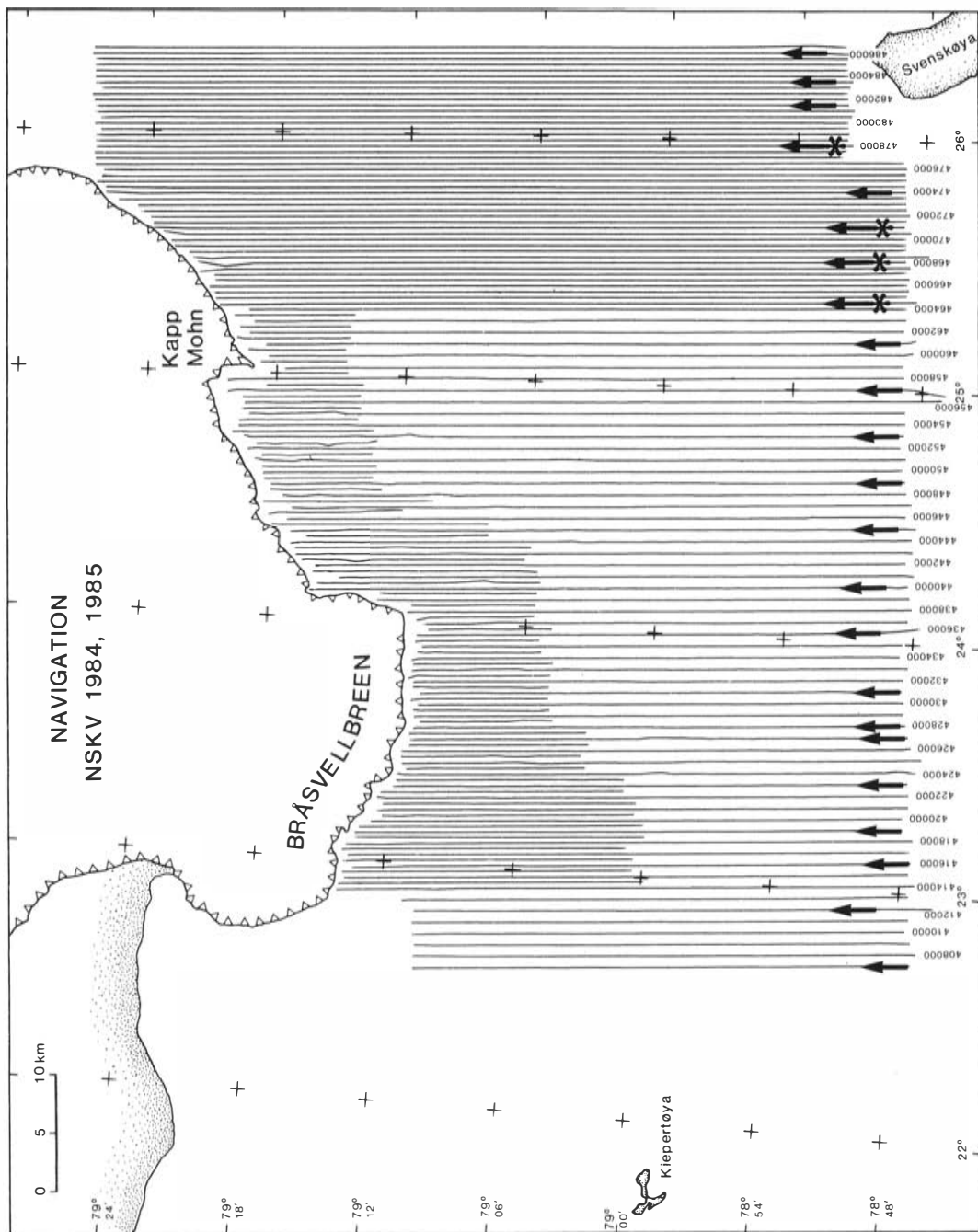
Materials and methods

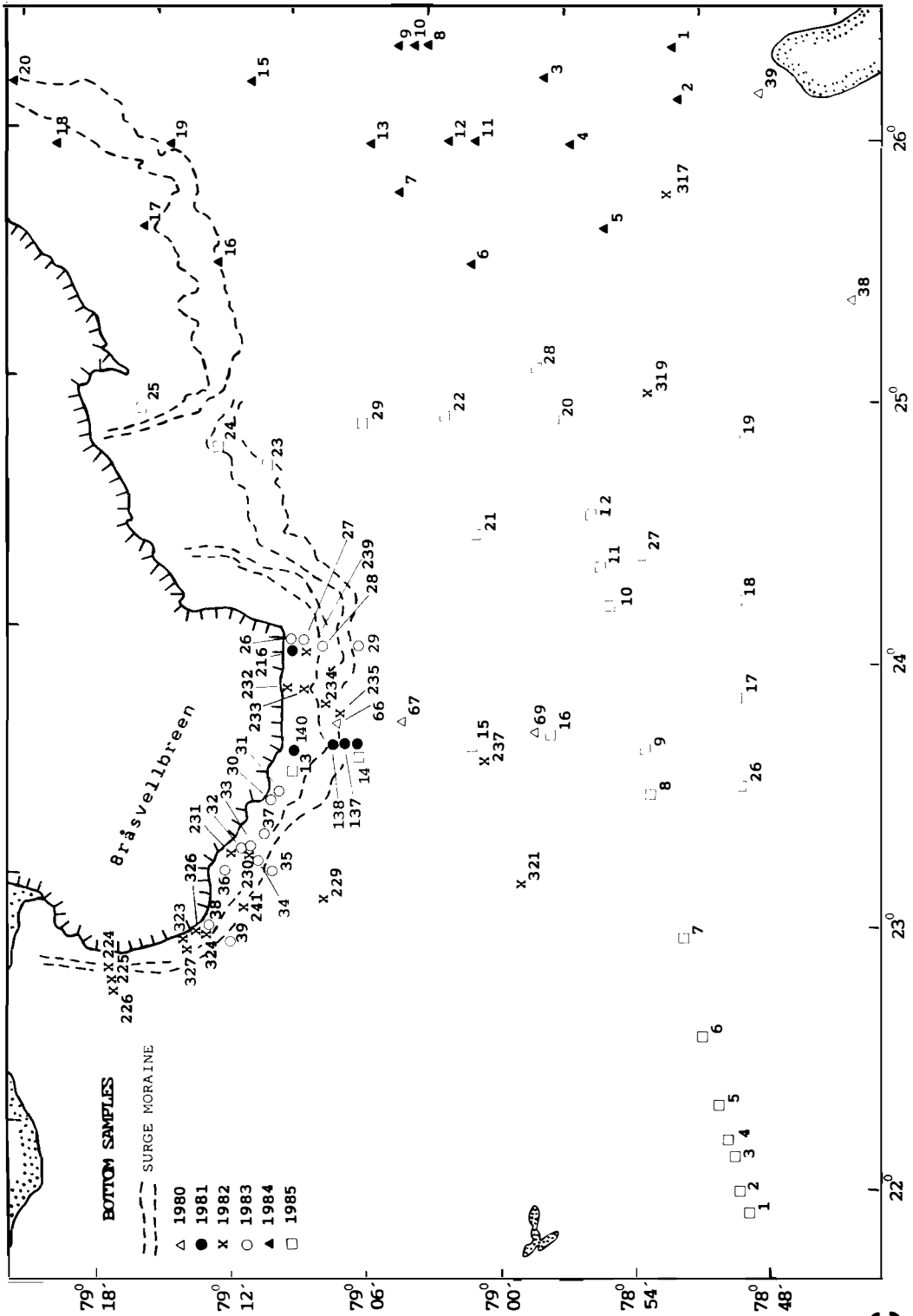
Coring and acoustic data acquisition

Reconnaissance work in 1980 and 1981 revealed that a thin layer of soft surface sediments covered overconsolidated material in front of Bråsvellbreen. Furthermore, the assumed surge terminal ridge separated this setting from that beyond it, where a thicker soft glaciomarine cover with no overconsolidated sediments was found within reach of 3 m coring equipment. A more detailed program of acoustic profiling and core sampling was then designed to verify if the 1936–38 surge was the cause of the morphology and sediment distribution. If verified, this would present a situation where the direct effects of a surging glacier and a subsequent ice load on a marine, glaciogenic sediment could be studied. For sediment distribution and sea floor morphology studies, a 3.5 kHz echo sounder and a side-scan sonar were considered particularly important. The laboratory analysis program was designed

Fig. 5. A. Acoustic profiles run by Norsk Polarinstittutt (NP) in 1980–83. Sparker was used in 1980 and 1983. A side-scan sonar was used in a small part of the 1982 lines, and along all 1983 sparker lines. All lines after 1980 have 3.5 kHz information. B. Acoustic profiles run by The Hydrographic Survey of Norway (NSKV) in 1984 and 1985. Lines 464500–486500 were run in 1984 and the rest in 1985. All lines have 3.5 kHz information. Sparker lines are marked with arrows. Lines with side-scan sonar data in 1984 are marked with asterisks. In 1985, essentially all lines were run with side scan. C. Sampling localities from all cruises. In 1984 and 1985, gravity cores were taken at 7 locations (1984 - 11, 12, 13 and 1985 - 26, 27, 28, 29). The rest were surface grab samples.







to investigate sedimentological and geotechnical differences between different sediment types, affected and unaffected by the surge, and to obtain information about sedimentation rates and their variability in the Erik Eriksenstredet basin. Acoustic profiles and sample locations are shown in Figs. 5A, B and C.

Sea ice and strong surface currents caused problems for work in the area. The ice situation was particularly problematic during the 1982 survey when the major part of the sampling program was planned. Current velocities in excess of 1 knot were observed, and abundant, large drifting ice floes made station work difficult. One aspect of the sampling program during the 1982 and 1983 surveys was to obtain long cores with penetration into the underlying overconsolidated unit. However, the overconsolidation, combined with a high clast content, made coring difficult at a number of localities. The total number of core stations appears high (Fig. 5C), but several of the cores were only partly successful. The total number of 3.5 kHz profile kilometres similarly appears high (Fig. 5A). This results from the fact that the 3.5 kHz echo sounder was running continuously, also during periods of searching for routes through the ice or suitable sample locations.

Satellite navigation with a Magnavox MX1105 single channel receiver integrated with the ship's log and gyro was used during the 1980–83 surveys. The accuracy of the system (approximately 300–500 m) is normally insufficient for detailed work. However, accuracy on a relative scale was improved using observed radar distances to the ice front. One or two good satellite fixes per hour were usually obtained and all core stations were positioned by at least one satellite fix with an accuracy of 100–150 m.

In addition to the NP cruises of 1980–83, the Norwegian Hydrographic Survey (NSKV) carried out hydrographic mapping in this part of Erik Eriksenstredet during the autumn of 1984 and 1985 and included a sparker, a 3.5 kHz PDR, and a side-scan sonar in the program (Fig. 5B). These surveys were run with lines in a N-S direction and nominal line spacing of 500 m in the eastern part and 1,000 m in the western part with infill lines of 250 and 500 m spacing, respectively. Part of the sparker data was of generally poor quality due to severe noise problems. In addition to the acoustic profiling, 7 gravity cores and 50 surface grab samples were recovered.

The NSKV surveys were run using a local Decca

Sea Fix navigation system, with slave stations positioned on the surrounding islands. Relative accuracy of the system is in the order of 10 m.

Sediment analyses

On board analyses of a selection of the sediment cores included:

- Description of core section ends and cutter/catcher material (long cores were cut in 1 m sections).
 - Munsell soil color.
 - Pocket penetrometer shear strength on core section ends.
 - Measurements of compressional wave velocity, by means of a PUNDIT (Portable Ultrasonic Non-destructive Digital Indicating Tester, trade mark of C.N.S. Instr. Ltd., England, ASTM 1983). This instrument measures travel time through the sediment with 1 μ s accuracy. Measurements were taken both along and normal to the cores. This was done immediately after retrieval of the plastic liner to ensure contact between the liner and the sample. Correction was made for travel time delay caused by measuring through the plastic liner.
 - Water content (% of wet weight) on samples from core section ends (only done on-board in 1982).
- Subsequent laboratory work included:
- X-radiographing of a selection of the cores prior to splitting. A few of the 1983 cores were also run through a computer tomograph.
 - Core splitting and visual description including Munsell soil color and photography of split cores. Cores with relatively stiff material were split by breaking in two halves, while softer material was cut with knife or wire saw.
 - Shear strength on split core halves by pocket penetrometer or fall-cone apparatus. The shear strength values given are usually averaged from several measurements in the same interval where this was possible.
 - Compressional wave velocity measurements with the PUNDIT, mostly on smaller sections of the cores, giving interval velocities. The main source of error is exact determination of the distance between the transmitter and receiver transducers, particularly when used in soft material. Velocities were measured both along and perpendicular to the cores, but no significant difference was recorded. To minimize the distance error, long intervals were preferred.

- Performance of consolidation tests (oedometer) on two samples to measure pre-consolidation stress of the material. The intervals chosen for consolidation testing were cut from the cores before splitting, after inspection of x-radiographs. A majority of the sampled material was too gravelly to be tested in standard sized equipment.
- Determining of water content (% of wet weight) and bulk density on subsamples of 100–200 g wet weight. Volume was measured by submerging the sample in kerosene. As the material generally had a high but varying content of gravel and pebbles, a correction was applied to obtain water content values that could be compared within the study area. Hence, a set of values is included that are corrected for material greater than 0.5 mm.
- Measurement of grain size distribution on a number of subsamples. Size fractions greater than 0.063 mm were separated by dry sieving, while clay and silt fractions were determined by Falling Drop Analysis (trademark Geonor A/S, Norway, Mowm 1966). This apparatus utilizes the falling time of a drop of sediment suspension through an organic liquid. It is largely temperature dependent, and as this apparatus did not have automatic temperature control, it was calibrated for every 0.5°C. Some samples were analyzed both with the falling drop method and in a sedigraph. Within small limits (<5%), the results were comparable. This was also the case for some samples where all the material was size-fractionated, in addition to falling-drop analyzed. We therefore consider the falling drop method reliable for the present purposes. The majority of the samples analyzed for grain size distribution were greater than 100 g wet sediment. Percentages were calculated only for material finer than 16 mm.
- XRD on oriented samples of clay and silt fractions.
- Determining of Atterberg limits after wet sieving through a 0.063 mm sieve.

Sea floor morphology

The sea floor morphology outside Bråsvellbreen was initially described by Solheim and Pfirman (1985) and based on acoustic data mainly from the 1982 and 1983 cruises. However, the NSKV

cruises of 1984 and 1985 have given a more detailed and complete data set and also cover a wider area. The total data base is used in this paper.

A range of different morphologic patterns in defined provinces have been mapped (Map 2, Morphological provinces, enclosed in back pocket). The most dominant morphological pattern is considered to define the signature of each province. However, there may be large variations within a province and changes between patterns may be gradational. The location of the boundaries is therefore a matter of interpretation in some areas.

The most striking morphological feature in the study area is the system of ridges that roughly parallels the ice front at a distance of a few kilometers. Solheim and Pfirman (1985) mapped the ridge in front of Bråsvellbreen and argued that it was the end moraine resulting from the 1936–38 surge. The dense grid of new lines confirms the continuity of the feature, and furthermore shows that there is a system of three ridges. A second ridge, similar to the Bråsvellbreen ridge, runs subparallel to the Basin 3 ice front, while a third ridge has an intermediate position. The latter merges with the Bråsvellbreen ridge, but apparently not with the Basin 3 ridge (Map 2). The following description and discussion will show that the ridges are terminal features. They will be referred to as surge moraines, and this term will be used below, even though evidence which confirms the Basin 3 and intermediate ridges to be surge-related features has not yet been presented.

The study area is divided into 3 zones, each with several characteristic features:

- *The surge moraines.*
- Inside the surge moraines, *the surge zone* (Solheim & Pfirman 1985).
- Outside the surge moraines, *the surge-distal zone.*

The surge moraines

The most typical cross-sectional shape of the Bråsvellbreen surge moraine is that of an asymmetrical ridge with a smooth outer (distal) slope of 1–3° and a steeper (3–6°, locally steeper) inner (proximal) slope (Fig. 6A, C and D). However, in places the moraine has only a minor topographic expression (Fig. 6B). The distal part of the moraine appears on the 3.5 kHz records as a

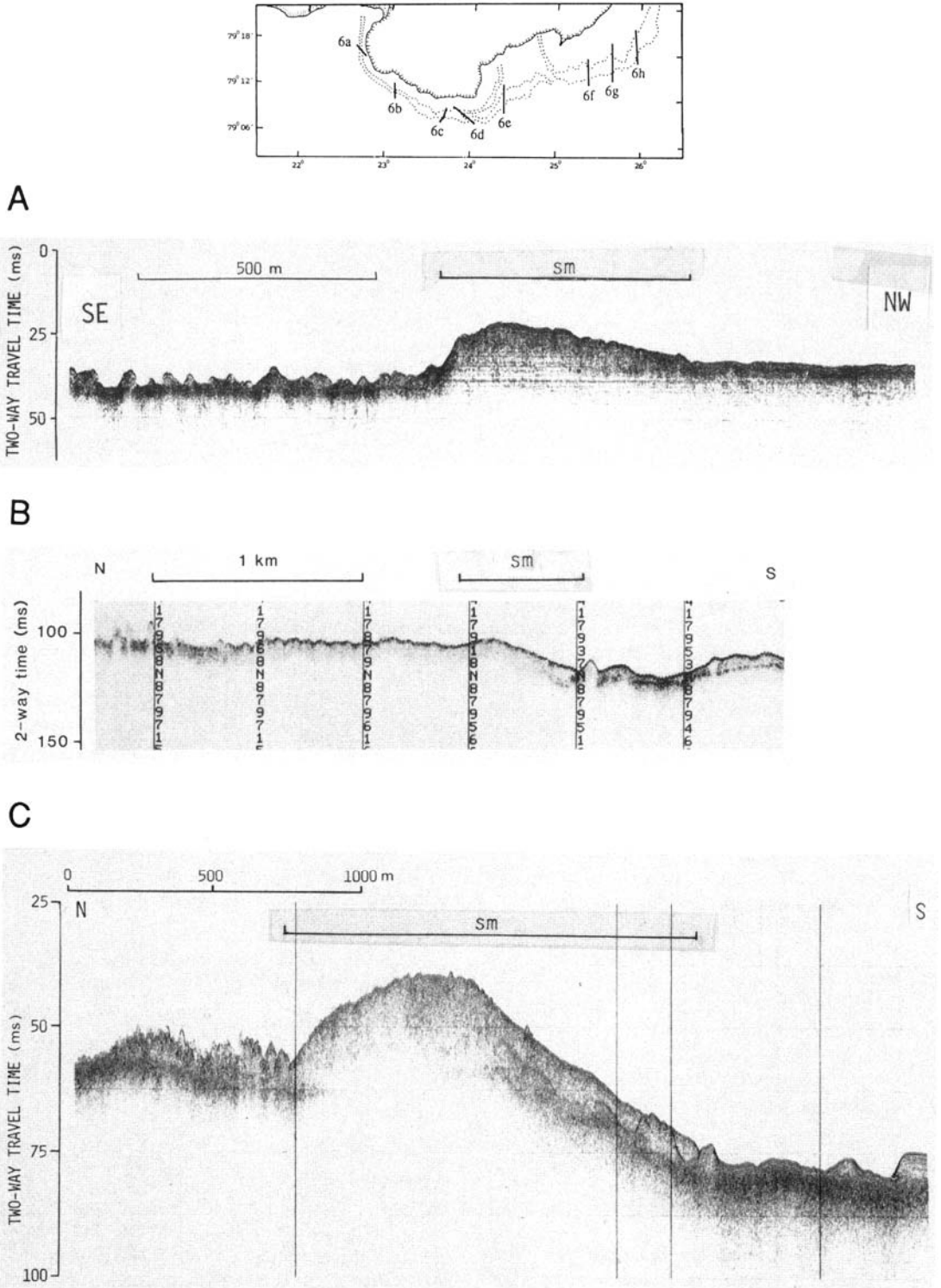
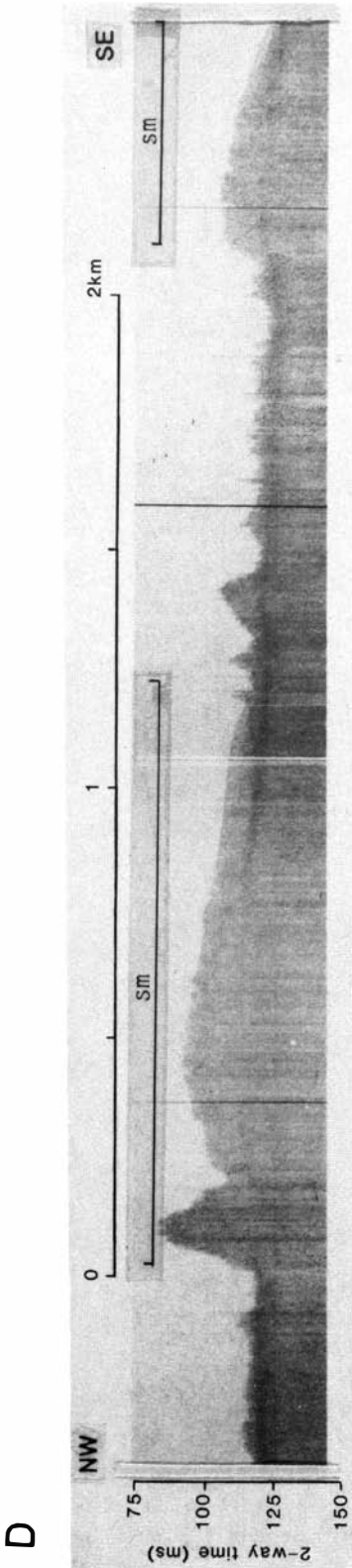


Fig. 6. A-H. 3.5 kHz and sparker records (Fig. 6E, lower part) across the surge moraines (sm).



smooth, acoustically transparent sediment lense which is draped over pre-existing topography and terminates abruptly (Fig. 6C). Its relief varies between 5 m and 20 m and the distance from the base of the proximal slope to the present-day glacier front ranges from 500 m to 3.5 km, the widest and most distinct part being in the area where it splits into two ridges. East of this, it is generally narrower and less distinct than further west. The easternmost two kilometers show little relief and are outlined only from its side-scan sonar character.

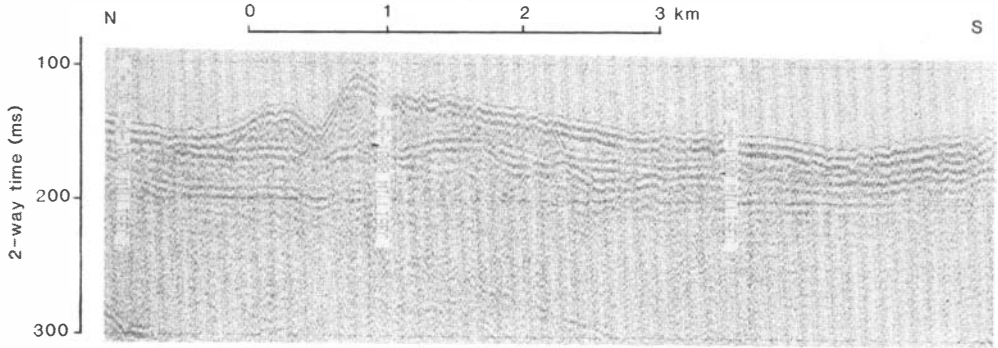
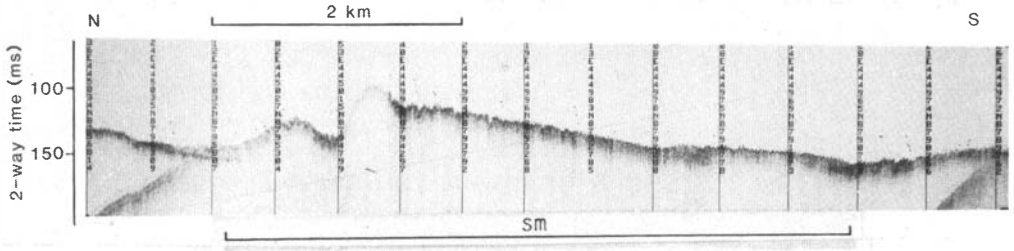
The intermediate surge moraine changes character from being a narrow, low-relief feature in its western part (Fig. 6D) to a wide, well-expressed feature further east (Fig. 6E). Towards its easternmost extension, it loses its bathymetric expression again. The central part of this ridge is wider (up to 3 km) and has a larger maximum relief (35 m) than the Bråsvellbreen ridge, but the overall shape is quite similar.

The Basin 3 surge moraine (Fig. 6F, G and H) has a character somewhat different from that outside Bråsvellbreen. The western part is narrow and poorly expressed bathymetrically (Fig. 6F), although locally it resembles the Bråsvellbreen ridge (Fig. 6G). In its central and widest part (up to 4.5 km), the moraine has the shape of a wide, low-relief sediment lense (Fig. 6H), and the proximal boundary is difficult to define. The distal part, however, is easily recognized by its draped, acoustically transparent character.

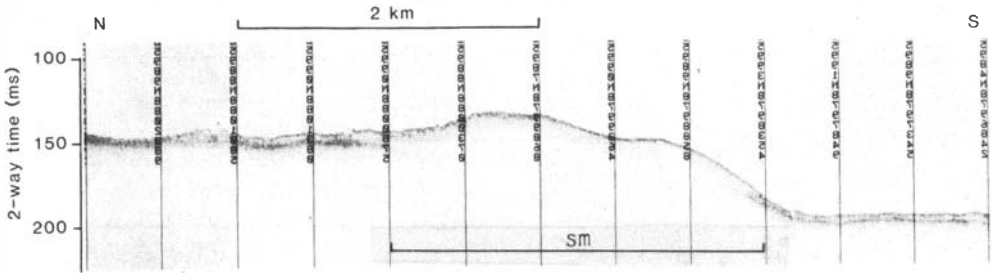
Common for the three surge moraines is that they mark a distinct change in the sea floor morphology between the area towards the glacier and the deeper parts of the basin (Fig. 7).

Although patterns mapped on either side of the ridge may continue on to the ridge proper, the Bråsvellbreen moraine ridge has a generally smooth surface, dissected by occasional iceberg plough marks. Side-scan sonograms clearly show the abrupt distal termination (e.g. Fig. 6C) to be the termination of slump lobes covering the pre-existing morphology (Fig. 8) which may be small compressional, slump related features, or could represent subsequent creep. Furthermore, the smoothness is disturbed by small irregularities forming a small-scale swell and swale morphology (Fig. 8). The disturbed areas usually terminate along the slump edge. Most likely these represent creep features in the soft, acoustically transparent sediments. In the upper left part of Fig. 8A, some vague, larger features can be seen that may

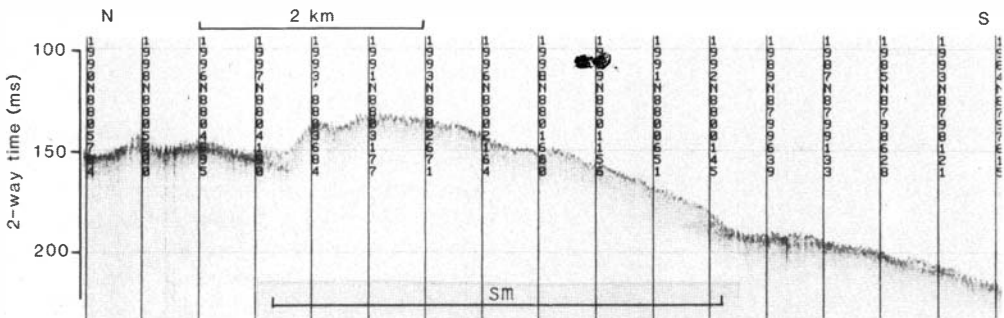
E



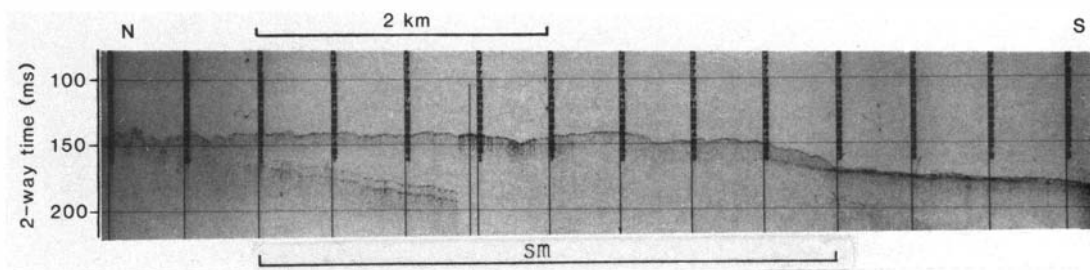
F



G



H



represent detachment scars caused by the slumping.

Side-scan sonographs from the moraines proper show that their small-scale surface morphology in general differs between the Bråsvellbreen moraine and the two other moraines (Map 2). Outside the eastern part of Bråsvellbreen, where the moraine ridge splits, the inner ridge is characterized by a smooth surface, obscured by small disturbances and occasional iceberg plough marks. The outer, intermediate moraine and its continuation eastwards, however, is dominated by iceberg plough marks. This is also the situation on the moraine outside Basin 3, but here the plough marks are

associated with small ridges, mounds and depressions, in both linear and random arrangements (Fig. 9). This is defined as a separate morphological province (Map 2). At the distal part there is again an area of smooth, slightly disturbed sea floor.

The surge zone

The area inside the Bråsvellbreen ridge was termed the surge zone by Solheim and Pfirman (1985) because this area was directly affected by grounded surging ice in 1936–38. Two different morphological patterns predominate. The main

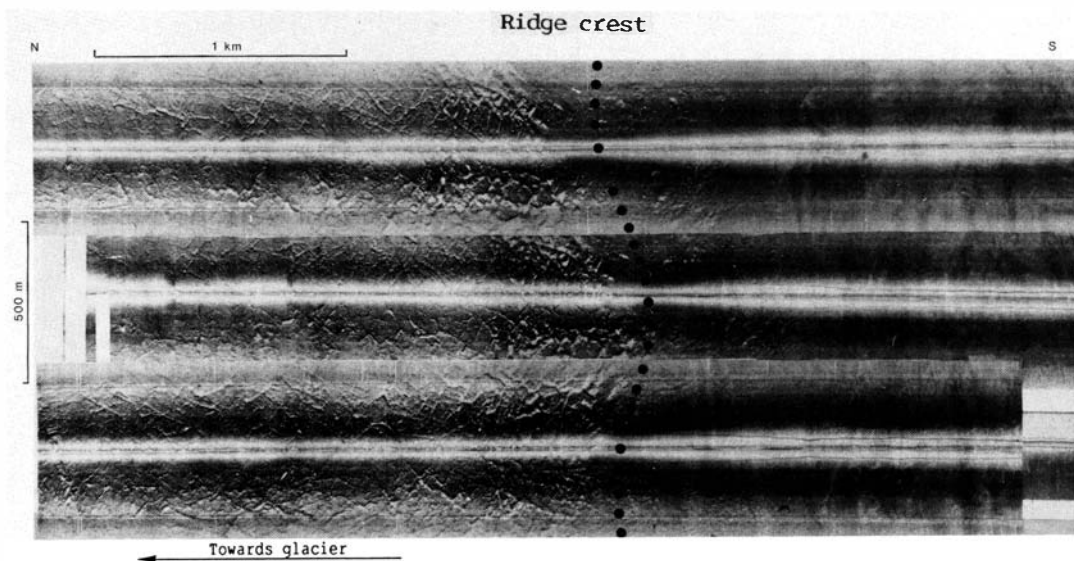


Fig. 7. Side-scan sonar mosaic across the Bråsvellbreen surge moraine. Notice the marked morphological change across the ridge. For location, see Fig. 10.

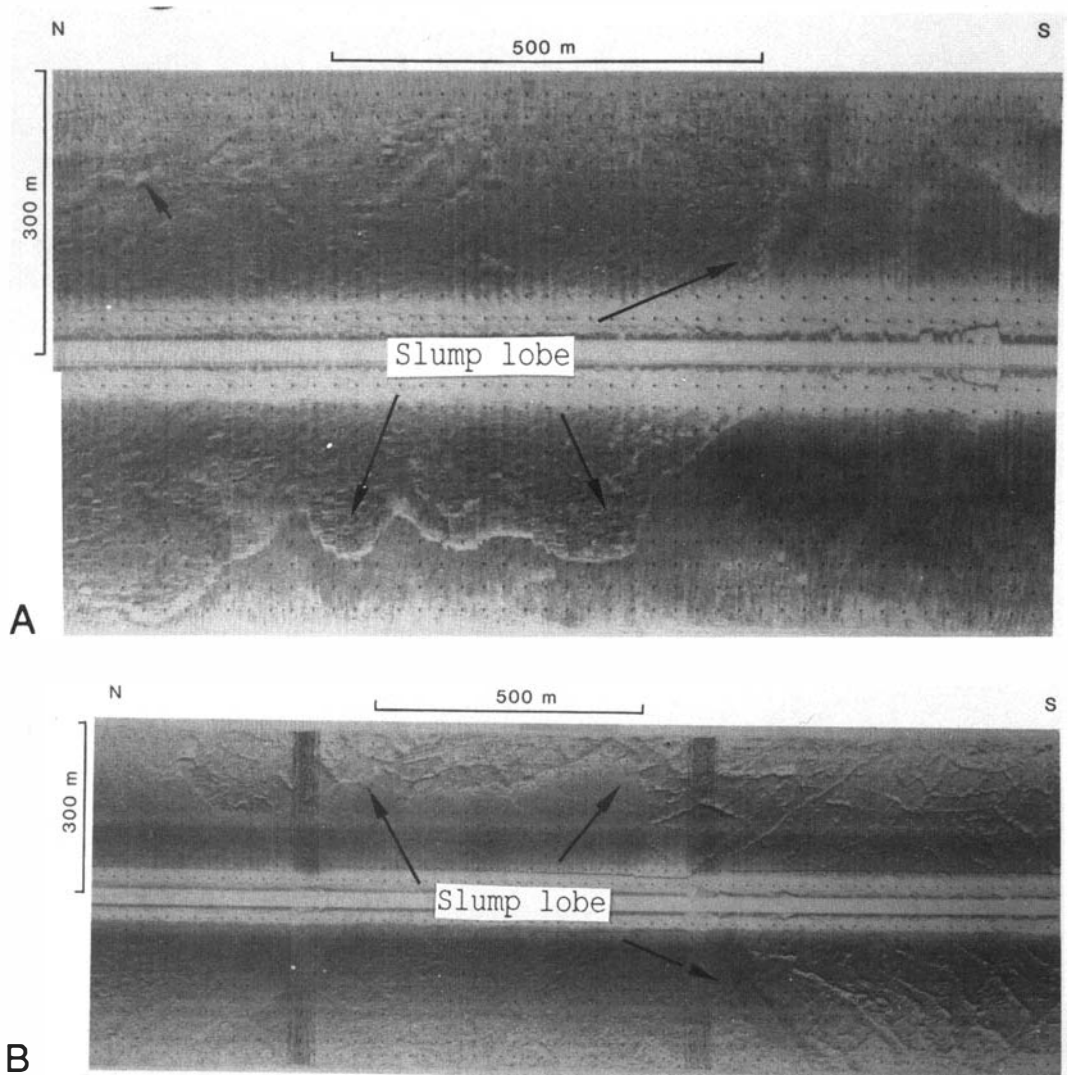


Fig. 8. A and B. Side-scan sonographs showing slump lobes on the distal part of the surge moraines. Note that the slumps cover pre-existing relief. Note also the small disturbances in the smooth slump lobe surface, and the possible detachment scars (short arrow) in A. For location, see Fig. 10.

part of the area, 0.5–1 km south of the ice front, has a system of smaller, linear ridges orientated in different directions that together form a rhombohedral cross-pattern (Map 2 and Fig. 10). The ridges have reliefs on the order of 5 m and spacing of 20–70 m. They are larger and more distinctly close to the surge moraine. Ridge directions vary, and 2–3 different directions may be present within a region (Fig. 11). Most often, however, there are directions sub-parallel and sub-perpendicular to the present-day ice front.

In general the distal limit of the rhombohedral pattern follows the proximal edge of the moraine, but in some locations it may extend on to the topographically-defined ridge. In the eastern part, where the moraine ridge splits into an outer and an inner ridge, a clear rhombohedral pattern exists between the two moraine ridges (Map 2 and Fig. 10B).

Although the side-scan data coverage is more sparse outside Basin 3, a rhombohedral ridge pattern can also be mapped here. It is best

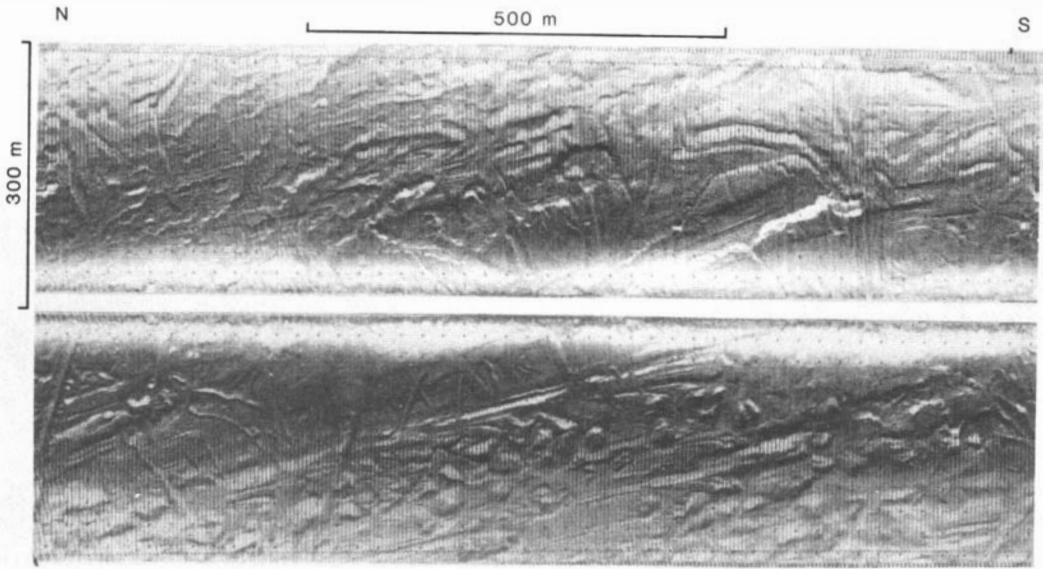


Fig. 9. Side-scan sonograph showing the “mixed morphology” indicated on Map 2. For location, see Fig. 10.

expressed in the eastern part, but is generally not as clear as that outside Bråsvellbreen. The distal limit roughly follows the proximal side of the end moraine, but the latter is more difficult to define, due to its lesser topographic expression. The inner limit of the rhombohedral pattern is generally 3–5 km off the present-day ice front, except close to Kapp Mohn.

Between the two drainage basins, a rhombohedral ridge pattern disturbed by smaller mounds and depressions prevails for a distance of approximately 4 km inside the moraine. The disturbances seem to overprint the rhombohedral pattern in this area.

In the western part of Bråsvellbreen the rhombohedral ridge pattern can be traced to the ice front (Fig. 10A), while further east, in a 500 m to 1 km wide zone adjacent to the ice front, a system of discontinuous arcuate ridges trending subparallel to the front prevails (Map 2 and Fig. 12). The relief and width of individual ridges are of the same order as the linear ridges forming the rhombohedral pattern. The zone of arcuate ridges widens markedly to the east of Bråsvellbreen, from approximately 1 km to generally 3–5 km in the rest of the area. Both adjacent to Basin 3 and Bråsvellbreen, the ridges are relatively distinct, and the glacier-parallel trend predominates even though other directions do occur.

Also within this morphological province the pattern is most varied and least distinct in the region between Bråsvellbreen and Basin 3. The above-mentioned pattern of mounds and depressions obscures the ridges, and directions vary from parallel to subperpendicular to the ice front. In the shallowest region, southwest of Kapp Mohn, the ridge system is overprinted by recent iceberg plough marks which define the dominant morphological features of this area (Map 2).

The surge-distal zone

Two broad classes of sea floor morphologic provinces prevail south of the surge moraine system, in the surge-distal zone;

1. Areas where iceberg plough marks predominate.
2. Areas where smooth sea floor predominates, but where a number of other features also exist.

Two classes of iceberg plough marks are defined in the study area:

- a) “Recent” plough marks, formed under the present-day water depth and glacier configuration.

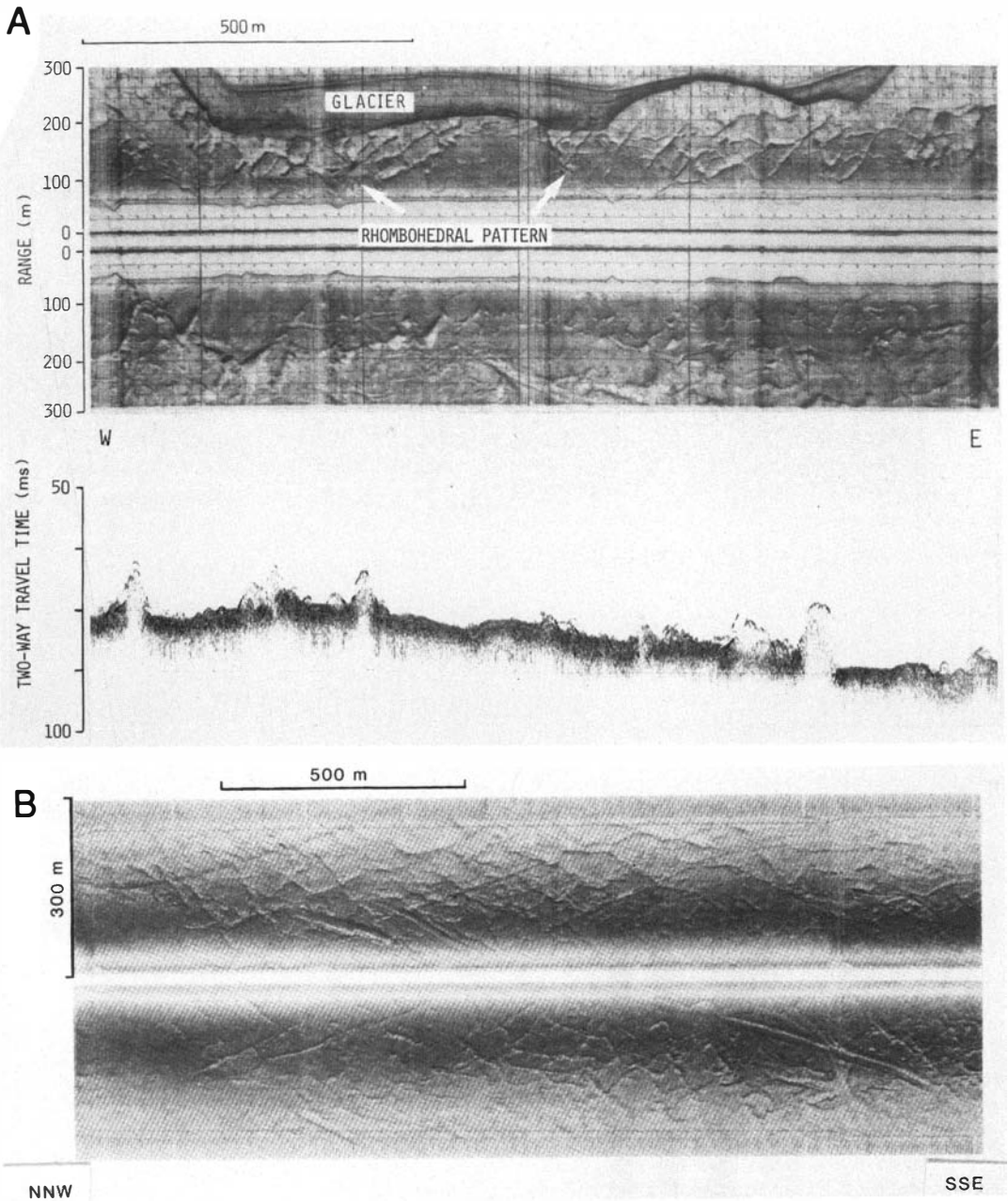
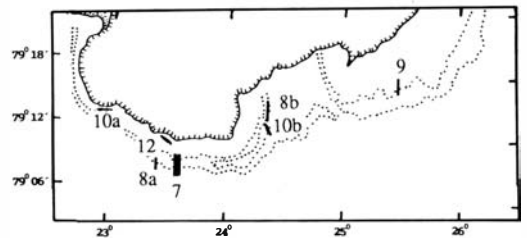


Fig. 10. Side-scan sonograms and 3.5 kHz echogram from the rhombohedral ridge pattern of the surge zone. A. Rhombohedral ridge pattern off the ice front in the western part of Bråsvellbreen. B. Rhombohedral ridge pattern between two moraine ridges in the eastern part of Bråsvellbreen.



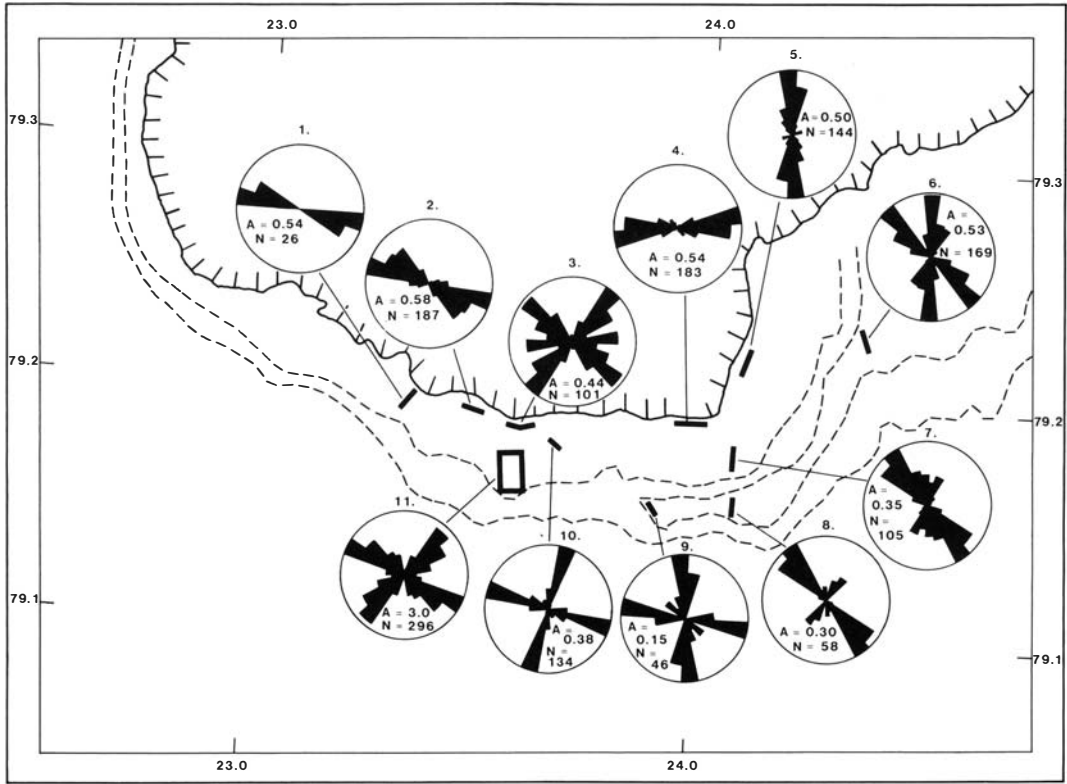


Fig. 11. Rose diagrams of directions of ridges in the surge zone. The analyses were done inside a sliding window of 100×200 m across each area. N = number of counts. A = measured area in km².

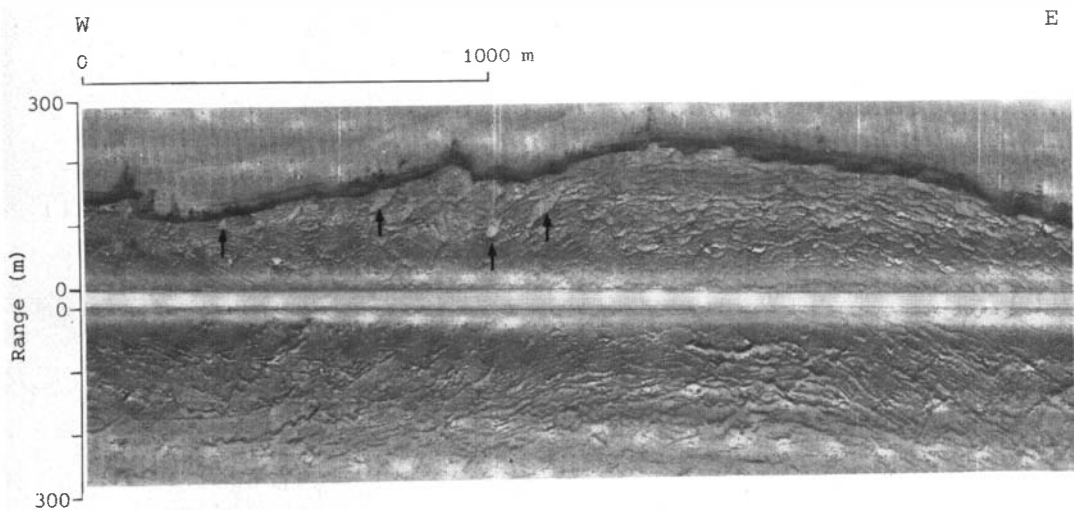


Fig. 12. Side-scan sonograph of the discontinuous, arcuate ridges subparallel to the ice front. Some possible iceberg calving impact features are marked with arrows. For location, see Fig. 10.

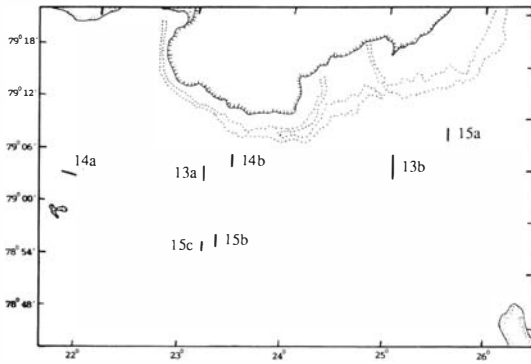
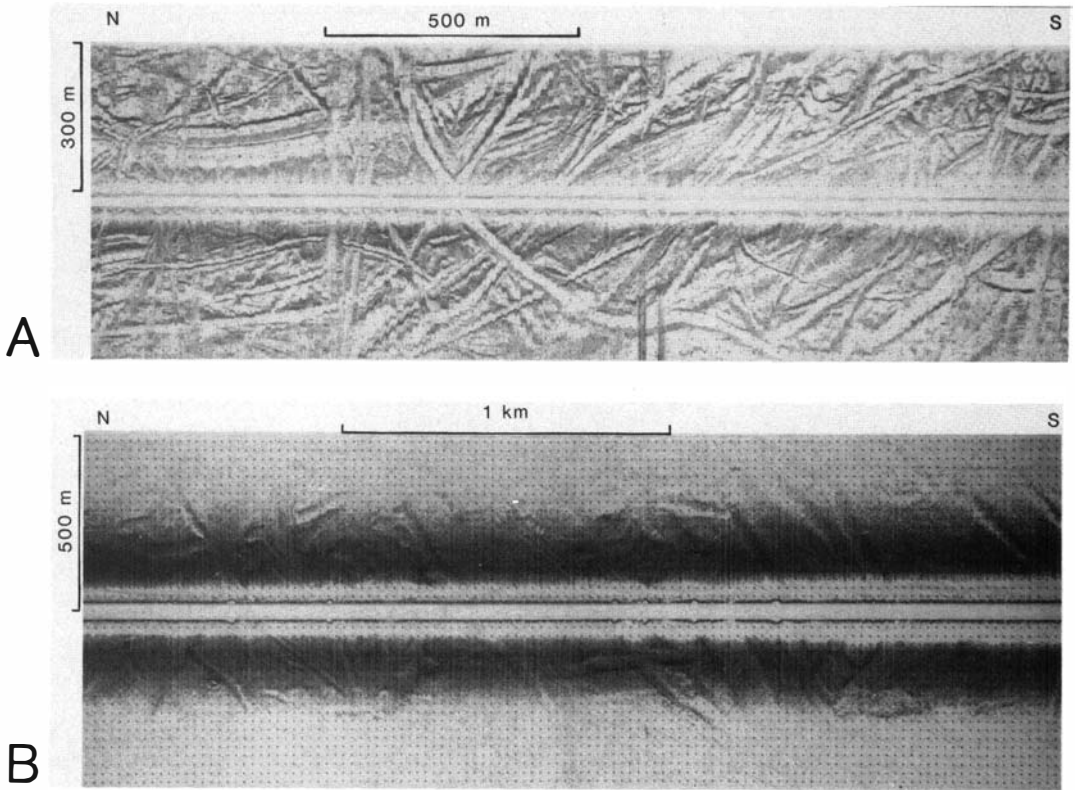


Fig. 13. Side-scan sonographs. A. Recent iceberg plough marks. B. Fossil iceberg plough marks.

b) “Fossil” plough marks, mostly found in water depths below the probable reach of present-day icebergs.

The distinction between a) and b) is made only from their appearance on the side-scan records. The recent plough marks have a sharp, fresh appearance which contrasts markedly with the weakly-pronounced, probably degraded, fossil marks (Fig. 13). However, the differentiation is

not always straightforward, as a range of plough marks intermediate between the two end members exists.

Most of the recent ploughing is found in the shallower surge-distal areas on either side of Erik Eriksenstredet, with the addition of the intermediate surge moraine, the area southwest of Kapp Mohn and occasional plough marks elsewhere in the surge zones. Typical widths of these plough marks are from 10 to 50 m, averaging

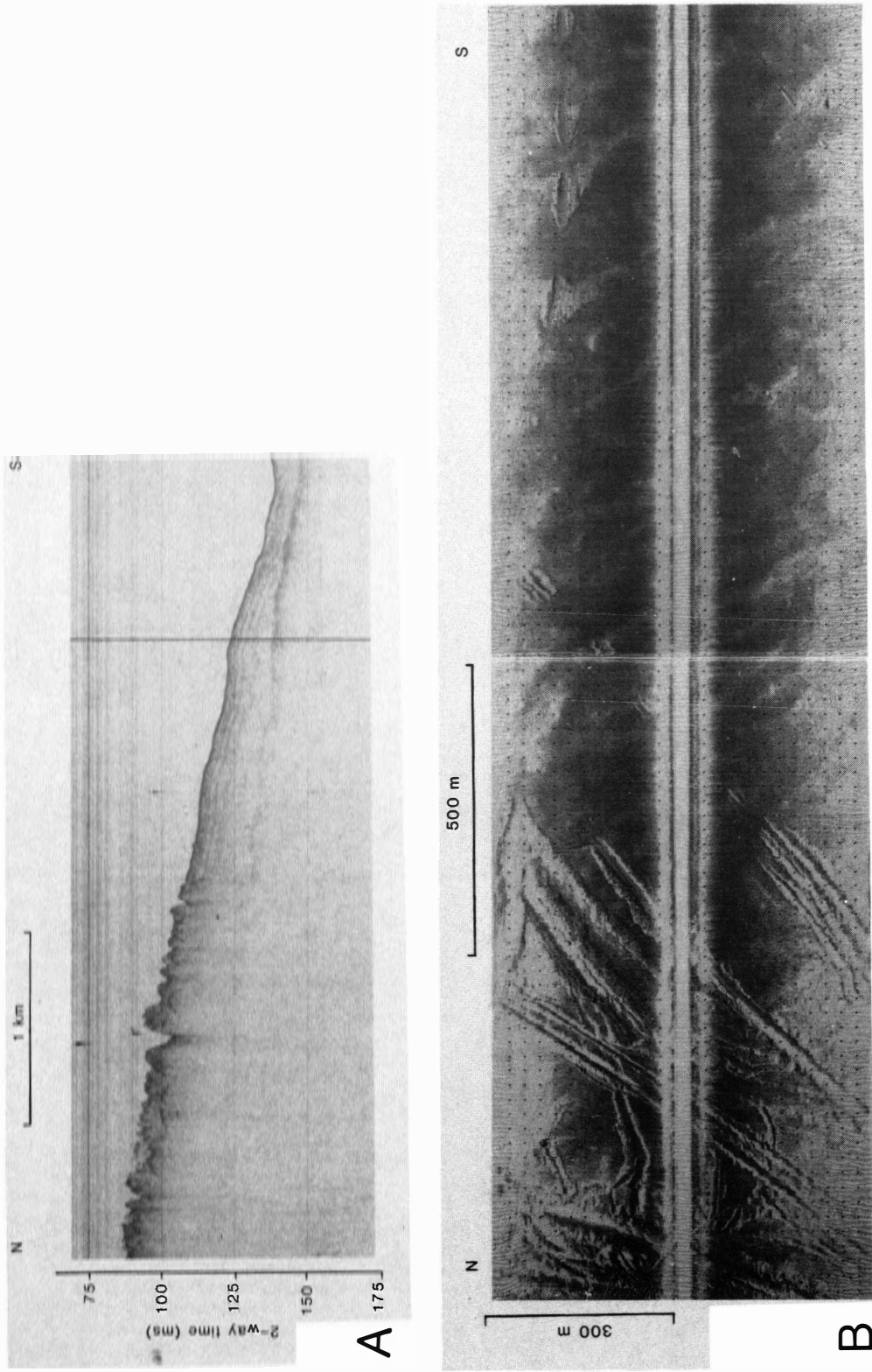


Fig. 14. A and B. 3.5 kHz record (upper) and side-scan sonograph (lower) showing termination of the recent iceberg ploughing. Note that the profiles are from different locations. For location, see Fig. 13.

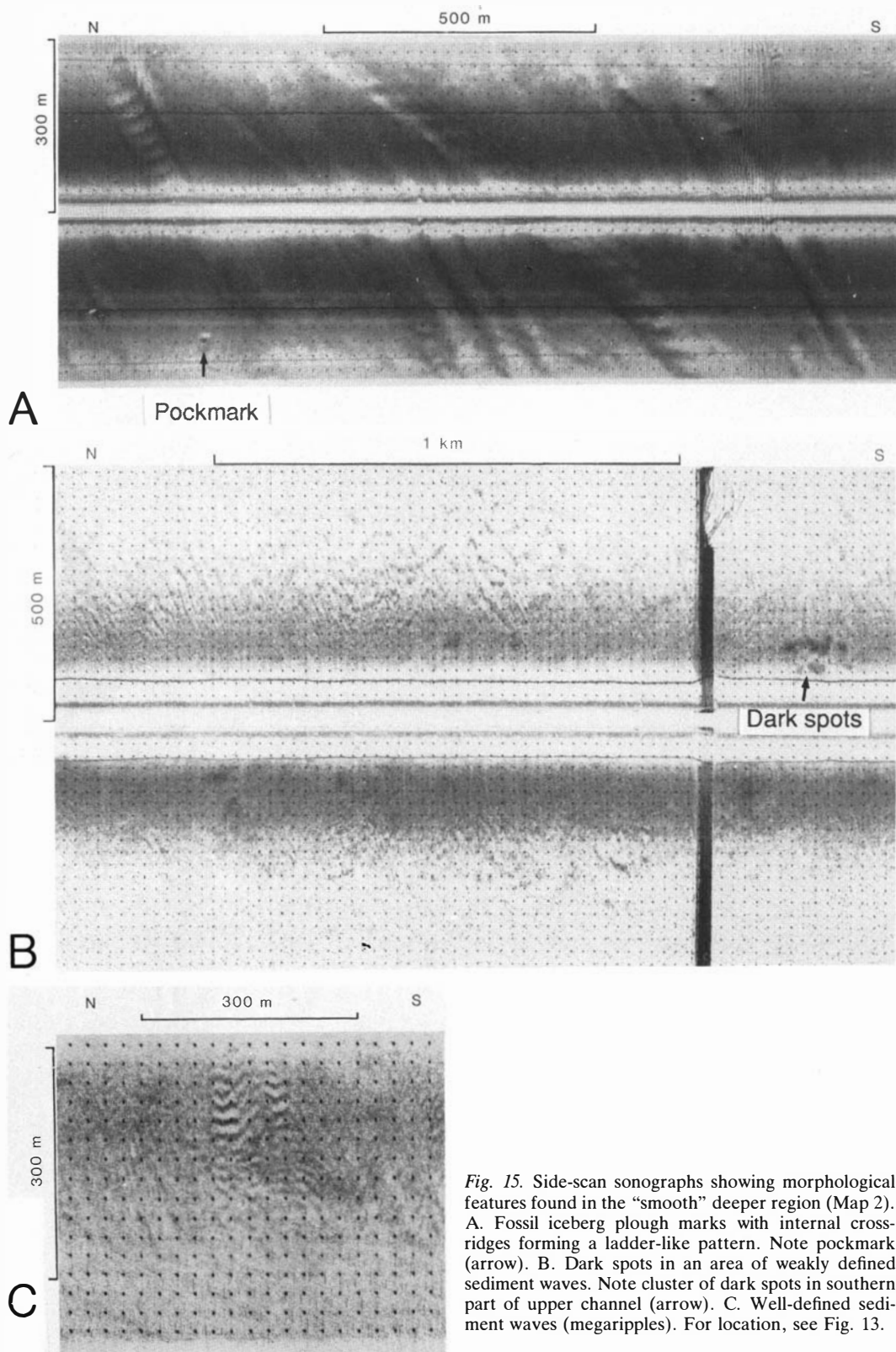


Fig. 15. Side-scan sonographs showing morphological features found in the “smooth” deeper region (Map 2). A. Fossil iceberg plough marks with internal cross-ridges forming a ladder-like pattern. Note pockmark (arrow). B. Dark spots in an area of weakly defined sediment waves. Note cluster of dark spots in southern part of upper channel (arrow). C. Well-defined sediment waves (megaripples). For location, see Fig. 13.

around 25 m (Fig. 13A). Relief (top of berm to bottom of trough) is on the order of 2–5 m. The lower limit for the recent iceberg ploughing varies between 120 m and 130 m water depth, corresponding well with a maximum submarine ice cliff height of 125 m for Austfonna (Dowdeswell 1989). This is well-expressed, both along the north slope and in the southwestern and southeastern parts of the survey area (Map 2). In the north-western part, the intense ploughing grades into a transitional zone of less intense ploughing at 50–100 m water depth which terminates at approximately 120 m water depth. Most often, however, the zone of intense, recent ploughing terminates abruptly and changes into smoother sea floor with older plough marks (Fig. 14). Locally this occurs at depths shallower than 120 m (Fig. 14A).

Dominating directions of the recent plough marks in the northern region generally vary from NW–SE in the western part, through a region of mixed directions in central parts, to more NE–SW directions in the east. In the southern regions, the ploughing directions are generally more variable (Map 2).

Fossil plough marks are found over the entire basin below 120–130 m water depth, including the large region of smooth sea floor. These gouges are degraded to various degrees. They may range from being barely visible on side-scan records and having no topographic expression within the resolution of the 3.5 kHz echo sounder, to being well-enough pronounced that a recent origin cannot be excluded. In general they have less well-defined berms than the recent plough marks. Widths range from 20 to 100 m, averaging approximately 50 m. The relief is often quite similar to that found for recent plough marks, but smoother. Directional trends are mostly similar to those of the recent plough marks, except for the southeastern region, where the fossil plough marks have a strong NE–SW component, and the small area in the deep, central part of the study area where there is a distinct NE–SW, NW–SE cross-pattern. In the easternmost region, smaller, transverse ridges in the plough marks give a washboard or a ladder-like appearance (Fig. 15A).

With the exception of the small areas of more concentrated old ploughing, the areas below the limit of recent iceberg ploughing are defined as one morphological province. In general this province is defined by a smooth sea floor of low reflectivity to the side-scan signals. However, several morphological features are observed:

- “Old” iceberg plough marks, as described above.
- Pockmarks. These are small (5–15 m diameter) circular depressions in the sea floor (Fig. 15A). They are sparse in number, but distributed over the entire area.
- Patches of more reflective sea floor, appearing as dark spots on the side-scan sonar records (Fig. 15B). These are of similar diameter, but more common than pockmarks. They may be found in groups covering areas of 100–200 m diameter. Dark spots and pockmarks may also be found grouped together. None of the two can be distinguished in echograms, implying that they have reliefs of <1 m.
- Sediment waves (megaripples) (Fig. 15B and C). In particular in the western half of the region, disturbances resembling megaripples are found. Often they are indistinct (Fig. 15B) and only rarely can dimensions and directions of sediment movement be measured. Wavelengths seem to be on the order of 15–20 m and measurable directions mostly vary between NW–SE and NE–SW, although E–W also occurs (Fig. 15C).

Distribution and acoustic stratigraphy of unlithified sediments

The sediment cover above bedrock in the major part of the study area is generally less than 10 ms (two-way travel time) (Fig. 16). Uncertainties in accurately determining the sediment thickness result from the following factors:

- Underlying bedrock is essentially conformable with the sea floor over large areas.
- Total sediment thickness is less than the resolution of the sparker system used over large areas.
- The 3.5 kHz penetration is poor due to over-consolidation and scattering of energy in sediments with high clast content.

An internally consistent, detailed acoustic stratigraphy is therefore difficult to map.

In the surge zone, the sediment thickness is mostly 2–5 ms, with some areas of 5–10 ms. The latter is most common along the surge moraine outside Basin 3. This is also the region where the proximal boundary of the moraine is difficult to define, and where sediment seems to be “smeared” out over a larger area than the ridge

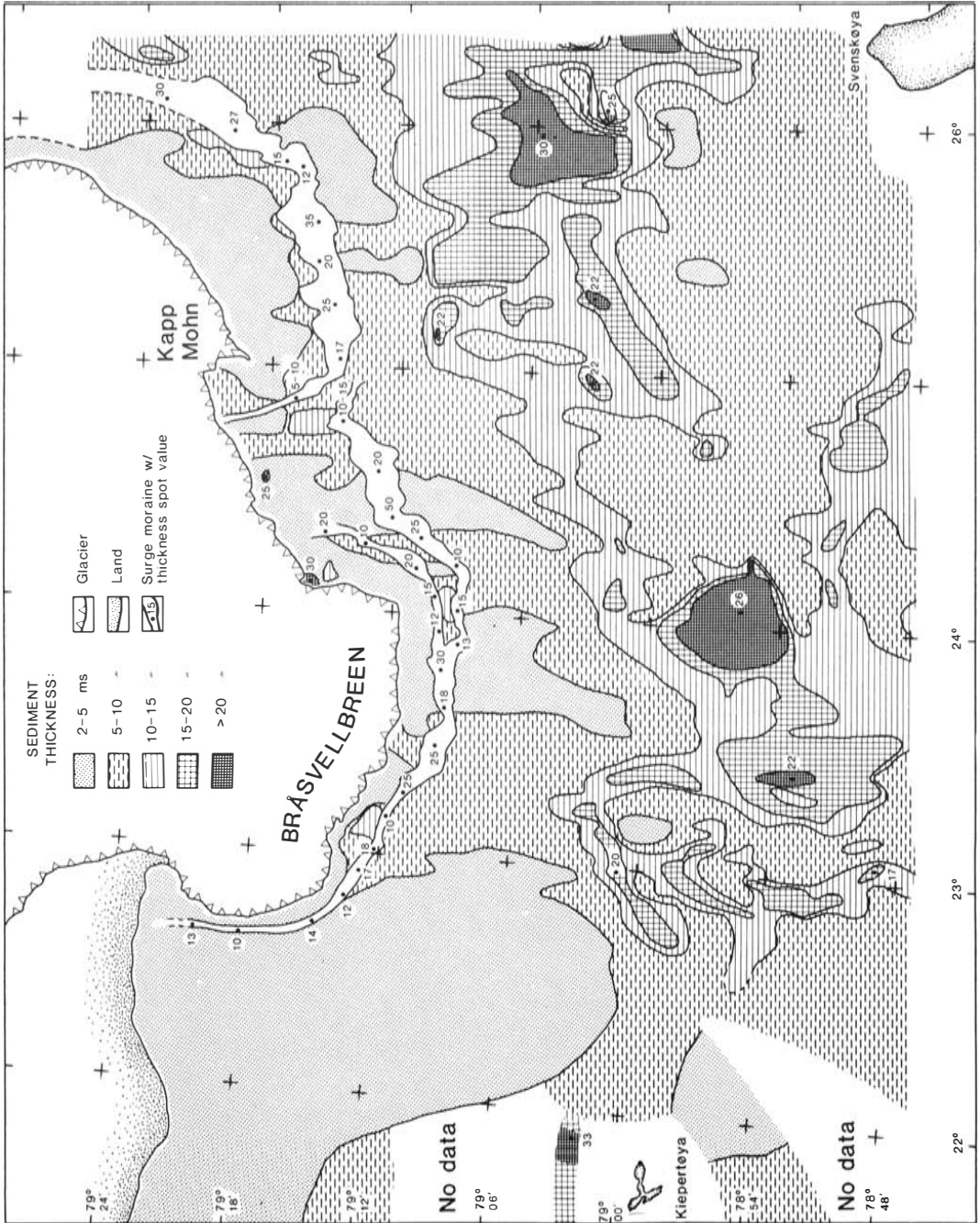


Fig. 16. Isopach map of total un lithified sediment cover. Thickness values in two-way reflection time (ms = milliseconds).

proper. Due to the irregular topography, thickness variations are large, and the map (Fig. 16) represents average values. Most irregularities are too local to be included in a map of this scale. Deviations from 2–10 ms thickness inside the surge moraines include: a small area of 10–15 ms in the western part of Bråsvellbreen (found in a local bathymetric depression that also appears to have escaped recent iceberg ploughing outside the surge moraine); two small accumulations which are associated with the meltwater outlet, one of which reaches 30 ms thickness; a local ridge close to the ice front in the intermediate region; and an area of 10–15 ms just inside the eastern part of the intermediate surge moraine.

The surge moraine system constitutes the most distinctive sediment accumulation in the region, although its relief and thus sediment thickness vary considerably. The intermediate moraine reaches the largest thickness, of up to 50 ms (Figs. 6 and 16). In the region where this moraine merges with the Bråsvellbreen moraine, the latter reaches its maximum thickness of 30 ms.

The large region in the western part of the study area, with 2–5 ms sediment, is part of the shallow sill at the mouth of Hinlopenstredet. Water depths in this area are generally less than 50 m. The major part of the deeper basin has 5–10 ms sediment thickness, but locally thicker lenses occur in the deeper part of the strait and thinner ones on the north slope. The trend of the thicker accumulations follows the bathymetric NE-SW trend, with a transition into the more N-S Olgastredet trend in the southwestern part of the map area.

Five acoustic stratigraphic units are defined within the present study area (Fig. 17), based on their character in 3.5 kHz records:

- Unit 1. Semitransparent top unit in the surge zone.
- Unit 2. The surge moraine ridge system.
- Unit 3. Transparent top unit in the surge-distal region.
- Unit 4. Intermediate, semitransparent unit.
- Unit 5. Opaque unit, underlying the transparent sediments over the entire study area.

Some of these units, in particular 1, 2 and 3, may be isochronous or at least overlapping in age, but their character and geometry are different enough to justify a separation. The most diagnostic features are acoustic transparency, character of internal reflections and surface roughness. There

are no systematic differences between the areas outside the different glacial drainage basins.

Unit 1 is the acoustic unit that forms most of the small-scale topography in the surge zone. Due to squeeze-up, ice push and occasional iceberg ploughing, the character of this unit is dominated by its rough surface structure which causes abundant diffraction patterns. The unit rests on a relatively smooth reflector, opaque to the 3.5 kHz signal. Its thickness varies frequently from zero between ridges to several meters in the ridges and other local accumulations. The ridges may be narrow enough to be represented only by a single diffraction hyperbola, and this may contribute to the acoustically transparent character of the sediment. Where Unit 1 is found as a more continuous accumulation, it has a more semi-transparent character, with abundant internal diffraction. Internal reflectors can be seen, but are local due to the patchiness of the unit.

As the surge moraine ridges comprise depositional features clearly different from the other stratigraphic units in the region, they have been classified as a separate unit, Unit 2. The Bråsvellbreen ridge has the best coverage of good quality data. Most of the ridge, in particular the central and inner (proximal) part, has a relatively homogeneous, semi-transparent character. On some of the 1982 lines, run with high sweep rate under favourable weather conditions, internal diffraction and discontinuous reflectors can be seen. In the profile of Fig. 17, the ridge terminates on the berm of a plough mark and some of the ridge material has spilled over and covers the plough mark floor with a 1 ms thick drape. No ridge sediment, resolvable by the 3.5 kHz echosounder, can be followed further out. The same structure is also seen in other profiles across the Bråsvellbreen ridge. The surge moraine ridges outside Basin 3 and the intermediate area have a more uniform acoustic appearance, but the data from these areas is of lower quality and vertical resolution.

Unit 3 is found as a thin, acoustically transparent layer in central parts of the basin at depths exceeding 140 m. This limit is most distinct along the north slope. Unit 3 reaches its largest thickness of 7 ms in the southwest, between 23° and 24°E, while the thickness generally varies from 1–3 ms over most of the region. The existence of a thin drape, below the resolution of the 3.5 kHz system (approx. 1 ms), also in waters shallower than 140 m cannot be excluded.

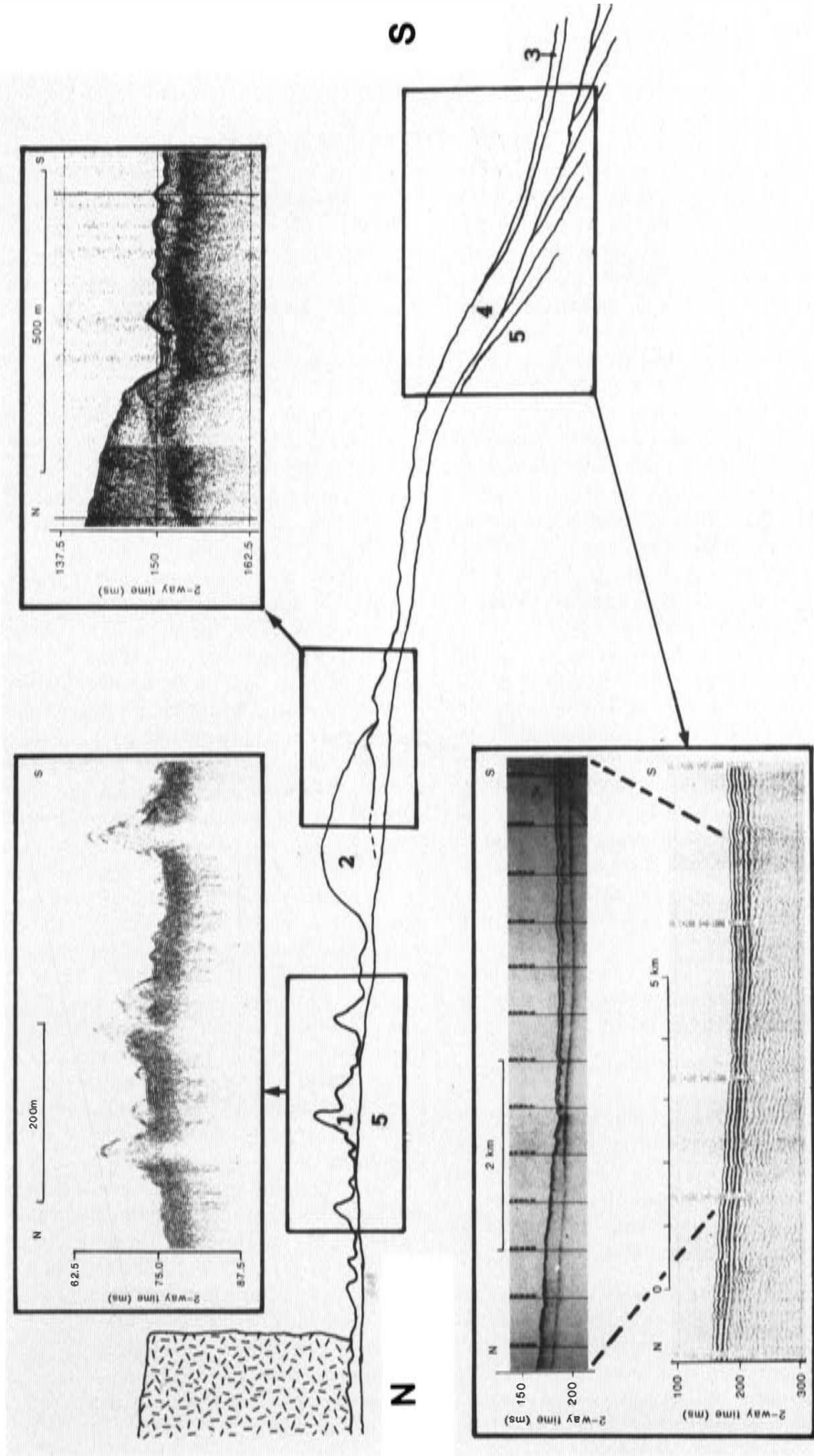


Fig. 17. Cross-section showing the different acoustic units (bold numbers 1-5). Note that the line drawing is only schematic, not drawn to scale.

Unit 4 constitutes most of the sediment thickness in the surge-distal zone. It varies in thickness from zero up to nearly 30 ms. Its distribution follows the general sediment distribution trend in the basin, with the thickest deposits in the deepest areas. The top surface has a gently undulating character, most likely resulting from old iceberg plough marks. In the central parts of the basin, this undulating surface is draped by Unit 3 sediments (Fig. 17). Its lower boundary is a smooth reflector that can be followed regionally over the area, also under the end moraines and in the surge zone. Internally, Unit 4 is mostly homogeneous and slightly less transparent than Unit 3. Occasionally, an undulating, discontinuous reflector can be seen in the lower part of the unit. From its less transparent character the material below this reflector may locally represent thicker till accumulations. Parallel layering, most distinct in the upper half of Unit 4, is observed on the slope towards Barentsøya (Fig. 14A). Internal acoustic layering can only be seen below the lower limit of recent iceberg ploughing. Above 120 m waterdepth, Unit 4 sediments are intensively disturbed by recent ploughing in front of the surge moraines. However, in the local deep in front of central Bråsvellbreen (Map 1) the top surface of Unit 4 is smoothly undulating from old, degraded ploughing, and it can be followed under the outer part of the moraine ridge (Fig. 17).

Unit 5 is used here as a collective term for all sediments below the smooth, lowermost reflector. It may represent in part the upper bedrock or a highly overconsolidated till, opaque to the 3.5 kHz signal. The sparker resolution is too poor to resolve a thin layer of till. When followed under the surge moraine (Fig. 17), the reflector seems to outcrop between ridges in the surge zone where coring has revealed highly consolidated, pebble-rich till. Thus, most of Unit 5 most likely represents an unresolvably thin and patchy cover of overcompacted till over the sedimentary bedrock.

Sediment composition and physical properties

The distribution of cores (Fig. 5C) may seem strongly biased towards the surge zone. This results partly from the sea-ice conditions during sampling, but also from the fact that many of the stations in the surge zone were considered

unsuccessful because the corer failed to penetrate down into the lower, overconsolidated layer (Unit 5). Fig. 18 shows the lithostratigraphy of a selection of the cores, arranged along profiles from the present-day ice front and out towards the Erik Eriksenstredet basin. Grain size distribution and physical properties are indicated along the sections to reveal any systematic changes in these parameters either downcore or lateral. Appendices 2 and 3 show lithology (grain-size distributions) and physical properties, respectively.

Lithology

In the *surge zone*, three different lithologies are found. The dominant sediment type, found in most of the cores, is a diamicton with a generally high but varying content of gravel and larger clasts (Fig. 19). There are large and frequent variations in the grain size distribution both downcore and laterally, without any apparent systematic trend.

The second distinct lithology is a clean sand, as seen in the top parts of cores 83-30, 83-31 and 83-26 (Fig. 18D and E). These are all well-sorted, fining-upward sands, with a minor content of gravel and mud-sized material. The typical sandy sequence is well-exemplified in the uppermost 0.3 m of core 83-26 (Fig. 18E) where the silt content decreases while the gravel content increases downcore. As there are only three cores with this lithology, little can be said about the distribution. However, from the generally high number of cores, it can be justifiably stated that the clean sands are relatively restricted in areal extent. Possible mechanisms for formation of the sands include wave action, currents, iceberg calving and scouring, and glacial meltwater activity. Pfirman (1985) suggested that severe storms could disturb and rework sediment down to 150 m water depth in the Barents Sea. The sands are sampled at depths ranging from 70 to 92 m. However, wave action, as well as currents, would be expected to result in a wider distribution of the sandy sediments (Johnson 1981). Also, during most of the stormy season, the area is covered by sea-ice, damping wave action and reducing wind-water coupling. The action of icebergs may stir up sediment and resuspend fines. This may occur during iceberg ploughing, but also from the impact of icebergs on the sea floor during the calving process (Powell 1985). The latter would indeed have a local effect. The sands are found within the zone of arcuate, subparallel ridges, but the data cover-

age and the navigation are not good enough to relate the samples to any ploughing or calving event. However, it is considered unlikely that such an event could cause 30 cm of well-sorted sand within the very short time-interval of its duration. This leaves glacial meltwater activity as the most likely mechanism, probably in the form of small local streams.

The third distinct lithology of the surge zone appears even more laterally restricted than the clean sand. A greenish fine-grained mud is found only in two cores: 83-31 in the interval 0.48 m to 0.85 m (Fig. 18D), and core 83-32 in the interval 0.58 m to 0.7 m. The mud is situated between gravel-rich diamictons and is characterized by an olive-gray color (Munsell color 5Y 4/1), minor amounts of sand-sized material and high shear strength. Analyses of the foraminiferal fauna indicate a more ice-distal environment than the present location of only 1.5 km from the glacial front although the data is sparse and the interpretation is not unambiguous (J. Nagy pers. comm. 1985). Based on color, lithology and foraminifera, this material resembles the Holocene muds usually found further out in the Barents Sea (Elverhøi & Solheim 1983) and hence indicates a pre-surge, ice-distal origin. The overlying diamicton further supports this interpretation.

The lithology of the *surge moraine* (cores from the Bråsvellbreen moraine only) consists essentially of the same relatively homogeneous, gravel-rich diamicton which dominates the surge zone (Fig. 19). Although no distinct boundaries exist, there is a tendency for more fine-grained, less gravelly deposits to occur towards the distal parts of the ridge (e.g. cores 82-234 and 82-235, Fig. 18D). However, the variation is large, and core 83-29 from the distal part of the outer ridge in the eastern part of the study area has a gravel content reaching 25–30%. Intervals of finer grained mud are also found in these deposits (i.e. 82-235, 0.8 m–0.9 m), but with no corresponding change in other parameters.

In the *surge-distal zone*, the sediments (acoustic Units 3 and 4) reach a thickness of several meters and consist of a sequence of olive-gray mud above darker mud with a higher content of dropstones. These sediments most likely represent Holocene mud and Late Weichselian glaciomarine sediment, respectively (Elverhøi & Solheim 1983). As a result of closer proximity to a source area for icebergs throughout the Holocene, the content of coarser material in the Hol-

ocene part is relatively high compared to further out in the Barents Sea. The material just outside the Bråsvellbreen surge moraine is clearly more fine-grained than the directly surge-affected sediments in the surge zone and the moraine ridge (Fig. 18). However, the variations here are also large and frequent. A high content of coarser material is found in the top of some cores (e.g. 82-229, Fig. 18C) as well as further downcore (e.g. 82-237, Fig. 18D). One core, (83-39, Fig. 18B) 0.5 km outside the end moraine, shows a well-sorted, upwards-fining sand with lumps of clay in its lower part. According to Powell (1984), the latter may represent basal debris, most likely released from icebergs.

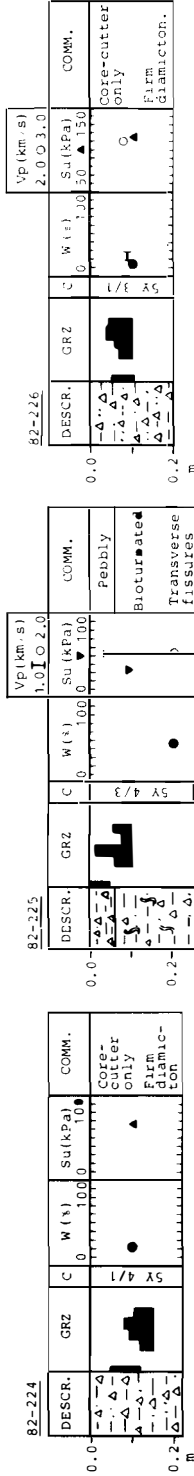
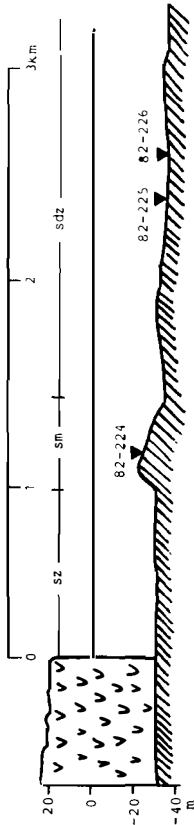
In summary, the grain size distributions for samples obtained in the surge-distal zone have stronger tendencies towards the mud fractions than the material in the surge zone and surge moraines (Fig. 20), but the variation is also larger in the surge-distal zone. This most likely results from the wider range of depositional environments spanned by this zone, which includes the shallow Hinlopenstredet threshold, where probably no or very little sedimentation took place during the Holocene, and the Erik Eriksenstredet basin with depths of more than 200 m and apparently continuous mud deposition. Furthermore, as the side-scan sonar records indicate sediment waves and pockmarks, the Erik Eriksenstredet basin sediments are affected by both bottom currents and gas seepage, both of which may cause depletion of fines. However, lithologies that bear relation to these processes were not sampled during this study. A slight tendency of more fines in the surge moraine than in the surge zone (Fig. 20) reflects the more fine-grained character of the distal parts of the moraine.

Physical properties

Although a large amount of geotechnical information exists from many high-latitude continental

Fig. 18. A–E. Profiles P1–P5. Sections showing lithology and physical properties of cores along profiles sub-perpendicular to the ice front. Note different scales, both down-core and within various parameters. C = colour after Munsell Soil Colour Charts. W = water content in % wet weight. Vp = compressional velocity. Su = undrained shear strength. B.D. = wet bulk density. OED marks samples taken out for consolidation tests in oedometer. For location of cores, see Fig. 5.

PROFILE P1



NOTE: Values are placed arbitrarily in cores 82-224 and 82-226, as only one piece of material was recovered in the core-cutter.

- DESCR.:
- Mud
 - Sand
 - △△ Gravel
 - ⊃ Larger clasts
 - sz : Surge zone
 - sm : Surge moraine
 - sdz : Surge-distal zone

- W : Bioturbation
- ∩ : Shells/shell fragments
- C : Colour
- █ : Sample
- W : Atterberg limits
- Su : Fall-cone
- ⊃ : Pocket penetrometer

- Vp : Measurement transverse to core axis
- ∩ : Measurement parallel to core axis
- : ¹⁴C dating

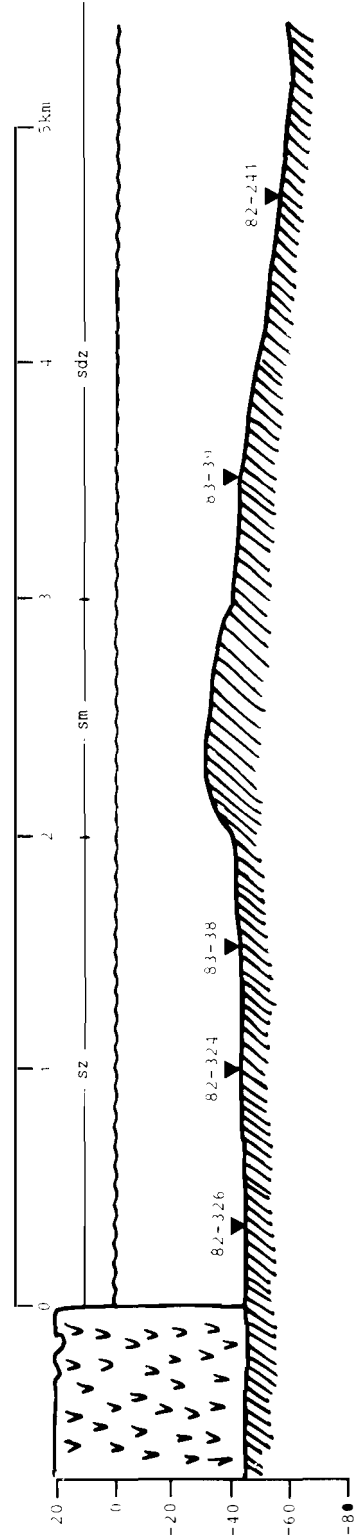
A

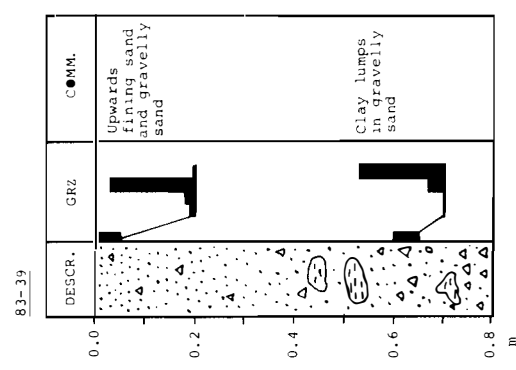
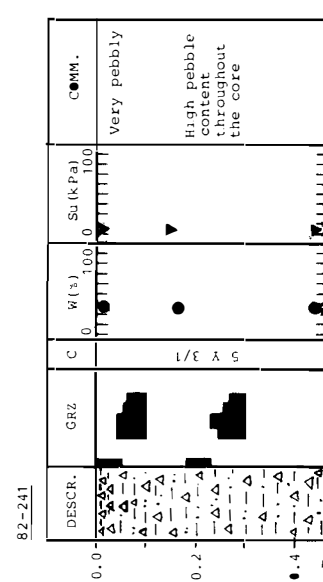
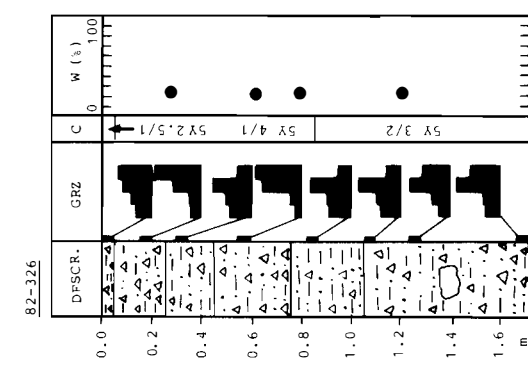
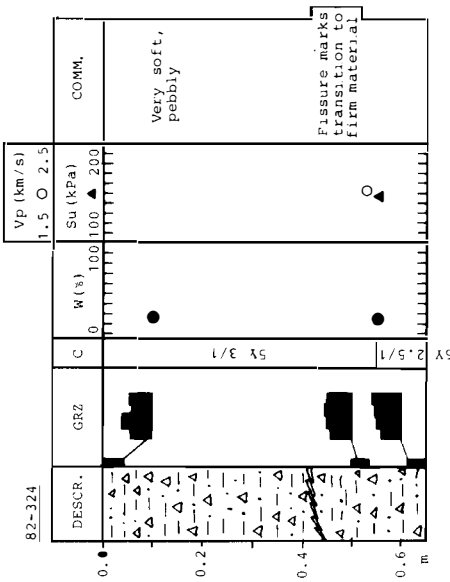
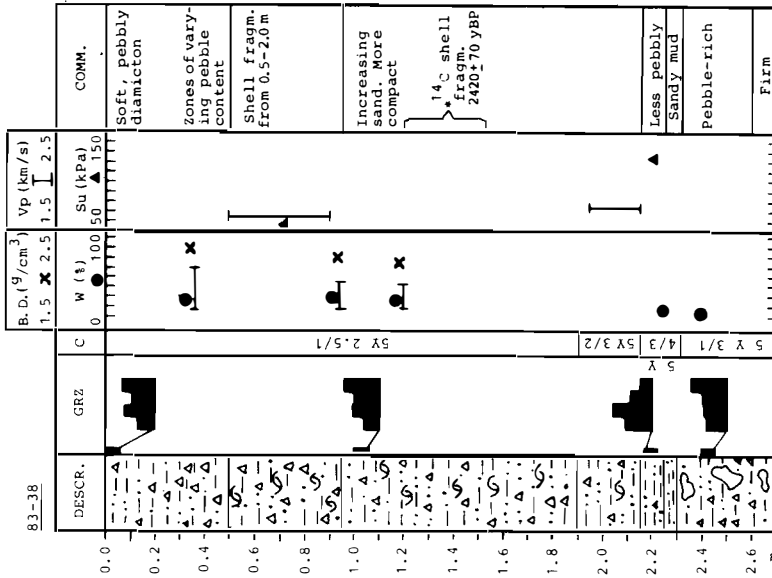
shelf areas, relatively little has been done to synthesize the information and to relate variations to different environments. Most of the work carried out on high-latitude sea-floor sediments covers relatively soft mud and sand (Clukey et al. 1978; Richards et al. 1975; Schwab & Lee 1983). Marine diamictions are still poorly understood geotechnically (Bennett & Nelson 1983). In the following discussion, the different physical characteristics of Erik Eriksenstredet sediments and their variations are discussed, both as a contribution to the general knowledge of marine diamictions and as an investigation as to whether any of the measured values or their variations can be related to glacier oscillations.

Undrained shear strength shows large variations in the surge zone diamictions, both laterally and downcore. The soft, acoustically transparent top material usually has an undrained shear strength of less than 20 kPa, and values less than 5 kPa have also been measured. Values are most likely over-estimated because of a generally high sand content, but nevertheless, they give an indication of the degree of consolidation. In general there is a downcore increase, from the soft top material, through an intermediate zone, and in some cores to a stiff material with values in excess of 100 kPa. The bulk of the material, however, plots in the intermediate range, with values between 30 and 100 kPa. A frequency histogram plot (Fig. 21A) shows the soft surface material below 20 kPa, the intermediately compacted material up to 20 and 100 kPa, and the lower, hard till between 120 and 160 kPa. Variations within each level follow no systematic trend, and changes usually are not connected to lithological changes. Exceptions to this are the intervals of fine-grained mud in cores 83-31 and 83-32 (Fig. 18D and Appendix 3). Core 83-31, 50–85 cm, in particular shows a distinct increase in shear strength, from less than 10 kPa in the diamiction above the compacted mud, to 100 kPa at the 55 cm level. The values decrease to 80 kPa near the bottom of the muddy section. The difference is not as distinct in core 83-32, where the values increase from 40–60 kPa in the diamictions above, to 80 kPa within the mud (Appendix 3).

The surge moraine diamictions show less varied and generally lower shear strengths than in the surge zone. All measurements except one fall below 40 kPa (Fig. 21B and Appendix 3) and the majority are below 25 kPa. In one core (82-234, 1)

PROFILE P2

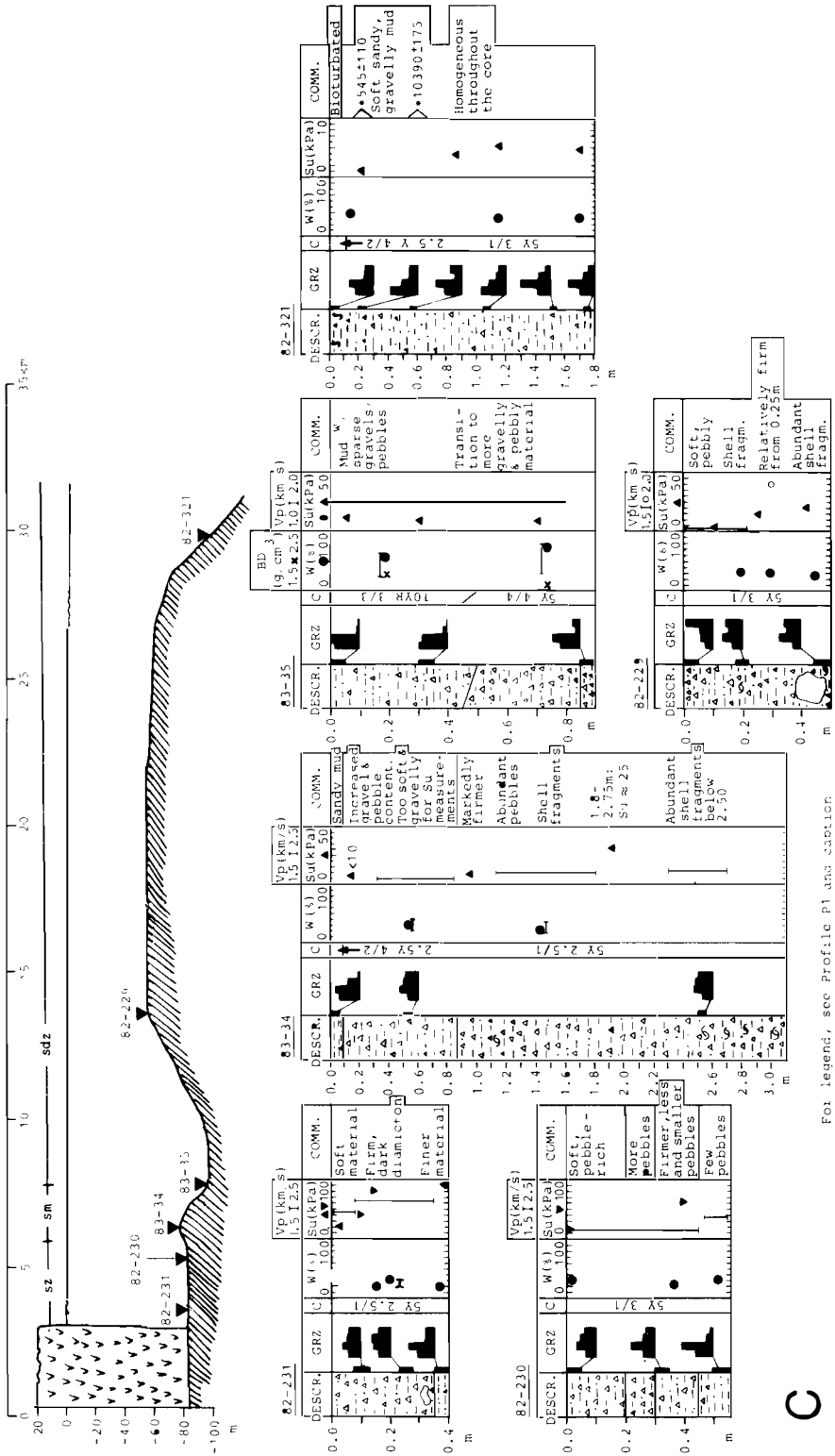




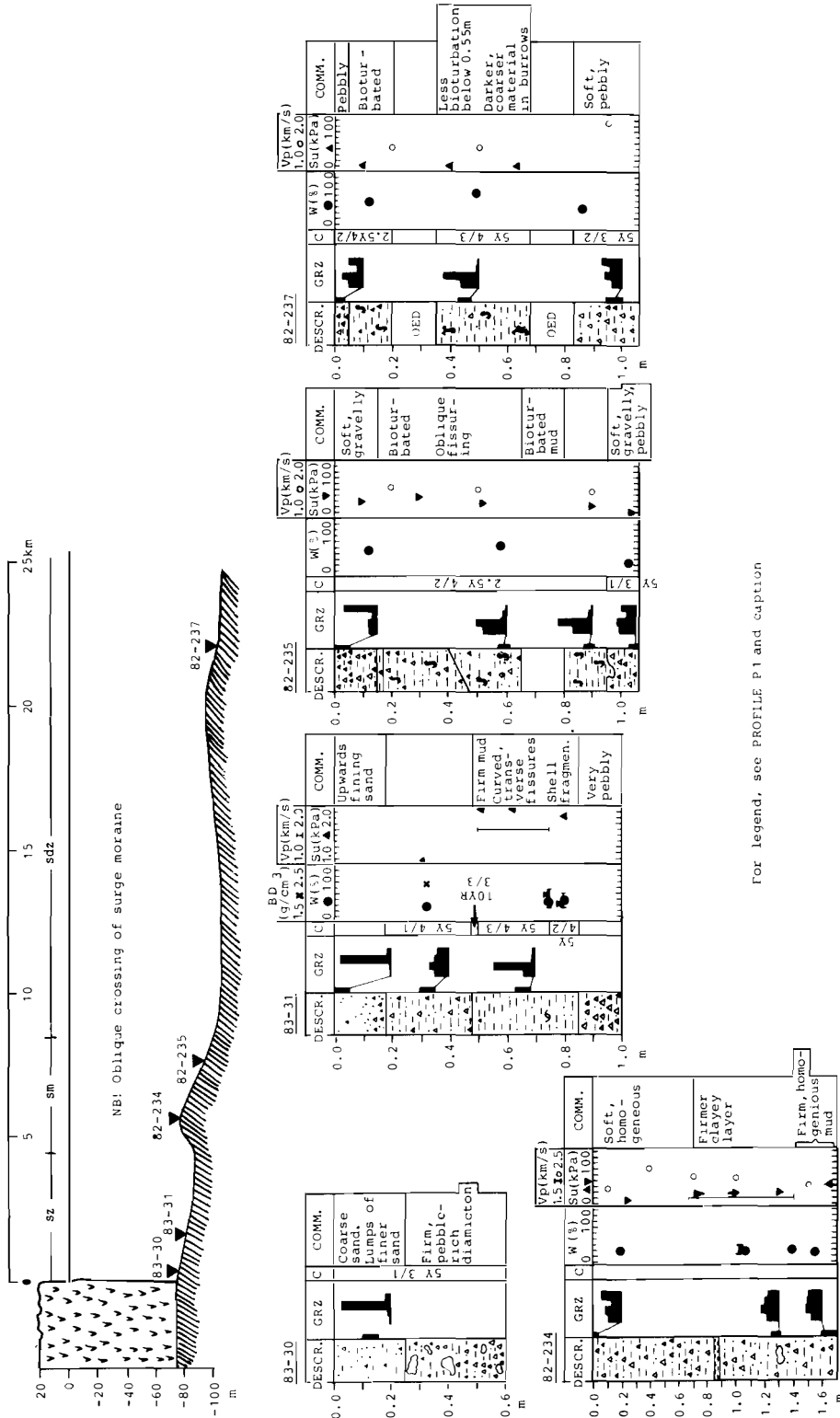
B

For legend, see PROFILE P1 and caption

PROFILE P3



PROFILE P4



For legend, see PROFILE P1 and caption

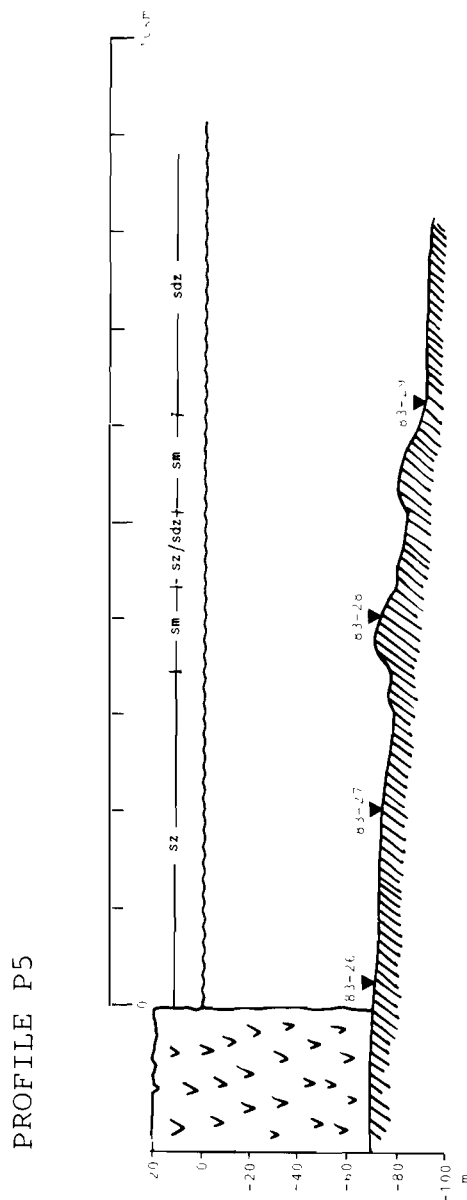
D

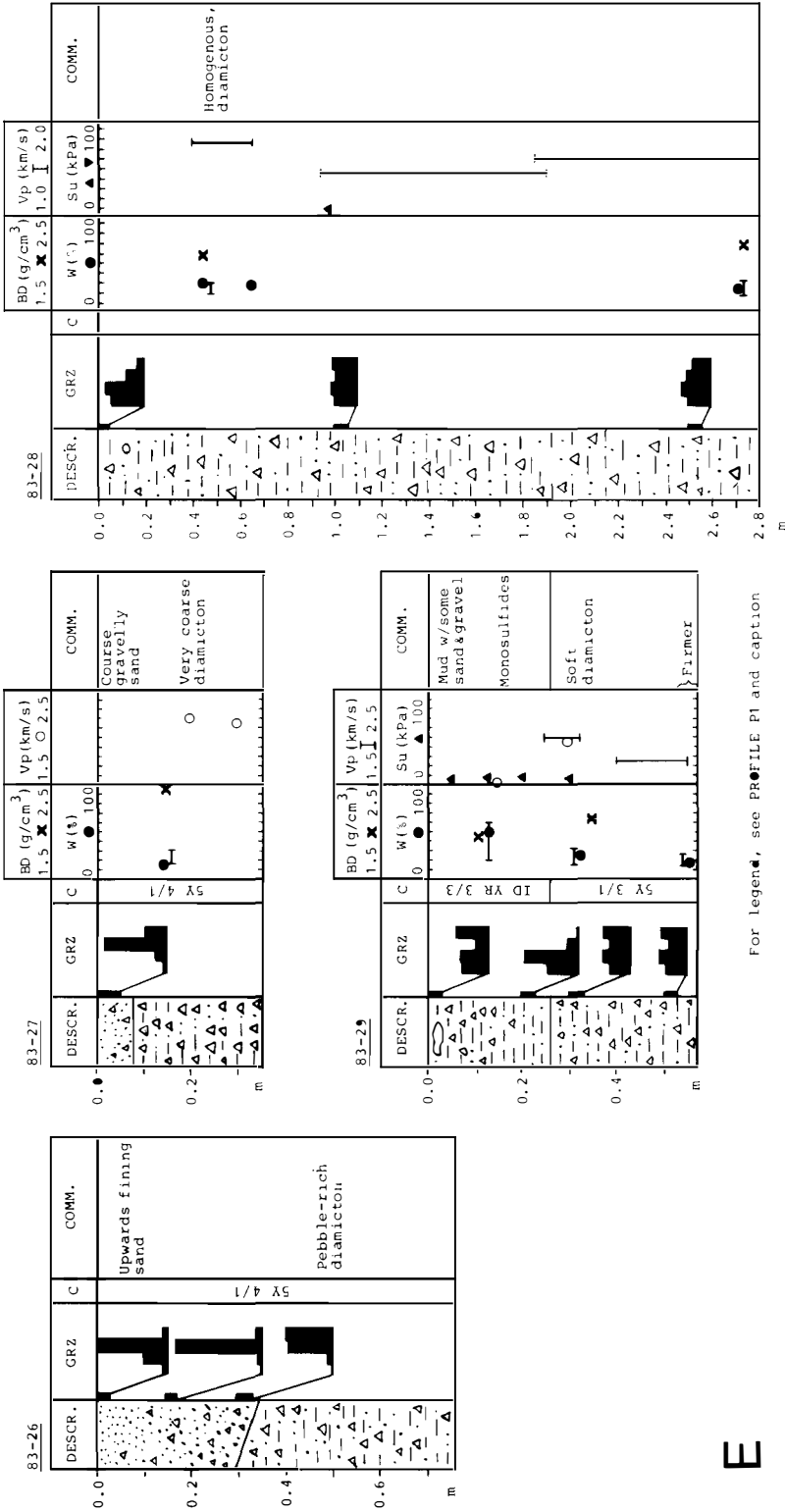
(Fig. 18D), there is a marked increase down-core, but generally no such trend can be identified. However, due to poor sample quality and the relatively few cores from the surge moraine proper, the number of shear strength measurements from this region is sparse and cannot be considered statistically significant.

Shear strengths below 10 kPa (Fig. 21C and Appendix 3) reflect the generally soft, muddy character of the Erik Erikstenstredet sediments outside the surge moraines. One sample (82-226) was strongly overconsolidated, with a shear strength of 110 kPa. This is located in the westernmost part of the study area, where the cover of soft sediments above the assumed Late Weichselian till is thin or non-existent. Material was only obtained in the core cutter and catcher and most likely represents the till.

Bulk density was measured only on the 1983 samples. The values vary between 1.74 g/cm^3 and 2.47 g/cm^3 (Fig. 22 and Appendix 3). Most of the measurements were made on surge zone samples, with only four and three values for each of the other two zones respectively. However, the values reflect to a great extent the lithology and water content. Much of the variation results from the unsorted character of the diamictons. The highest values were obtained in the compacted surge zone diamictons, while the lowest were found in the soft surge-distal muds. The four values from the surge moraine ridge are relatively high, $2.07\text{--}2.17 \text{ g/cm}^3$. This results from the generally coarse-grained lithology of the ridge sediment. Within the surge zone, the lowest bulk densities are found in the compacted fine-grained mud sections of cores 83-31 and 83-32, despite the over-consolidated character of these samples. These findings further reflect the importance of lithology.

The water content of the surge zone material generally falls below 30% (Fig. 23). Correction, for fractions $>0.5 \text{ mm}$ shifts the peak by 5–10%, but values are still low (Appendix 3). The uncorrected values are used in the subsequent discussions. The low values, also for the soft surge zone diamictons, indicate that compaction has rarely reduced water content with more than 10% in the sediments studied. Again, the compacted mud sections of cores 83-31 and 83-32 appear slightly anomalous. The three values measured on this material are the highest in the surge zone



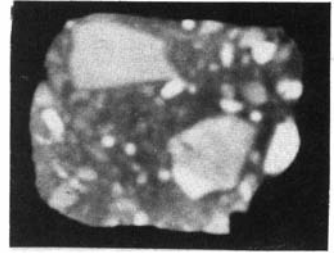
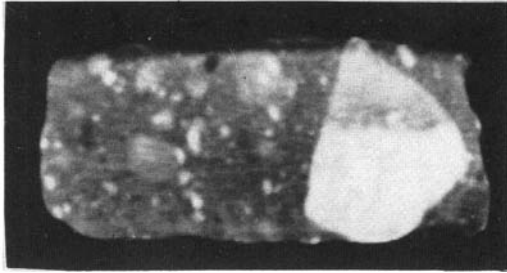


E

For legend, see PROFILE P1 and caption

83-32

83-37



19 36 cm

35 42 cm

Fig. 19. Computer tomographs of two core samples from the surge zone. Note that the highest density has the lightest colour. For location, see Fig. 5C.

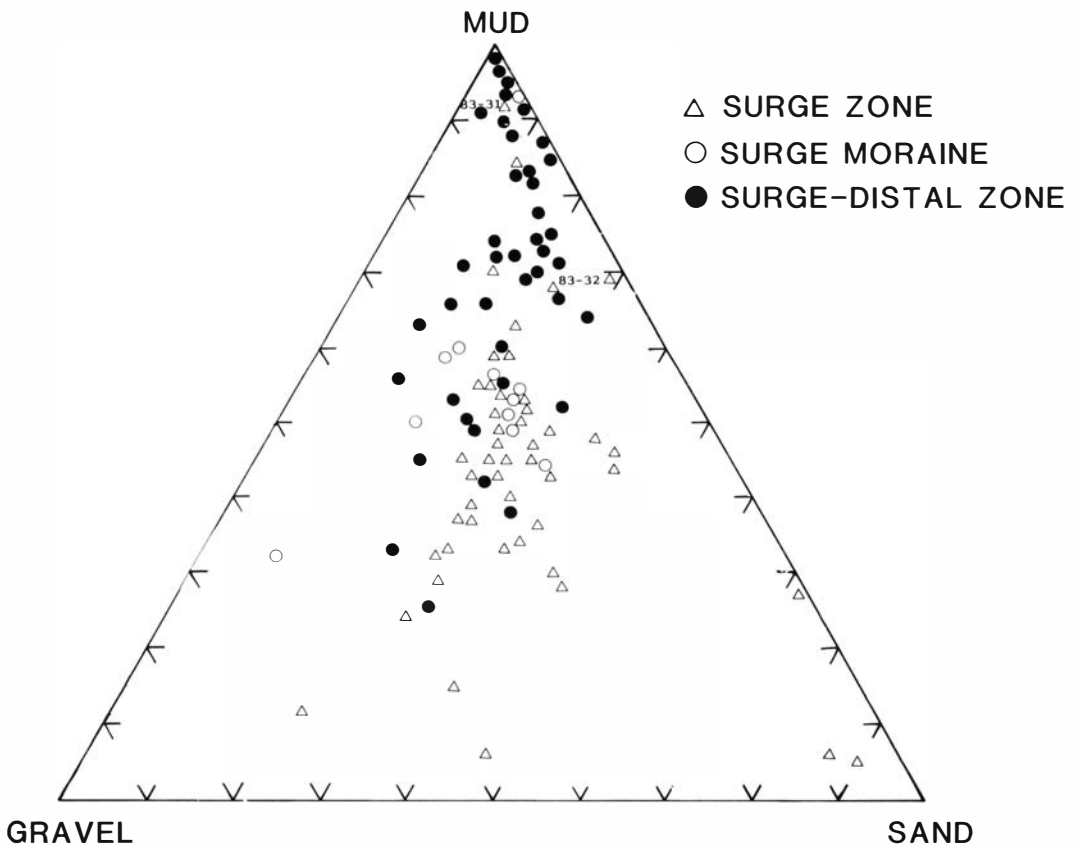


Fig. 20. Ternary diagram showing relative amounts of mud, sand and gravel in samples from the surge zone, surge moraine and surge-distal zone off Bråsvellbreen.

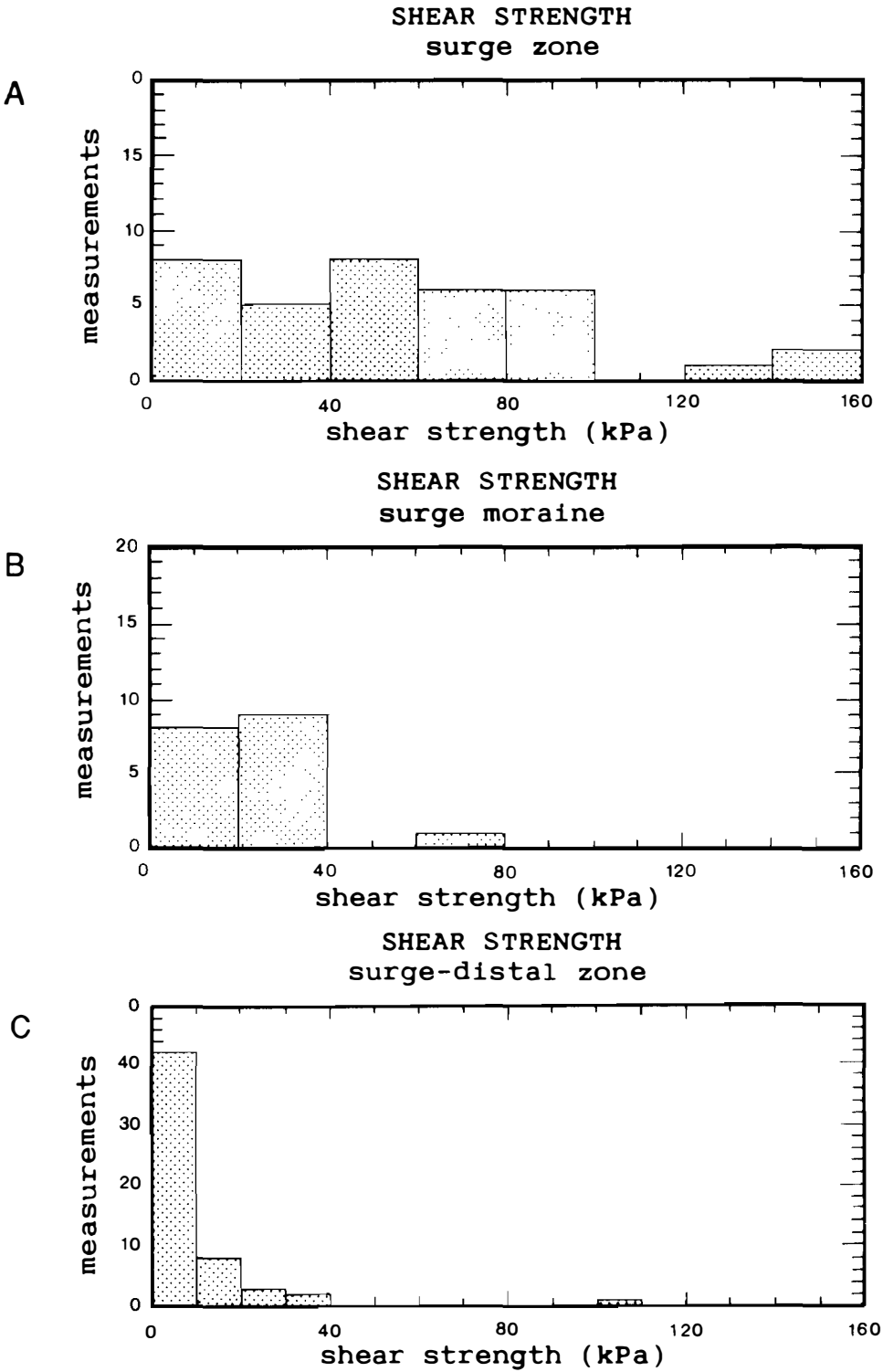


Fig. 21. Frequency histograms of undrained shear strength off Bråsvellbreen (pocket penetrometer and fall-cone) A. In the surge zone. B. On the surge moraine. C. Outside the surge moraine.

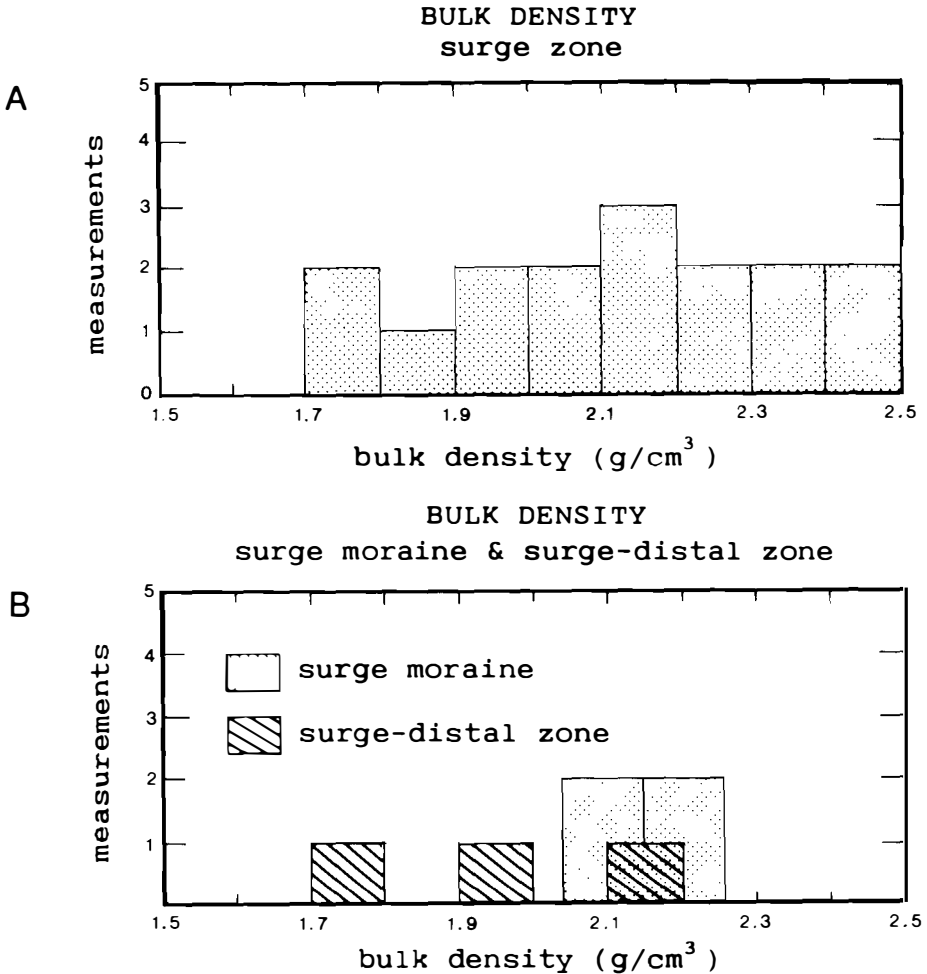


Fig. 22. Frequency histograms of bulk density in sediments off Bråsvellbreen. A. In the surge zone. B. In the surge moraine and surge-distal zone.

(Fig. 18D and Appendix 3), while the sediment is obviously overcompacted.

With the exception of core 82-235 (Fig. 18D), the water content of the surge moraine sediments falls in the same range of values as the surge zone diamictons. The surge-distal sediments, on the other hand, have a larger range of values. Generally they are higher, with a maximum of 73%, which reflects the more fine-grained character of the surge-distal zone sediments.

Compressional wave velocity varies from 1,470 m/s to 2,600 m/s (Fig. 24). Within the surge

zone, where most of the measurements have been made, the bulk of the samples falls between 1,800 and 2,200 m/s. The velocity distribution generally follows no distinct trend as to what sediment type the different velocities can be ascribed to, but the lowest value in the surge zone, 1,573 m/s, is found in the overconsolidated fine-grained mud in core 83-31. This indicates an important effect of lithology in addition to compaction. On the surge moraine, the majority of the velocity measurements are below 1,800 m/s, with only 2 samples of core 82-234 around 2,000 m/s. The surge-distal area again shows some variation, but the bulk of the values fall below 1,600 m/s. The highest

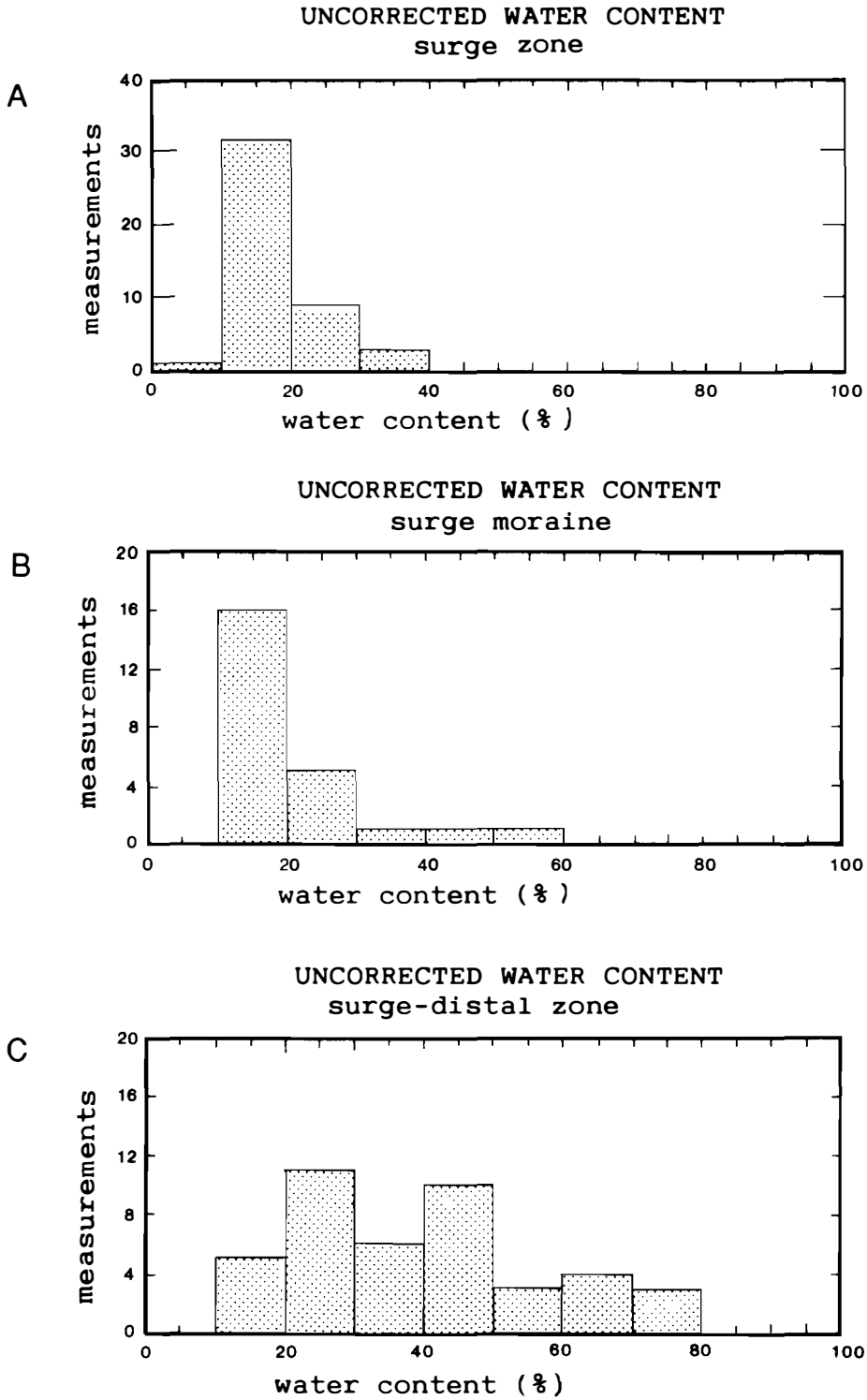


Fig. 23. Frequency histograms of water content, % of wet weight, in sediments off Bråsvellbreen. A. In the surge zone. B. On the surge moraine. C. Outside the surge moraine.

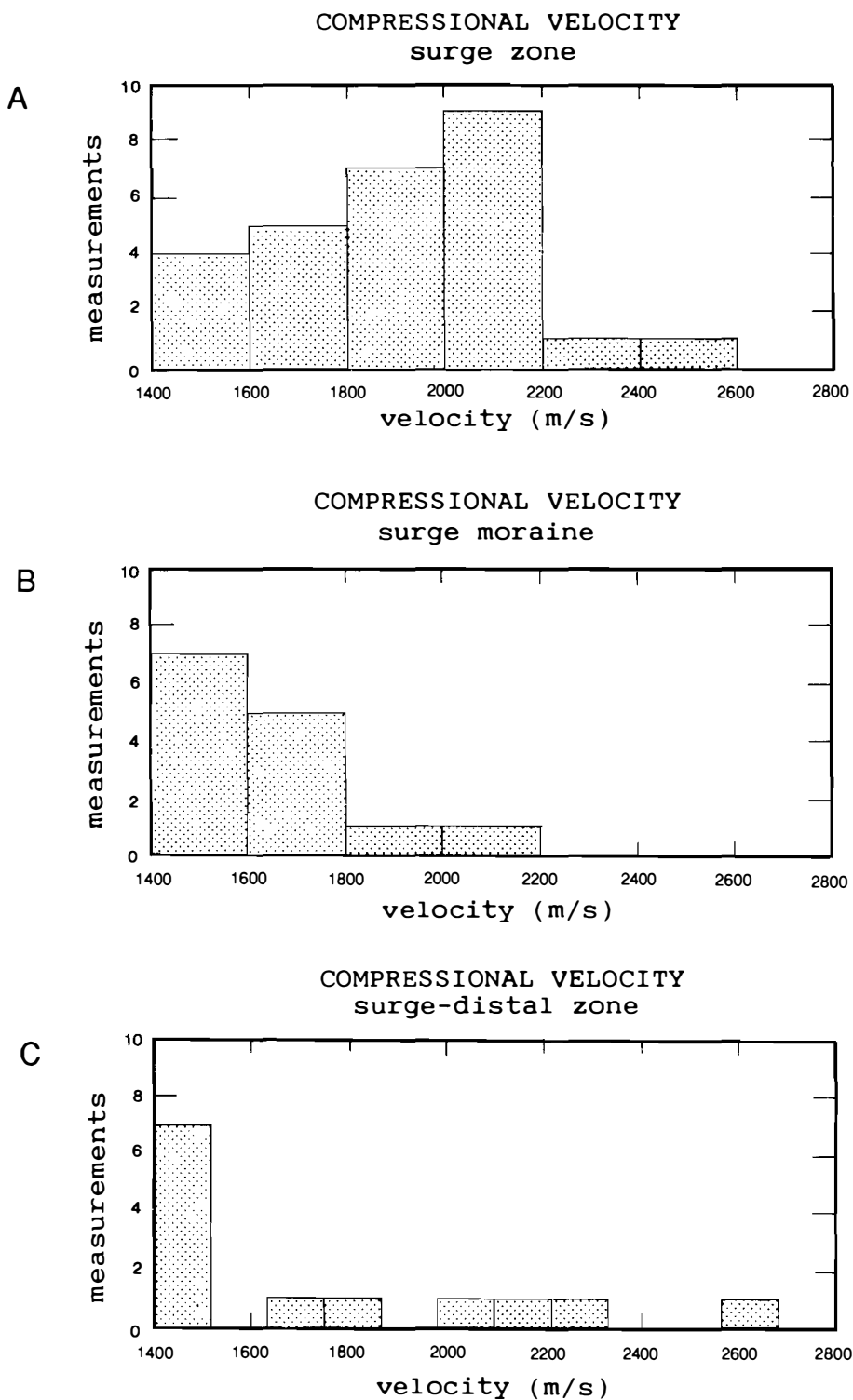


Fig. 24. Frequency histograms of compressional wave velocity in Bråsvellbreen sediments. A. In the surge zone. B. On the surge moraine. C. Outside the surge moraine.

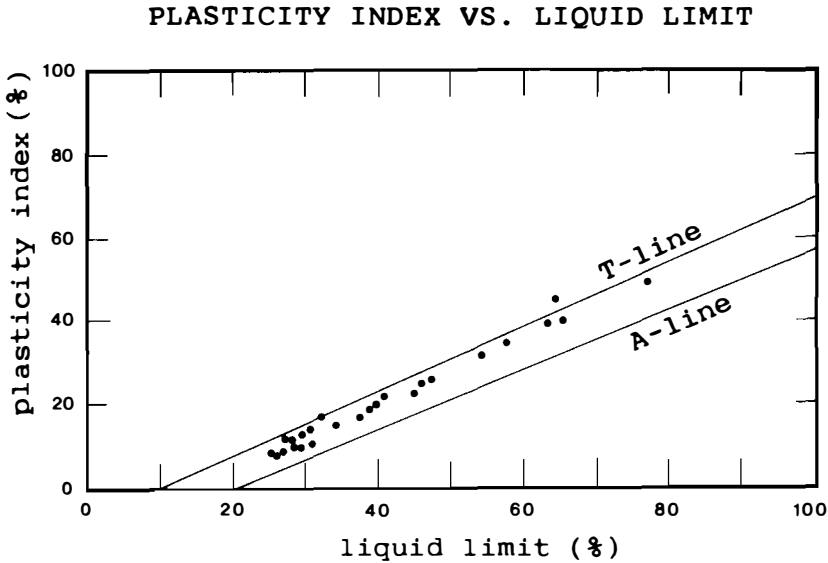


Fig. 25. Plot of plasticity versus liquid limit for sediments outside Bråsvellbreen. The A-line (Casagrande 1948) marks the division between sediments of a broadly inorganic nature (above the line) from those with a significant organic content (below the line). The T-line is defined for lodgement tills from Iceland and Spitsbergen (Boulton & Paul 1976).

values are mostly found in the more gravelly parts of the surge-distal cores, and in particular in the western part. The highest value of 2,600 m/s is measured in overconsolidated, assumed Late Weichselian till (acoustic Unit 5) at station 82-226.

Where measured, the *Atterberg limits* generally embrace the natural water content of the sample, hence showing the weakly to non-overconsolidated character of the bulk of the sediments. In a plot of the plasticity index versus liquid limit (Fig. 25), the Erik Eriksenstredet samples fall above the A-line (Casagrande 1948) as also has been observed on the shelf off mid-Norway (Rokoengen et al. 1980). The Atterberg limits are essentially a function of the type and amount of clay minerals of a sediment. Boulton & Paul (1976) defined a "T-line" (Fig. 25) along which lodgement tills from Iceland and Spitsbergen plot. In general, an increase in clay content will move the sediment towards the right along the T-line, while winnowing of the finest fractions will tend to move the sediment below the line and towards the left. The same effect is found for sediments where the fine fractions to a large degree consist of rock flour (Boulton 1976). The position of the bulk of the samples of this study in the left part

of the diagram most likely reflects fine fractions consisting of rock flour rather than winnowing of fine fractions. The samples are generally characterized by a high proportion of silt relative to clay-sized material, and the entire mud fraction has a large content of non-clay minerals. The same grain size distributions are found in the soft material of acoustic Units 3 and 4, and of Unit 5 where they are interpreted to be of the Late Weichselian basal till.

Relation to the acoustic stratigraphy

Most lithologic variations in the surge zone sediments are too local to be resolved by acoustic profiling systems with near surface source and receiver. Furthermore, the division between soft, normally consolidated sediments and sediments in the intermediate shear strength range (20–100 kPa) is gradational and highly irregular. Therefore, both the soft and the intermediately compacted diamictos, sands and muds are included in acoustic Unit 1. The most distinctive subbottom reflector observed in the 3.5 KHz records is the relatively even, opaque reflector that can be followed under the entire study area. This reflector seems to be exposed locally in

troughs in the surge zone, where stiff, highly overconsolidated material has been cored. Acoustic Unit 5 is therefore ascribed to this material, and it is suggested that the top reflector of Unit 5 is the top of the Late Weichselian till. Where the till is locally absent, the reflector represents top bedrock.

The soft mud cored in the deeper parts of the basin belong to acoustic Unit 3 (e.g. cores 85-26, 28, 84-11 and 13). None of these cores was long enough to identify a sedimentological change that could correspond to the division between acoustic

Units 3 and 4, which is usually found at a depth of 2–3 ms in these areas. However, cores from areas where Unit 3 is apparently non-existent (e.g. 82-237 and 82-321) should represent Unit 4 material. Although the number of samples is strongly biased towards Unit 3, Appendix 2 shows that both 82-237 and 82-321 generally have a higher gravel content than the Unit 3 cores. Thus, from the relatively sparse number of samples, we tentatively relate the difference in acoustic character between Unit 3 and 4 to a difference in gravel content. Similar relationships for acoustic

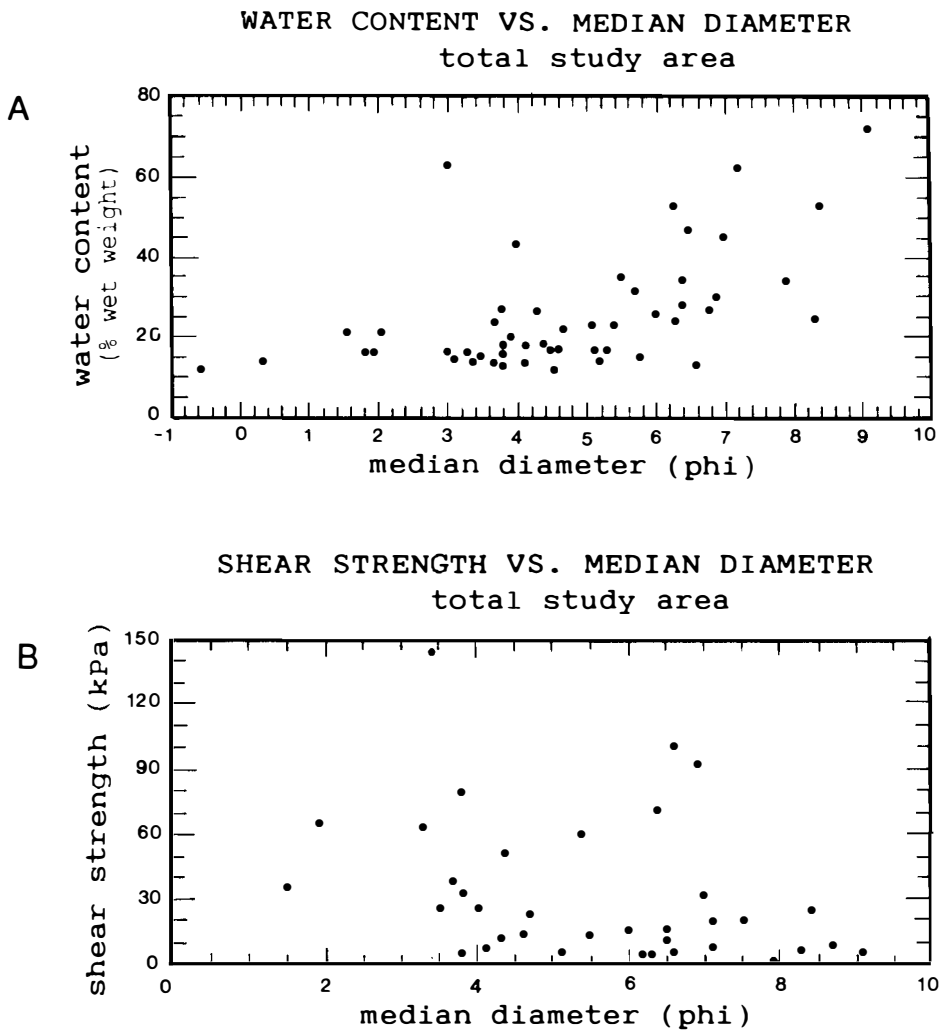
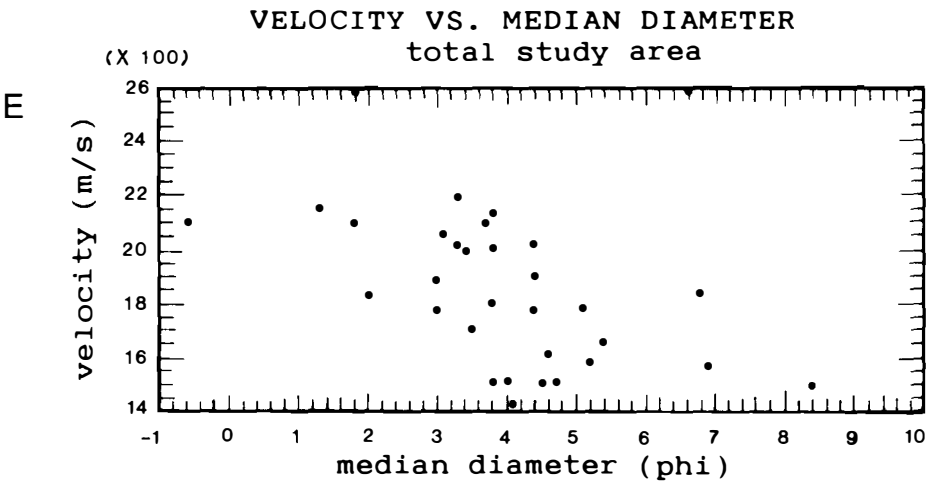
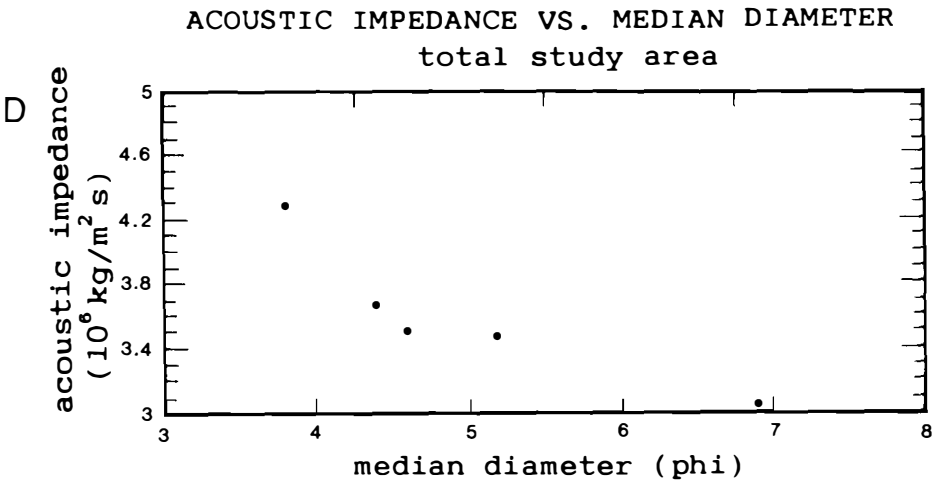
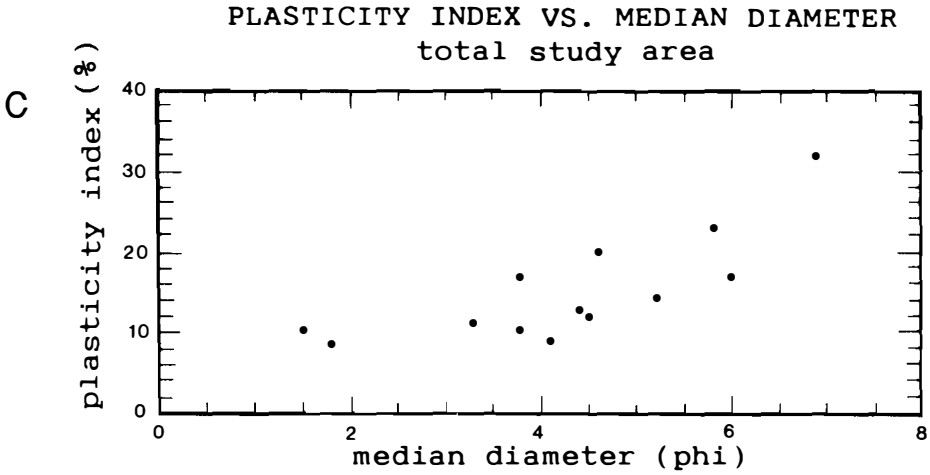


Fig. 26. Physical parameters plotted versus median grain diameter. A. Uncorrected water content. B. Undrained shear strength. C. Plasticity index. D. Acoustic impedance. E. Compressional velocity.



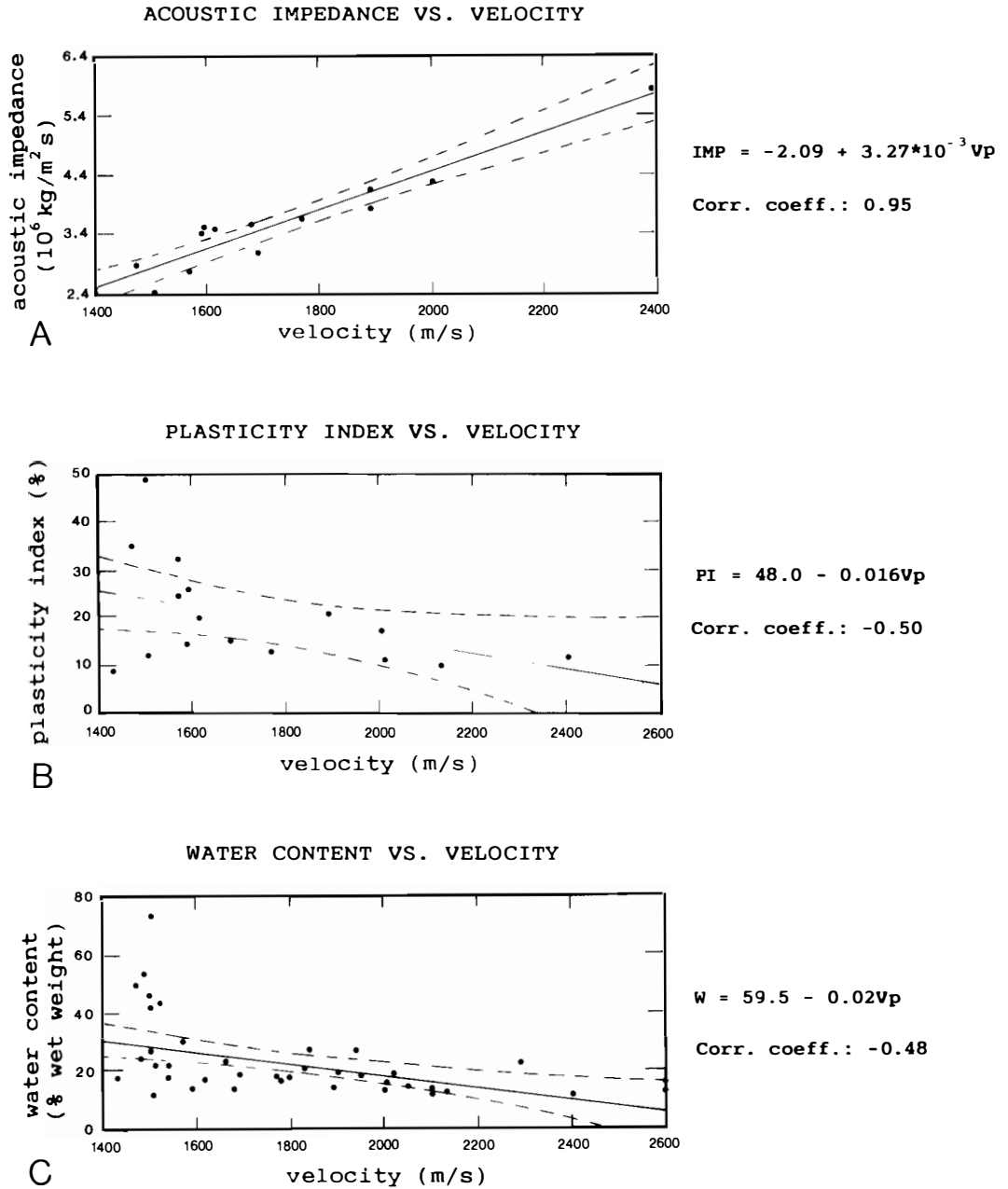
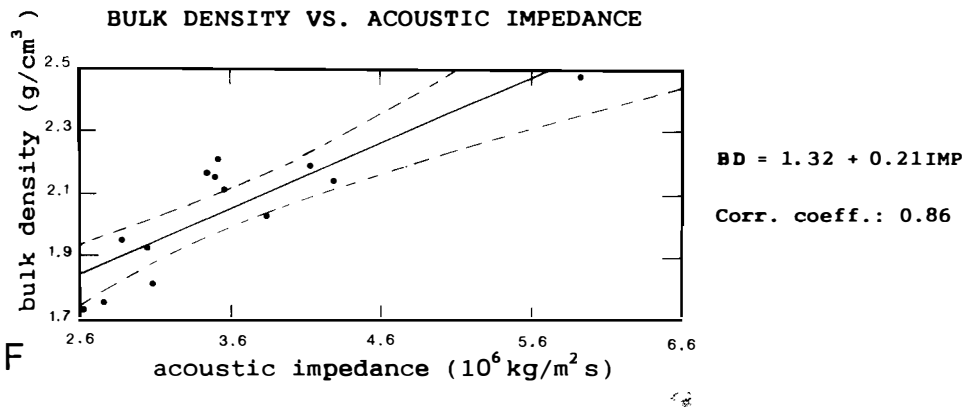
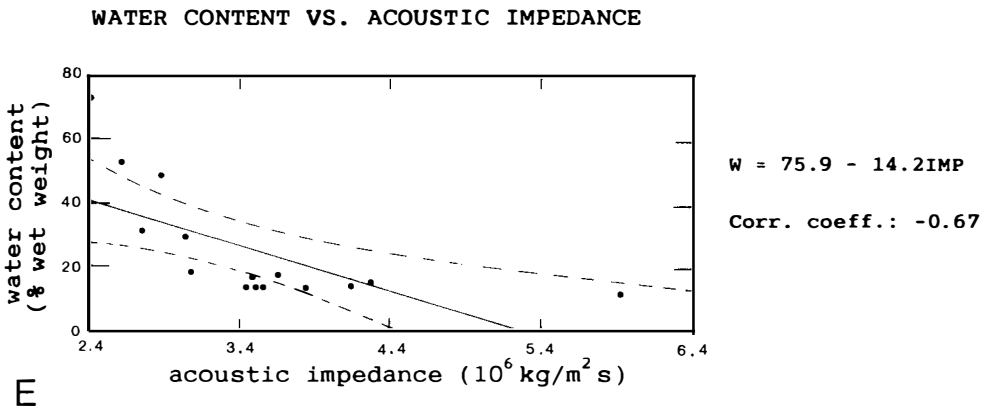
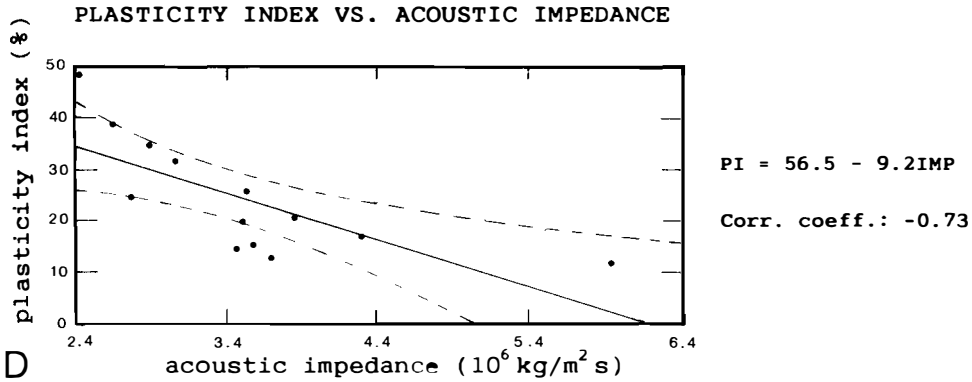


Fig. 27. Correlation between acoustical and other physical parameters. A. Acoustic impedance versus compressional velocity. B. Plasticity index versus velocity. C. Uncorrected water content versus velocity. D. Plasticity index versus acoustic impedance. E. Uncorrected water content versus acoustic impedance. F. Bulk density versus acoustic impedance. Correlation is done by simple, linear regression analyses. 95% confidence limit is shown by stippled lines.



character and grain size distribution were reported by Elverhøi et al. (1983) from the Kongsfjorden area in Spitsbergen.

Parameter correlation

By far the majority of published correlations

between different acoustic and geotechnical parameters are from deep sea sediments (e.g. Akal 1972; Buchan et al. 1972; Horn et al. 1968; Taylor Smith 1975; Hamilton 1974, 1980). This probably results from the more homogeneous conditions found in the deep sea. In the shallow regime, large and frequent changes, both laterally and

down-core, are typical, in particular when the sedimentary sequence is glacially influenced. The establishment of empirical correlations between different parameters is of interest in order to reduce the number of analyses necessary in a geotechnical reconnaissance survey. Relationships between acoustic and geotechnical/sedimentological parameters would be particularly useful. (e.g. Taylor Smith 1975; Bryan 1980).

The importance of grain size distribution for physical properties is shown by plots of different properties versus the median diameter (Fig. 26). All plots have considerable scatter, clearly showing the heterogeneous character of the ice-proximal environment.

The water content (Fig. 26A) is essentially constant for median diameters above 0.016 mm (ϕ_6), and then increases markedly. This demonstrates the greater importance of the fine silt-clay fraction in creating large porosity and hence large water content. Shear strength (Fig. 26B) has a large scatter, and the only trend seen is the tendency of high values for coarse-grained sizes in the diagram. This reflects the predominance of generally coarser material in the surge zone, where the majority of the overconsolidated samples were collected. The plot in general also reflects the source of error that may be involved in shear strength measurements on relatively sandy material. Plasticity (Fig. 26C) should be more or less independent of grain size distribution, as the samples picked for Atterberg limits were sieved through 0.063 mm and the Atterberg limits are mainly a function of the types of minerals present in the clay fraction. The low plasticity observed for the majority of the samples (Fig. 26C) again reflects the dominance of rock flour, giving rise to a less plastic sediment. The linear increase in acoustic impedance with an increasing median diameter (Fig. 26D) (only based on 5 datapoints) is mostly a function of the velocity increase with increasing grain sizes (Fig. 26E). In the velocity plot, the two anomalously high values of 2600 m/s most likely result from larger stones in the measured interval.

Average values for the above parameters are not significantly different from those found in other polar and subpolar shelf areas (e.g. Eide 1974; Løken 1976; Bugge 1980; Rokoengen et al. 1980; Josenhans et al. 1986; Paul & Jobson 1987) for texturally similar sediments, but the values obtained in this study may show a larger scatter. This results from the nature of the sediment, both

the large variability and the fact that this type of material is difficult to analyze due to the high content of gravel and larger stones.

Acoustic velocity and impedance show, despite the variability, a relatively good correlation with other physical properties (Fig. 27). The two acoustic properties themselves correlate with a coefficient of 0.95 (Fig. 27A). Hence, obtaining velocity information from this or a similar area gives a relatively good estimate of impedance. This information in turn can give an indication of the sediment bulk density. Other parameters that correlate reasonably well with the acoustic parameters are the plasticity index and the water content (Fig. 27B, C, D and E). Shear strength, on the other hand, shows very poor correlation with the acoustic parameters (Fig. 28). This was also noted by Buchan et al. (1972), who found better correlation with acoustic impedance by including other parameters (e.g. liquid limit, velocity and grain-size parameters) in a multivariate analysis. The more complex nature of shear strength as a property could then be shown. The present data set is not considered adequate for this type of analysis.

Sedimentation, sediment dynamics and formation of the sea floor morphology off S Austfonna

Derivation of sediments for the surge moraines

Several lines of evidence support the surge moraine origin for the continuous ridge outside the Bråsvellbreen glacier: 1. Photographic documentation of the recent surge; 2. the continuity, which is confirmed by the new, dense grid of acoustic profiles; 3. the cross-sectional shape, characteristic of formation in close contact with an ice front; 4. the marked change in sea floor morphology across the ridge; 5. the decreased frequency of iceberg plough marks inside the ridge, relative to the distal side. However, it now also seems likely that the major part of the ridge is formed through at least two advances, both presumably surges. In the eastern part of Bråsvellbreen, the last (1936–38) surge did not reach as far out as the previous one(s), thus giving rise to two surge moraines. Two evolutionary stages

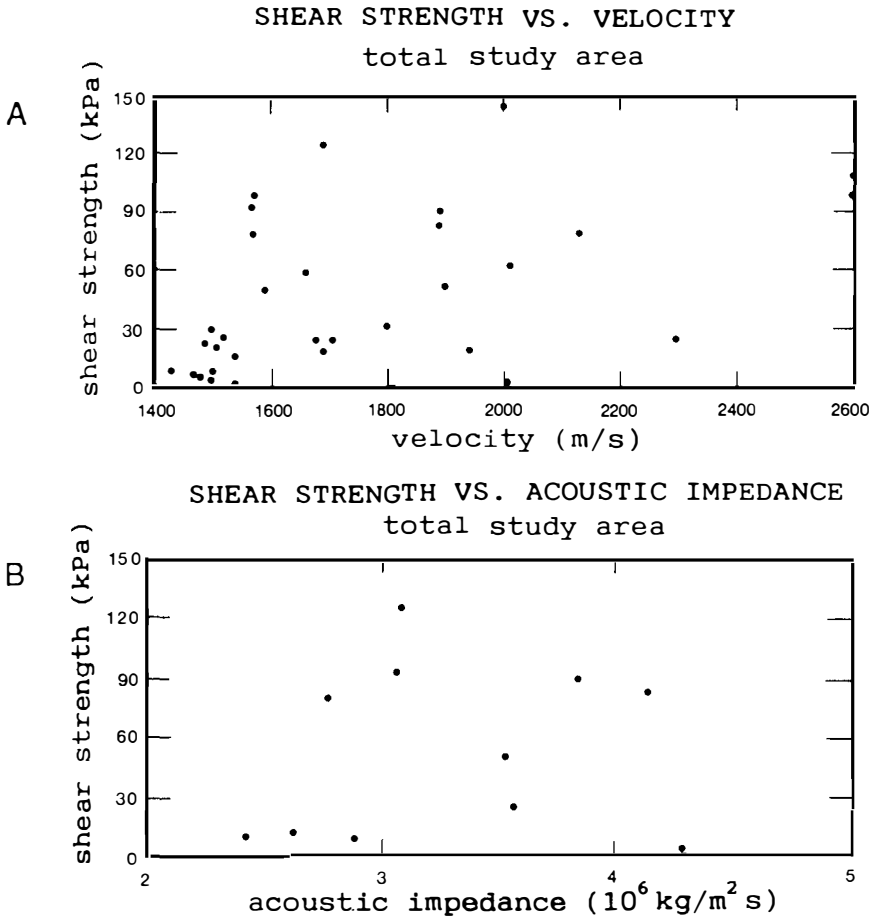


Fig. 28. Plots of undrained shear strength. A. Undrained shear strength versus compressional velocity. B. Undrained shear strength versus acoustic impedance.

in the formation of the morphology in the three zones are shown schematically in Fig. 29.

Two mechanisms may be important for formation of the ridge, deposition from meltwater and ice push. Solheim & Pfirman (1985) argued that both mechanisms were important, and that its final shape was partly modified by slumping, which is obvious several places along the distal parts (Fig. 8). Before addressing the ridge formational mechanism, the availability of pre-surge sediments and how sediments are supplied to the surge zone during surge should be discussed. Two modes are important; transport of debris embedded in glacier ice (subglacial debris) and transport by meltwater.

Subglacial debris.—As the pattern of surge moraine ridges bears evidence of at least one previous Bråsvellbreen surge, the sediment dis-

tribution and characteristics in the surge zone prior to the 1936–38 surge were probably similar to those of today. The situation before onset of the surge activity was most likely similar to that of the surrounding areas at the present: a thin veneer of till above the sedimentary bedrock and a cover of soft, Late Weichselian ice-proximal sediments and Holocene mud with a thickness depending on the time of onset of the surge activity, which is unknown. Previous surges reworked the sea floor sediment, brought in sediment carried in the glacier sole and sediment transported by meltwater. The glacier oscillations formed a pattern of soft and intermediately compacted, topographically irregular sediments similar to those observed in the area today and which were encountered by the 1936–38 surge. As supraglacial input of debris is insignificant on Austfonna, the only source of englacial debris

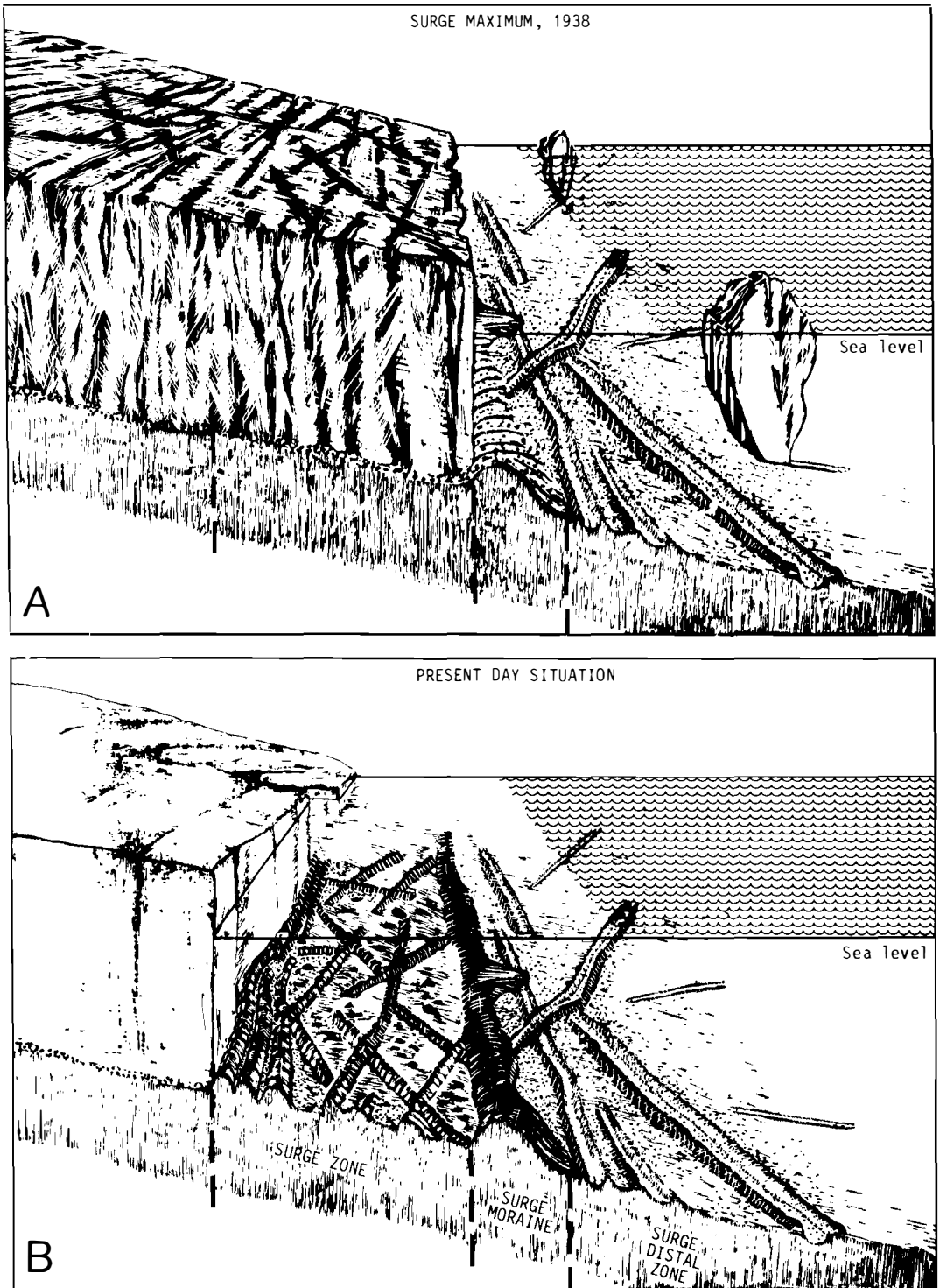


Fig. 29. Schematic model showing the evolution of the surge-related morphology in two stages. A. During surge, with the glacier snout in its maximum position. B. The present-day situation. Note that individual features are not drawn to scale. Drawn to scale, the surge moraine in particular would appear wider in many areas.

is subglacial sediments. These sediments form a debris-rich zone of basal ice, and may, according to Boulton (1970), be brought up through shearing and thrusting, or by repeated folding (M. Hambrey, pers. comm. 1988). The most important factor in supplying material to the surge zone is probably transport of subglacial material along and close to the glacier base. The thickness and concentration of subglacial debris layers may vary considerably (Drewry 1986). Important factors are the temperature regime and the character of the substratum, both of which are largely unknown for Austfonna. Boulton (1972) stated that the debris layer of temperate glaciers usually was thinner than 0.1 m and only exceptionally reached 1 m. Hagen et al. (1986) observed sediment in the lower 4 m of the temperate Bondhusbreen in Norway, but concentrations in excess of 10% of weight were found only in the lowermost meter. Cold glaciers, on the other hand, have thicker debris zones, and 17 m thickness was observed at Camp Century in Greenland (Herron & Langway 1979), while the cold based Foxfonna (Liestøl 1974) in Svalbard had up to 20 m of debris-rich basal ice over large parts (O. Liestøl, pers. comm. 1987). The debris concentrations also showed large variations. Based on literature studies, Pessl & Frederick (1981) suggest an average value of 25% for basal debris bands in temperate glaciers, reaching as high as 30–90% in marginal zones. Clapperton (1975) found that the debris content in surging glaciers on Iceland and Svalbard was higher than in non-surging glaciers. He attributed this to enhanced regelation because of the increased amounts of subglacial water in which increased heat transfer took place. Glaciers that surge over outwash and/or fjord bottom sediments have been observed to become particularly rich in debris (Clapperton 1975).

The considerations above show that the amount of subglacial debris may vary considerably among glaciers. There is also a marked lack of information on sub-polar glaciers. Any estimation regarding the amount of subglacial debris brought to the surge zone would be speculative, but a reasonable assumption would be a 1 m thick layer with a debris concentration of 25%. How much of this sediment contributes to the total sediment volume of the surge zone and the surge moraine is uncertain. The amount deposited in the surge zone depends on the rate of basal melting. Frictional heating during the surge and the fact that the surge covered unfrozen sea floor would

enhance the rate of basal melting. Lodgement processes (Boulton 1975) are here considered to be of minor importance, given the short time that active ice covered the surge zone. Lodgement till would also tend to be more dense and compacted (Lawson 1979) than most of the sediments seen in the area. On the other hand, calving is the most important mode of retreat in this environment, and a significant amount of the subglacial material might also have been carried away with icebergs, and hence not deposited in the surge zone.

Meltwater.—Both theory and field observations indicate high rates of meltwater output during surges (Weertman 1969; Thorarinsson 1969; Humphrey et al. 1986). A significant difference from non-surging glaciers is that in the case of a surge, large amounts of meltwater will also be generated during winters (Kamb et al. 1985). Meltwater has been shown to be a more efficient agent for transport of subglacial material than englacial transport. In a temperate glacier in Norway, a nine-to-one ratio between the two modes of transport has been found (Hagen et al. 1986). Any pre-surge subglacial drainage system or newly formed conduits will constantly be disrupted and changed during a surge. Kamb (1987), in fact, proposes such changes to be a cause of surges. Meltwater would probably be discharged along the entire frontal zone, as opposed to the present-day situation of Bråsvellbreen, where there is only one large meltwater outlet which is located at the very eastern margin of the basin. Disruption and frequent shift of channels would have led to increased release of material from the glacier, as well as erosion of the substratum. With the exception of three cores (83-26, 83-30 and 83-31, Fig. 18D and E) that had well-sorted sand in the upper part, the sediments in the surge zone and surge moraine show no widespread sorting indicative of meltwater action. Hence, from the sediment cores, the main effect of meltwater activity in the surge zone proper during the surge may have been to enhance subglacial meltout and to redistribute bulk sediment volumes without leading to sorting effects significant enough to be detected by the level of sediment sampling during this study. The importance of increased subglacial meltwater activity for the total sediment volume in the surge zone is difficult to evaluate due to lack of diagnostic criteria.

Thorarinsson (1969) noted an increase in meltwater discharge from a surging glacier in

Iceland before the frontal advance proper. The most significant increase, however, occurred when the surge had propagated to the snout and the advance of the ice front started. Syn-surge meltwater activity most likely will transport and deposit relatively high loads of soft, unstable sediments at the front, making more material available for reworking, mixing with the pre-existing soft sediments and push by the advancing glacier.

Surge moraine formation

Pushed material probably forms the major part of the surge moraines. When the advance of the glacier front stops, however, high discharge of meltwater and thus sediment may still continue for some time. A pulse of very turbid meltwater appears to coincide with the end of the surge (Kamb et al. 1985). The acoustically transparent sediment drape of the distal slope of the surge moraine ridge may be a result of this final meltwater pulse, in addition to parts of the pushed sediment, which also may be soft, unstable and susceptible to slumping. This gives rise to the characteristic appearance of the distal part of the surge moraine ridge system (Fig. 6). Although the number of cores from the ridge proper is inadequate for a detailed textural picture of the ridge sediments, the importance of slumping is shown by the unsorted character of all parts of the ridge. The most distal parts may have a somewhat finer grain-size distribution, but the material still encompasses a considerable amount of gravel and larger clasts. Some of this may be dropped from floating icebergs, but it is unlikely to be the main source considering the relatively large thicknesses and short periods of time involved.

Slump lobes are only observed on the distal side of the surge moraines. As the proximal side is steeper, this indicates that the major part of the mass movement took place during a relatively short period of time, when the glacier front was in its maximum position and stabilized the proximal slope. The relatively low slope of the proximal side, compared to slopes of up to 45 degrees of marine push-up ridges in Canada (Lewis et al. 1977), may point toward some slope modification after ice retreat, but direct evidence for this has not been observed. Local steeper slopes may represent true ice contact slopes.

The whole system of sea floor morphologies, including a continuous, terminal ridge, in front of Basin 3 clearly resembles that found in front of

Bråsvellbreen. As there are several indications of a Basin 3 surge, it is considered most likely that the patterns also found here result directly from surge and post-surge activity. This was also argued by Solheim (1986), but only from the few 1984 side-scan lines. The more expanded data set strongly supports this.

The main difference between the surge moraines in the two regions is the relatively less-marked bathymetric expression of the Basin 3 moraine. The proximal boundary is difficult to define, while the distal part shows the same type of acoustically transparent lense character. As it was argued that the Bråsvellbreen moraine mostly resulted from push, but with meltwater supplying sediments to the front, the difference in character may be explained by less efficient push in the Basin 3 region. This explanation is supported by differences in water depths between the two regions. While the Bråsvellbreen moraine is mostly situated shallower than 90 m, the major part of the Basin 3 moraine is between 100 and 110 m water depth. As the size of the drainage basins and amount of advance are comparable in the two regions, buoyancy would have decreased the bulldozing capacity of the Basin 3 surge front to a larger degree than for Bråsvellbreen. Pushed material in shallower water closer to the present-day ice front may be overriden and partly redistributed by the surging glacier when water depth came below a critical value. The low relief character of parts of the Basin 3 surge moraine can be explained in this way.

The rhombohedral pattern

Several indications point towards the rhombohedral ridge pattern having been formed through squeeze-up of sediment into subglacial fractures during and immediately after the surge, as is also suggested by Solheim & Pfirman (1985):

- The ridges show directional trends that match within 10–20° with the crevasse pattern seen from aerial photos of the surface of the surging glacier (Fig. 4B). The surface crevasses show three distinct directions, one roughly parallel to the glacier flowlines and two directions with an angle to the flow lines. All these directions are recognized in the present-day sea floor topography (Fig. 11).
- The pattern is only found proximal to the surge moraines.

- As the ridges forming the pattern have directions at various angles, up to perpendicular, with the ice front, they can not have been formed by push from the grounded glacier. For the same reason, the ridges are not likely to have been formed by deposition from meltwater or direct melt-out along the ice front during its retreat.
- The material forming the ridges is soft and hence not likely to represent a pre-existing till topography.

Terrestrial landforms, also interpreted as having resulted from crevasse fillings, have been described from several regions. Bjørklund (1985) ascribed parallel ridges in Sweden to a process of infill from supraglacial and englacial debris during a phase of glacier stagnation. This ablation type crevasse filling is also discussed by Gravenor & Kupsch (1959) and by Johnson (1975). However, infill from above seems unlikely in the case of Bråsvellbreen, due to reasons discussed in the Introduction. Both the glacier surface and the exposed part of the front appear clean at present.

Gravenor & Kupsch (1959) also discuss Hoppe's (1952) model of sub-glacial squeeze-up. Ridge systems in Canada show similar dimensions and patterns as those of Bråsvellbreen. According to Hoppe (1952), squeeze-up requires that most of the debris is under the ice (little englacial material), and that the subglacial debris is unfrozen (susceptible to plastic deformation). Both these requirements seem to hold for Bråsvellbreen, as the surging glacier moved over glacial and glacial marine sediments.

Sharp (1985) describes ridges in front of a surging glacier in Iceland that most likely result from crevasse fillings. These ridges have directions oblique to the local ice flow directions. They can be followed into the present-day glacier front where they are continuous with the subglacial lodgement till. Found also here are ice structures similar to those interpreted by Hambrey & Muller (1978) to be crevasse traces in a non-surge cold glacier. The ridges are thought to have been formed during the very early part of the quiescent phase of the surge cycle, when the heavily crevassed glacier stagnated and sank into its bed, causing subglacial till to flow from areas of ice overburden into crevasses at atmospheric pressure (Sharp 1985). A similar process has been suggested by Boulton (1972) for flowage of

sediments into cavities on the lee side of large boulders under Svalbard glaciers.

Ordinarily, crevasse depth rarely exceeds 30 m in temperate and subpolar glaciers. In cold glaciers crevasses may reach greater depths (Hambrey & Muller 1978). However, Smith (1976) calculated that crevasses filled with water to a level equal to or greater than 94.6% of its depth can penetrate the bottom of the glacier. Weertman (1973) found a similar value of 97.4%. Water-filled crevasses is most likely to have been the situation for Bråsvellbreen, surging out in up to 100 m water depth.

From the above discussion, a crevasse-fill origin through squeeze-up during the early phase of post-surge stagnation seems likely for the rhombohedral ridge pattern, similar to that found terrestrially by Sharp (1985) in Iceland.

Post surge preservation of the morphology

A major problem with the sub-glacial squeeze-up formation theory is the post-surge preservation of the ridges. An absolute requirement is that later movement in the glacier sole is insignificant, or that the glacier moves completely detached from the substratum. The latter is unlikely as the glacier rests on a deformable till bed. Boulton and Jones (1979) proposed models for glacier flow on this type of substratum, where a large part of the glacier movement was contributed to by deformation of the bed rather than of the glacier. Two preservation modes may be considered if the squeeze-up mechanism is viable:

- Freezing to the bed.
- Post-surge stagnation of the snout.

Schytt (1969) suggested a "cold ring" structure for the Nordaustlandet ice caps in which a core of temperate ice was held in by a ring of cold ice. This is consistent with Clarke's (1976) numerical modelling experiments which indicate that the glacier snout soon refreezes to the bed after a surge of a cold glacier, thereby leading to the quiescent phase.

However the glacier surged out over the unfrozen sea floor, it was severely crevassed and thus possibly allowed the penetration of sea water, at least in the outermost parts. In addition, as will be shown in the next chapter, the front probably withdrew from the zone of the rhombohedral pattern in a maximum of approximately 30 years. It is here considered unlikely that the gla-

acier would freeze to its bed in this situation within the time frame presented. Furthermore, the cores and the seismic data show that the glacier rests on deformable sediment, most likely till, at least 3 m thick. In the case of a frozen bed, the detachment surface for calving of basal ice probably would be somewhat down in the sediment, or at the sediment-bedrock interface. Hence, the frozen bed would have been included in the calving of basal ice, causing significant distortion of the morphological pattern.

From the above discussion, post-surge stagnation, caused by mass deficiency in the accumulation area and not involving freezing to the bed, is considered the most likely mechanism for preservation of the subglacial morphology found in the major part of the surge zone. Retreat took place mainly by calving. The temperature regime during the last part of the post-surge period and at present is uncertain, but this will be briefly discussed below.

The discontinuous, arcuate ridges

Discontinuous, arcuate ridges, which sub-parallel the glacier in the innermost part of the surge zone (Map 2), are features which may have resulted from:

- *push*, probably on an annual basis.
- *squeeze-up*, similar to the mechanism proposed for the rhombohedral ridge pattern.
- *deposition* of englacial debris directly from the ice front or of basal debris from meltwater.
- *impact* by calving icebergs (Powell 1985).

The latter is considered an unlikely mechanism to produce such a regular pattern, although structures that can be ascribed to impact do occur. These, however, seem to be superimposed on the arcuate ridges (Fig. 12). Deposition directly from the glacier does not seem capable of producing ridges of this size, and the action of meltwater would most likely result in more localized accumulations. Squeeze-up is also excluded as a likely mechanism. The aerial photographs from the Bråsvellbreen surge indicate a consistent crevasse pattern normal to the flow lines, but the surface fractures appear straight for relatively long distances and do not show the discontinuous, arcuate character seen on the present-day sea floor.

This leaves annual push moraines as the most likely explanation for these features. Annual push

moraines typically have relatively low relief and occur in groups of several ridges with short interridge spacing (B. Andersen, pers. comm. 1987; Larsen et al. 1988). Both this and the fact that the ridges can be seen to reflect the overall shape of the ice-front support a push moraine origin. Boulton (1986) has described in much detail similar features from Svalbard, Iceland and Canada, both in marine and terrestrial environments. Annual moraines of comparable size are described from Late Weichselian deposits in northern Norway by Sollid & Carlsson (1984). The size of the ridges, however, will most likely vary with glacier dynamics and the amount of material available. Andersen & Sollid (1971) report presently-forming annual moraines with a width of 2–3 m and a relief of <1 m from southern Norway. Price (1970) describes series of short, arcuate ridges in Iceland that are joined together, forming a similar pattern as that found off Bråsvellbreen. Although these are interpreted as annual features, Price (1970) attributes their formation to the squeezing out of water-soaked till from beneath the glacier front, rather than to simple push. Hence, processes are involved similar to those envisaged here for the formation of the rhombohedral ridge pattern. Pebble fabric and a distal slope that is steeper than the proximal are the main arguments for the squeeze-out theory. In the Bråsvellbreen area there are no pebble orientation studies (no oriented cores were taken). The cross-sectional shape shows no significant trend in ridge asymmetry, and no other indications of a squeeze-out origin can be found.

A consequence of the annual push moraine explanation of the ridges is that the Bråsvellbreen front is no longer totally stagnant. Sharp (1984) interpreted similar ridges on Iceland to be annual moraines and used this pattern as a possible diagnostic feature to indicate that a glacier was not a surge-type glacier. If the Bråsvellbreen ridges are interpreted as annual moraines, this will show that surging glaciers also have a period of slight activity, producing small push ridges during the quiescent stage. Although no velocity measurements are available from Bråsvellbreen, a set of crevasses parallel to the present-day ice front indicates slight movement of the glacier. Information from other surge-type glaciers on Svalbard during their quiescent phase further supports this. Nathorstbreen on Spitsbergen, another surging glacier, has been measured to have an average velocity of 10 cm/day at the front, and ridges seen

on echograms from Van Keulenfjorden in front of Nathorstbreen have been interpreted as annual moraines (Liestøl 1976). Pushed sea ice in front of Negribreen, east Spitsbergen, shows that this glacier also advances during the winter (O. Liestøl, pers. comm. 1986). Negribreen is probably the most comparable surging glacier relative to Bråsvellbreen on Svalbard, both in size and surface profile.

The size of individual ridges is dependent on both the amount of readvance of the glacier and the amount of material available for involvement in the ridge formation. Boulton (1986) points to the association between the ice marginal fan complexes and push moraines. Outside Bråsvellbreen, the largest of the push-moraines are found just off the main meltwater outlet, where the largest amount of recent sediment is also expected to be found.

The discontinuity of the push moraines is probably due to the differential movement of the glacier and the varying amounts of material available to form ridges. In the case of large readvances, annual ridges may be destroyed in favour of the formation of larger ones. Side-scan lines from 1982 and 1983 that run along the glacier cover only the innermost 500 m, while the 1984 and 1985 lines normal to the glacier do not run close enough to record the innermost area. The 1982 and 1983 navigation is not accurate enough to merge the two data sets in detail. Thus, we do not have a continuous coverage between the ice front and the proximal boundary of the rhombohedral pattern. However, counting ridges thought to be annual push-moraines along 4 profiles from the ice front and 500 m seawards gives from 16 to 17 ridges. With a maximum width of the arcuate pattern of 1,000 m in the frontal zone of Bråsvellbreen, the major part of the glacier has then been active for the last 17–34 years, leaving a completely stagnant period which lasted for 16–33 years. The criterion for selecting the ridges to be counted was a minimum length of 100 m. Including all smaller ridges, the numbers varied between 24 and 29 over the 500 m distance. In the western, thinnest part of the glacier, however, stagnant conditions still prevail, which is shown by the fact that the crevasse-fill pattern can be followed up to the glacier proper (Fig. 10).

The formation of annual moraines confirms the conclusion that preservation of the rhombohedral ridge pattern requires stagnant ice. When the glacier again resumes normal activity, this pattern

is reshaped into push ridges. This may also give some indications about the temperature regime. The formation of push-ridges implies sliding of the glacier, which is inconsistent with a frozen bed. Furthermore, sediment cores obtained within 100 m from the present-day glacier front (Solheim & Pfirman 1985, and below) did not bear evidence of permafrost conditions. However, extrapolation of temperature gradients measured in shallow boreholes points toward frozen bed conditions (J.A. Dowdeswell, pers. comm. 1988). An explanation may be that Austfonna is a true subpolar ice cap, as proposed by Schytt (1969), but that there is an outer zone of unknown width where non-frozen conditions exist in the contact zone between glacier ice, sediment and sea water. Ice movement mainly takes place then through deformation in the frozen part, but is transferred to a component of basal sliding in the outer, non-frozen part.

The intermediate region

As the same suite of morphologic features—terminal moraine, rhombohedral and arcuate ridge patterns—is also recognized in the intermediate region, the above discussion leads to the conclusion that this region has also been covered by surging ice. This conclusion is in addition supported by the fact that the end moraine in the region merges with the Bråsvellbreen moraine. It has clearly been formed by an advance that also included Bråsvellbreen. A merge with the Basin 3 moraine is not observable from the present data, but from the appearance of the ridges it seems likely that formation of at least the eastern part of the intermediate moraine also involved in a Basin 3 advance. From this we can infer that both Bråsvellbreen and Basin 3 had previous surges that were somewhat more laterally extensive than their last surges. Changes in surge directions of previous advances to cover the intermediate region with surging ice seem unlikely for Basin 3, which is situated in a well-defined bedrock depression (Dowdeswell et al. 1986), but may not be excluded for Bråsvellbreen (Fig. 3B). These questions can not be conclusively answered from the present data base, but the directional trends of the rhombohedral and parallel ridges, although rather inconsistent, seem to indicate both advance and retreat directions sub-perpendicular to the present-day glacier front also in this region.

Both the intermediate moraine ridge and the

Basin 3 ridge have more frequent iceberg plough marks than the Bråsvellbreen ridge. The susceptibility to grounding of icebergs results from the topographic expression of the ridge system, but the relative differences in plough mark abundance clearly reflect the age differences. The intermediate ridge, which is dominated by plough marks, is older than the other ridges, and it has also experienced the large production of icebergs during the latest Basin 3 and Bråsvellbreen surges. The Basin 3 moraine also has more abundant plough marks than the moraine off Bråsvellbreen, due to its longer exposure to drifting icebergs. Nevertheless, most of the surface area of this ridge has been classified as a "mixed morphology", characterized by iceberg plough marks and numerous smaller mounds and depressions (Map 2 and Fig. 9). Sometimes these disturbances appear as 25–50 m wide craters with a circular berm. This pattern is found mostly on the proximal part of the end moraine and immediately inside it, but also in a small area outside the ridge, inside the easternmost part of the intermediate moraine (Map 2). Due to the location of this pattern in the area of an assumed heavily crevassed surge front, it is likely that the disturbed sea floor results from iceberg impact during calving. Powell (1985) has described this effect from the Antarctic. He found that calving icebergs may have a great effect on the sea floor, also without direct contact, because of the preceding pressure wave. On a sloping sea floor, these processes would lead to small-scale slumps and gravity flows.

The surge-distal regions (non surge-related features)

The major part of the study area, outside the surge moraine systems, is characterized by two main classes of sea floor morphology: smooth sea floor with other features and iceberg ploughing, both recent and relict. Iceberg plough mark distribution is governed by iceberg production, currents, local and regional bathymetry and time of exposure of the area to drifting icebergs. The lower depth limit of recent plough marks is approximately 120–130 m. However, outside the Bråsvellbreen surge moraine there is a region with smooth sea floor, i.e. lack of plough marks, despite being shallower than 120 m (Map 2). Comparison with the bathymetry (Map 1) shows that this area matches with a local deep in front

of the surge moraine. The bank south of the gouge-free area has most likely acted as an efficient trap for icebergs drifting in from other areas than Bråsvellbreen. Icebergs entering from deeper waters would have had to adjust their drafts to cross the shallow area and would thus no longer ground in the local trough. Likewise, bergs from Bråsvellbreen would have to cross the surge moraine, and would then float in the deeper trough. Occasional plough marks are also seen on the ridge crest.

In the surge zone outside Bråsvellbreen, as well as outside Basin 3 and the intermediate region, there are generally only few plough marks, the least outside Bråsvellbreen. There are two reasons for this: Firstly, the glacier is grounded, has sparse activity and thus only limited iceberg production. Secondly and more important, this area has only been exposed to drifting icebergs during a relatively short time interval since the last surge. This time interval is shortest for Bråsvellbreen and longest for the intermediate region. In the latter, as well as in the western part of the Basin 3 surge zone, there is a small region of more extensive gouging (Map 2). This again is strongly influenced by bathymetry. The area is shallow, the surge moraine ridges are not well-expressed topographically and they do not efficiently prevent icebergs from entering the area from outside. Furthermore, the shape of the glacier front at Kapp Mohn (Map 1) is unstable and indicates extensive calving.

The plough mark directions (Map 2) are functions of the prevailing current regimes in the region. Close to the mouth of Hinlopenstredet, tidal currents will move bergs both NW and SE. Although there are large calving glaciers further north in Hinlopenstredet, bergs from these glaciers probably do not reach the study area until their size is greatly reduced, due to the shallow sill at the southern end of the strait. The south-westerly flowing current through Erik Eriksenstredet dominates the iceberg transport in the eastern part of the basin, while the combined effect of this current system and the Hinlopen tidal component causes the unsystematically varying directions in the central part of the study area. The tidewater terminus of the Austfonna ice cap is the main iceberg producer, particularly in the surging drainage basins. During main phases of iceberg production, i.e. at the end of and shortly after surges, when the glacier front is in an extended position, strong katabatic winds may

also reach the area and influence the ploughmark direction pattern, at least locally.

As the fossil plough marks are found over the entire study area and down to depths of at least 270 m, these must result from a period with considerably larger icebergs. Since this entire region was glaciated during the Late Weichselian (Elverhøi & Solheim 1983), the fossil plough marks may date back to the period immediately after the retreat of the Late Weichselian ice sheet. Salvigsen (1981) recorded 10 kA old beaches at 100 m.a.s.l. at Kong Karls Land which implies that icebergs with drafts in the order of 370 m may have existed in the region. Variation in the abundance of fossil plough marks are therefore not just a simple function of modern bathymetry.

Other features than the relict, degraded plough marks that appear in the areas of smooth sea floor are pockmarks, "dark spots" and sediment waves. It is now largely accepted that pockmarks are formed by gas ascending through the sea floor, removing fines and preventing deposition, thereby creating a semicircular crater (King & MacLean 1970; Hovland 1983; Solheim & Elverhøi 1985; Hovland & Judd 1988). Because of the close association found between pockmarks and dark spots, a possible explanation for dark spots is that they are pockmarks in an early stage of evolution. No crater large enough to cause an acoustic shadow has been formed, but the fine sediment fractions have been brought into suspension and removed, thereby causing patches of more reflective sea floor. Currents capable of transporting sediment are indicated by the fact that sediment waves (megaripples) (Fig. 15C) exist over a large part of the study area. Due to the fact that Erik Eriksenstredet terminates in sills dividing it from Hinlopenstredet and Olgastredet, the currents forming these features are most likely tidal. Oscillatory movement set up by storm-generated waves could be another explanation for sediment waves at these water depths (Pfirman 1985), but as the area is ice-covered through most of the stormy season, this is considered a less likely mechanism.

Mineralogy and carbon content

Based on outcrops surrounding Austfonna (Lauritzen & Ohta 1984), the Permian calcareous bedrock of the Bråsvellbreen drainage basin most

likely differs from the Heckla Hoek-dominated basins further north. XRD analyses were carried out on a number of samples to investigate if there is a carbonate signal diagnostic of variations in sediment output from Bråsvellbreen.

The main mineral assemblage consists of 14, 10 and 7 Å minerals, quartz, feldspars, dolomite and calcite (Fig. 30). To focus on variations in carbonate content, clay minerals, quartz and feldspar percentages are combined and termed "non-carbonates" (Appendix 4). Analyses were performed on three different fractions: <63 µm, <4 µm and <2 µm. In one sample, 82-229, 40–49 cm, all the silt fractions were also analyzed. Quantification of the diffractograms was done by multiplying the top height with the width at the 50% intensity level (Norish & Taylor 1962). Analyses were first performed on the <63 µm fraction and subsequently on selected samples of the <2 µm fraction. This procedure showed that the calcite and dolomite contents decreased significantly relative to the non-carbonate group of minerals in moving from the coarse silt to clay fraction (Fig. 31). The high dolomite sample 82-229, 40–49 cm shows that the proportion of dolomite decreases more rapidly than calcite with a reduction in grain size. This test showed that carbonates should be present at least in the finer silt fractions, which also could be transported into the deeper basin. The remaining analyses were performed on the <4 µm fraction.

Mineralogy of the surge zone and surge moraine

The general trend (Fig. 32, p. 67) in the surge zone sediments outside Bråsvellbreen is a dominance of calcite, with values as high as 86% in the <63 mm fraction. Dolomite content is lower, with an average of 15–20%. These percentages decrease in the clay fraction, but calcite content still ranges between 32 and 50%. Although the number of measurements is small in each core, there seems to be no systematic down-core change. Considering the unsorted, homogeneous character of the surge zone diamictos, this is also to be expected.

Two surface samples from the surge zone of Basin 3 show only 3–5% calcite and dolomite in the <4 µm fraction, thereby indicating that Basin 3 drains non-carbonate rocks and that calcite is an adequate tracer for sediments delivered from Bråsvellbreen.

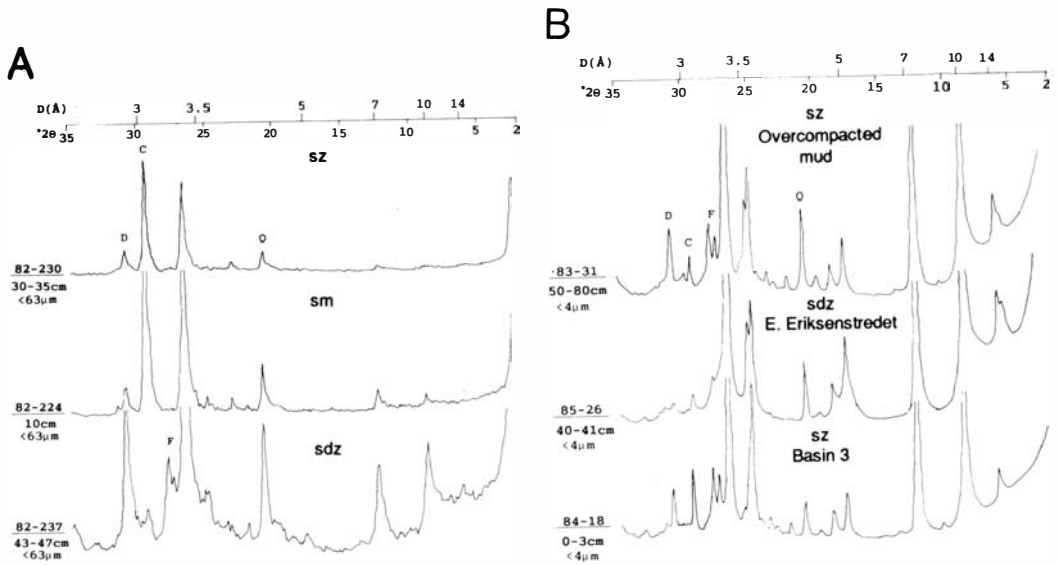


Fig. 30. X-ray diffractograms of some selected samples. A. $<63\ \mu\text{m}$ samples from the surge zone (sz) (82-230), the surge moraine (sm) (82-224) and the surge-distal zone (sdz) (82-237). B. $<4\ \mu\text{m}$ samples. 83-31 is the overcompacted, fine-grained mud found in the surge zone. 85-26 is from the central Erik Eriksenstredet basin and 84-18 is from the surge zone of Basin 3. Note the marked difference to the Bråsvellbreen surge zone sample in A (even when considering the different fractions used in the analysis). For location, see Fig. 5C.

The most anomalous mineralogy found in the surge zone samples is that of the overconsolidated mud sections of cores 83-31 and 83-32 (Figs. 30 and 32, Appendix 4). 92 and 87% non-carbonates in the $<4\ \mu\text{m}$ fraction show that this material has had larger input from other sediment sources than the surrounding diamictons.

Only two samples from the surge moraine ridge have been analyzed. These show carbonate contents of the same magnitude as the surge zone diamictons. From the homogeneous character of the surge moraine cores (Fig. 18), the two samples are considered representative.

Mineralogy of the surge-distal zone

The surge-distal zone shows more variation in mineralogy than the surge zone and the moraine. This might be expected since the sediments in the latter regions are deposited from and in direct contact with the Bråsvellbreen glacier, while further out the Bråsvellbreen sediments are diluted with material brought in with currents, icebergs and sea ice from other source regions.

In the northwestern part of the surge-distal area, overconsolidated diamictons in cores 82-225

and 82-226, apparently similar to the surge zone sediment, show carbonate contents similar to those of the surge zone. Core 82-229, somewhat further east (Fig. 32), shows high calcite content in the top sediment, decreasing downcore, while the dolomite content is considerably higher in the bottom of the core than in the top. This also corresponds with an increase in shear strength in the bottom of the core (Fig. 18C). Thus it seems that the upper and lower halves of this core have experienced different deposition and loading history. Core 83-29, which also is outside the Bråsvellbreen surge moraine, similarly has a high calcite content in the $<4\ \mu\text{m}$ fraction of the surface sample (34%) and in the lower half (34–73%). The 40–45 cm level, which also corresponds to less sandy and gravelly grain size distributions, has only 4% calcite.

There is a general tendency of decreasing carbonate content away from Bråsvellbreen, both southwards (82-237 and 82-321 $>$ 85-26 and 80-37) and eastwards (82-237 $>$ 85-29 $>$ 84-11 and 84-13). The most significant change is in the calcite content (e.g. 80-37, with no calcite throughout the core). Two cores, 82-321 and 85-26, were analyzed in greater detail (Fig. 32). 82-321 shows

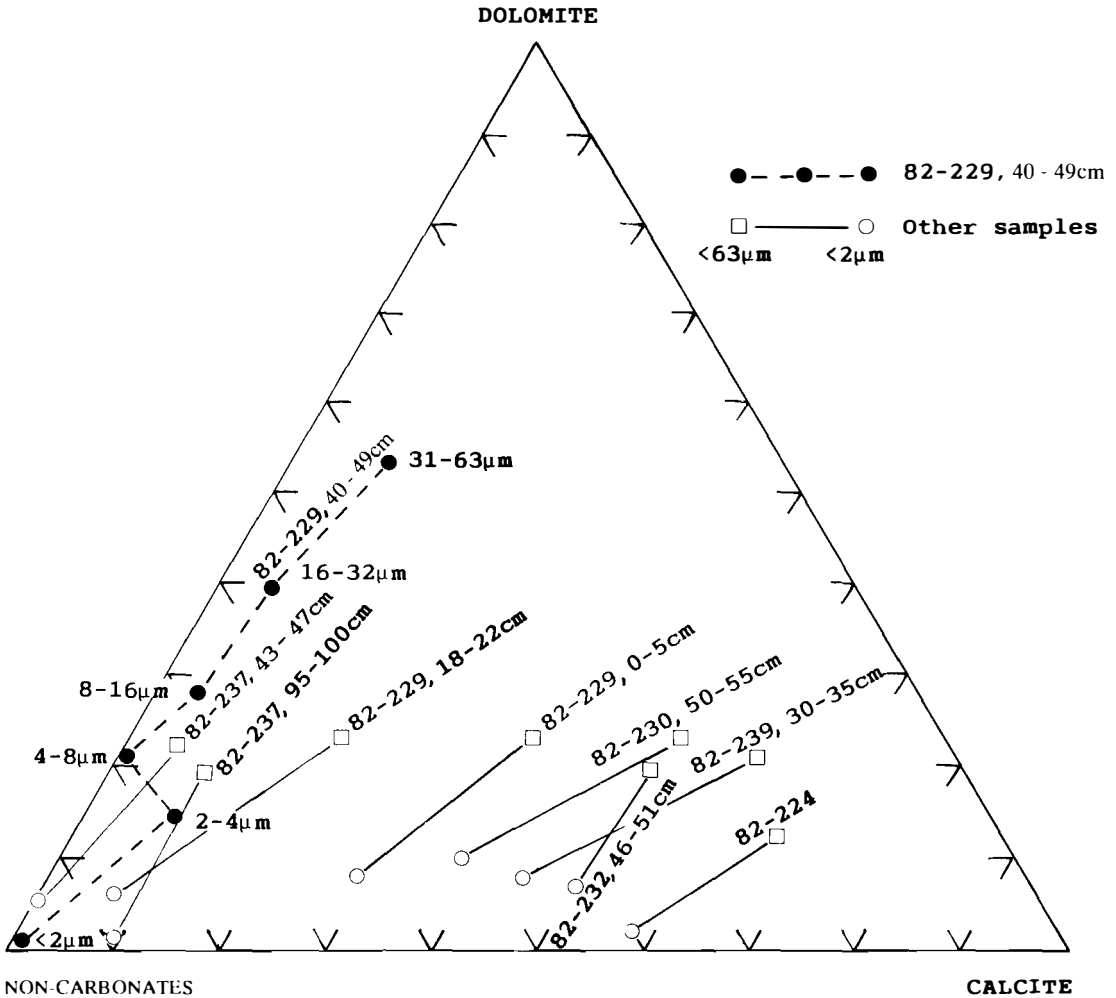


Fig. 31. Ternary diagram showing the variations in Calcite, Dolomite and "non-carbonates" with changing grain size in the <63 μm fraction.

a decrease in both calcite and dolomite from the surface to approximately 20 cm, and then a slight increase again down to 40 cm, the largest changes being in the calcite content. Calcite content is zero in the upper 13 cm of 85-26. However, the surface sediment was lost for this core during retrieval of the liner (Martinsen 1985). It then varies in the 1–3% range before steadily increasing to 12% in the lower part of the core. Dolomite is 4% in the top and decreases to zero at 46 cm. Core 85-29, which is the core east of Bråsvellbreen that is closest to the end moraine, shows a calcite minimum in the interval 20–60 cm, increasing to around 10% in the lower part of the core. The

remaining of the eastern cores, 85-28, 84-11, and 84-13 seem to have a small calcite increase below 20 cm.

Conclusion

The above discussion shows that carbonate content, in particular calcite, can be used as a qualitative indicator of sediment input from the Bråsvellbreen drainage basin. While the generally homogeneous surge zone and surge moraine cores show little systematic variation in mineralogy, several cores in more distal locations show similar trends of variation that may be ascribed to vari-

ations in Bråsvellbreen sediment yield. This signal, although possibly filtered due to under-sampling and bioturbational mixing, may hence give indications of previous surges or periods with varying surge frequency, and of the possible effects of these on sedimentation rates, if used additionally to dating.

Carbon content

The total carbon content (TC) of the surge zone and surge moraine material is generally high, around 6% (Fig. 33, Appendix 3). Except for the assumed Late Weichselian till in core 82-226, the values are lower in the surge-distal zone, 2.5–4.7%. For the total organic carbon (TOC), the values are generally small in the surge zone and the surge moraine samples, with the majority between 0.4 and 0.8%. In the surge-distal zone, on the other hand, values are between 0.9% and 2.0%. The above numbers show that in the surge zone and surge moraine, the majority of the carbon results from carbonate minerals transported from the Permo-Carboniferous bedrock of the adjacent parts of Nordaustlandet, and that this amount is reduced relative to the organic carbon in the more distal parts of the basin. As most of the carbonate is found in the silt fraction, the difference is a function of transport distance, in addition to increased dilution by sediments from other sources than the Bråsvellbreen drainage basin, in the distal areas. This is further demonstrated by plotting TOC and TC versus median grain diameter (Fig. 33B). The TC value drops off in the fine end of the plot, while the opposite is true for TOC. Both changes in slope occur at approximately φ 4–6. This demonstrates the importance of this grain size boundary; most of the carbonate rock fragments occur mainly in the fractions >0.016 mm. This is in accordance with the results of Vagners (1969) and Dreimanis & Vagners (1971), who found that the “terminal grades” after glacial comminution were centred around φ 6 for calcite and from φ 4 to φ 6 for dolomite. The organic carbon is found mainly in the fine silt and clay fractions, although the increase at this grain size may also partly result from lack of dilution by the rock fragments.

The organic carbon may be either primary or redeposited. TOC values for Late Weichselian sediments in the Barents Sea are mainly found to consist of reworked, Mesozoic coal, and dark

shale fragments, while Holocene sediments may contain significant amounts of recent carbon (Forsberg 1983). Primary production decreases considerably northwards in the Barents Sea, and is an order of magnitude less at 80°N than in the area of the oceanic polar front at approximately 74°N (Rey et al. 1987). However, the variation should not be significant within the study area. There are few sources for organic carbon on Nordaustlandet. Hence, whereas the TOC values in the more proximal regions may represent mostly primary carbon, the increased values in the surge-distal zone probably reflect increased influx of recycled carbon, for instance from Mesozoic coal beds in Kong Karls Land.

The most distinct deviation from the trend described above is again the compacted mud sections of surge zone cores 83-31 and 83-32 (Fig. 33A). These clearly fall within the highest TOC values measured in the surge-distal zone. However, the number of analyses in surge-distal samples is too small to give a representative average for this region. A better comparison is provided by average values for Barents Sea Holocene muds, which show comparable values, in the range of 1–2% (Elverhøi et al. 1989). Among the surge-distal zone samples, the most comparable in appearance is the muddy mid-section of 82-237 (Fig. 18D), which again is similar to northern Barents Sea Holocene muds, both in terms of color and grain size distribution.

Sedimentation rates

Whether the surging behaviour of glaciers has any effect on sedimentation and sedimentary processes outside the region directly influenced by the glacier is an important question in the interpretation of older sequences and formerly glaciated areas. A main problem in Erik Eriksonstredet, and also for the rest of the northern Barents Sea, is to obtain datable material. Seven samples have been dated from the study area (Fig. 34). Three samples have been dated by conventional ^{14}C techniques (Lab. ref. T, Fig. 34), while four samples were dated by accelerator methods (Lab. ref. Ua, Fig. 34). Datable shelly material is rare, and to obtain a sufficiently large sample of foraminifer tests it is necessary to use all individuals from a relatively large interval (Fig. 34). Resolution is therefore limited. For statistical

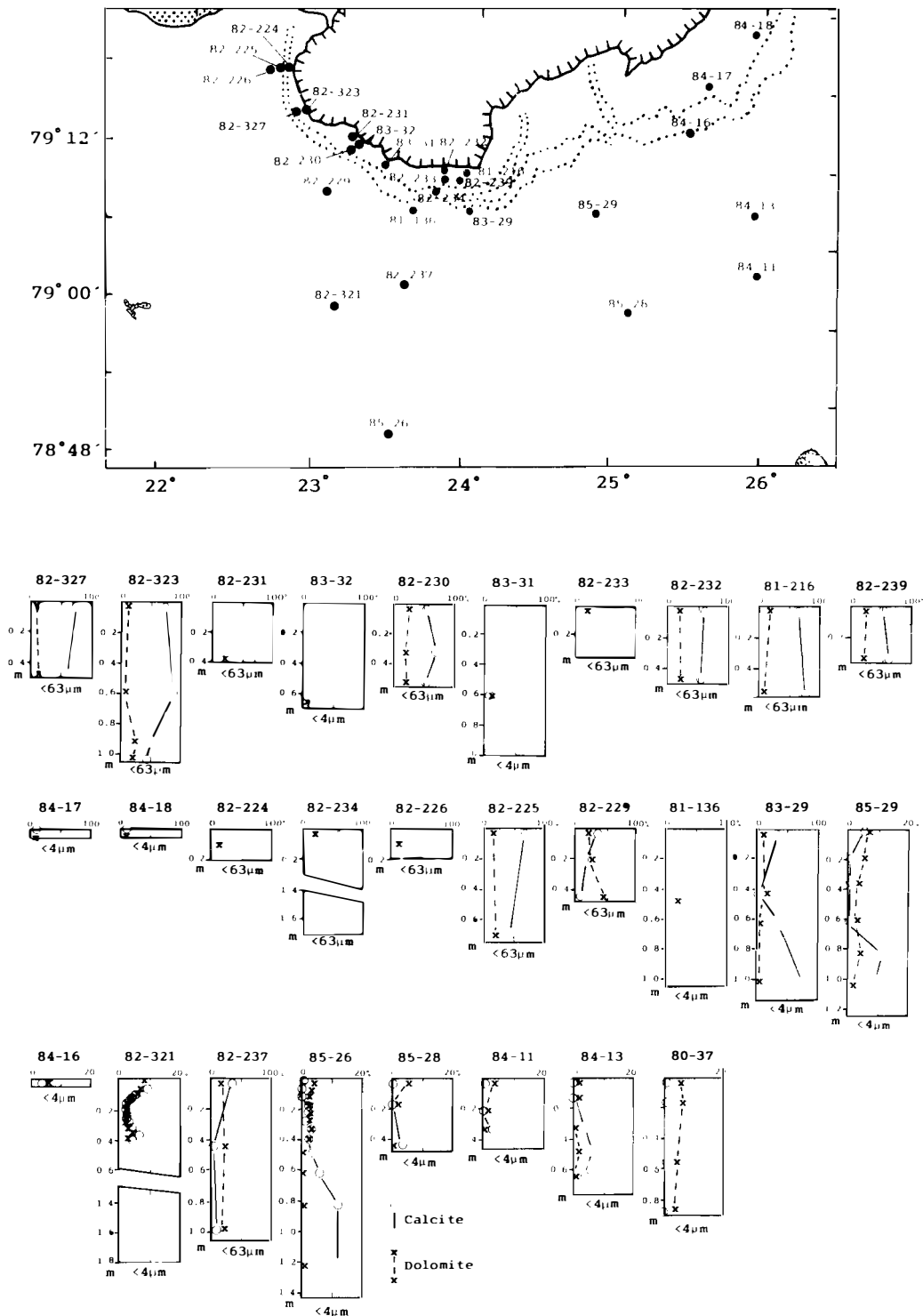


Fig. 32. Calcite and Dolomite content in all analysed samples. Note variable horizontal (%) scale in the lower two rows of cores.

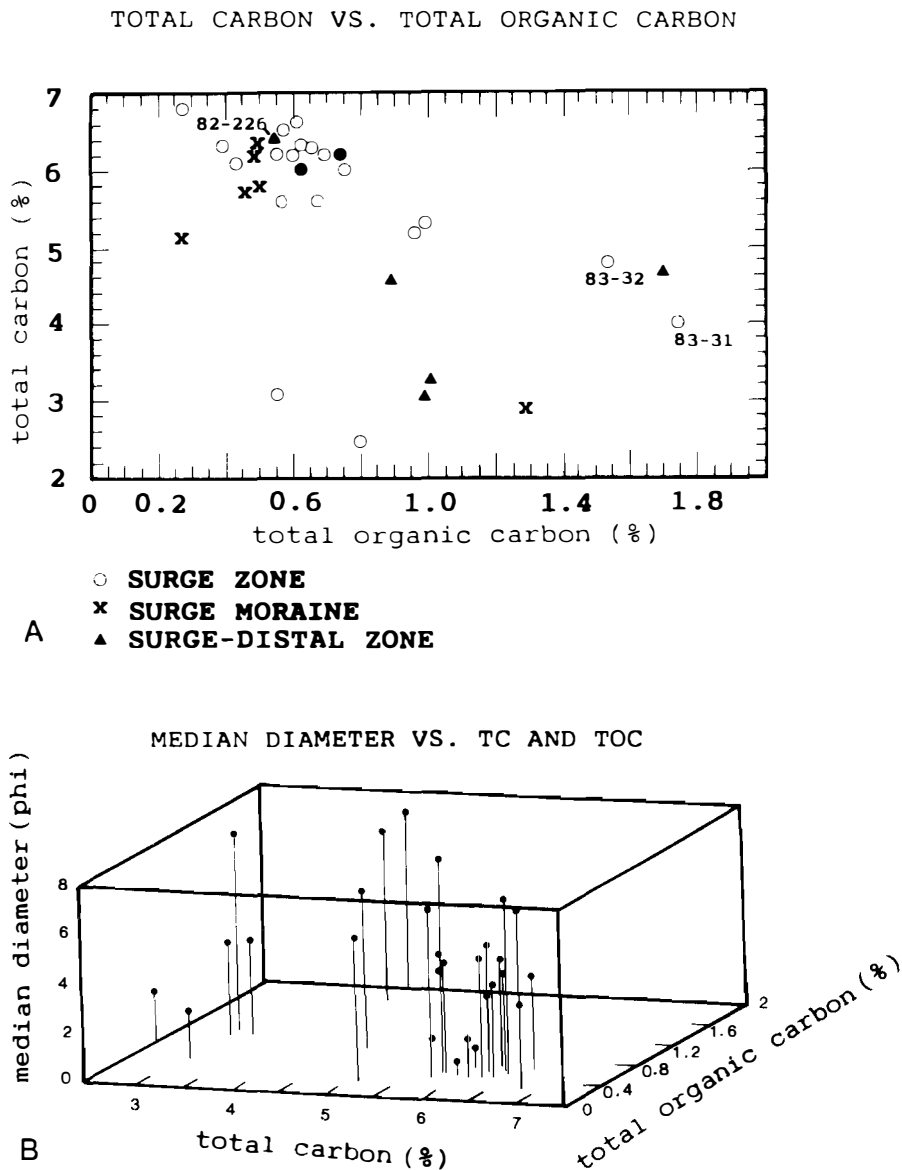
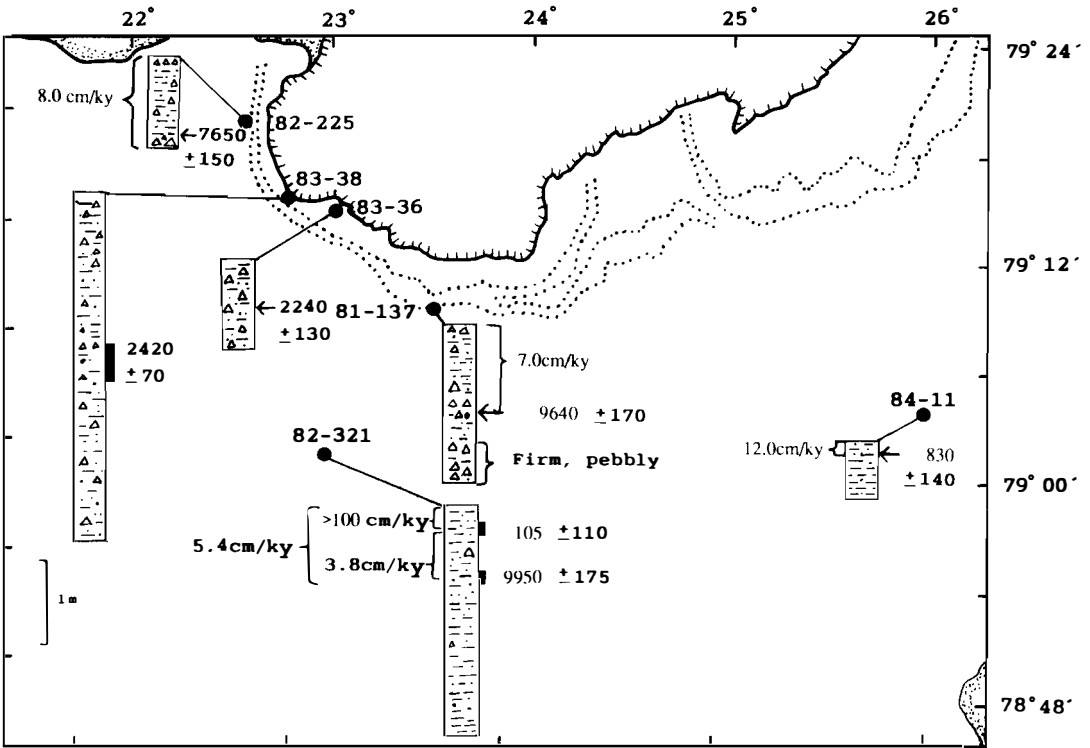


Fig. 33. Carbon content is used as a qualitative indicator of sediment input from the Bråsvellbreen drainage basin. A. Plot of total carbon (TC) versus total organic carbon (TOC). B. TC and TOC plotted versus median grain diameter.

significance a larger number of analyses would be necessary, but some inferences can be extracted from the obtained dates in terms of sedimentation rates.

The two dates from the surge zone (cores 83-36 and 83-38) are both shell fragments from diamicton in the intermediate shear strength range,

previously interpreted to result from reworking and loading by the surging glacier. Due to the reworking, the dates only give a maximum age for the sediment. The dates thus confirm that this is not Late Weichselian (or older) till, but sediment resulting from advance(s) since approximately 2,300 y.B.P.



Core	Level	Lab.ref.	Material	¹⁴ C age
82-225	61cm	T-5234	Mya truncata unruptured	7650 ± 150
83-36	36-38cm	T-5830	Shell fragments	2240 ± 130
83-38	120-150cm	T-5829	Shell fragments	2420 ± 70
81-137	68cm	Ua-302	Portlandia arctica life position	9640 ± 170
82-321	13-20cm	Ua-300	Astarte sulcata 1 valve	105 ± 110
82-321	50-58cm	Ua-301	Foraminifera	9950 ± 175
84-11	10cm	Ua-303	Portlandia arctica life position	830 ± 140

Fig. 34. Table of dated samples and map showing cores with ¹⁴C dates and calculated linear sedimentation rates. Bulk densities are not taken into consideration. All ages have a 440 years correction for reservoir effects.

In the two innermost cores in the surge-distal zone (82-225 and 81-137), sedimentation rates of 8.0 and 7.0 cm/ky (Fig. 34), calculated down to the dated intervals, are somewhat higher than the average 2–5 cm/ky Holocene rates reported by Elverhøi & Solheim (1983) for the central Barents Sea. However, given all the uncertainties and the fact that there are great local variations in the Barents Sea, the two rates compare with the higher of the Barents Sea sedimentation rates. As the highest rates, 8 cm/ky in 82-225, only range back to 7,650 y.B.P., there could be a trend towards increased rates with decreasing age. It should be noted, however, that core 82-225 is located in an area which most likely is strongly affected by recent iceberg gouging. 81-137, on the other hand is located in a smooth region, where no, or very little, ice gouging has been detected. Core 82-321, which is further away from the glacier and in a region without apparent recent iceberg ploughing, shows large variations in sedimentation rate with time. The uppermost age of 82-321 may be considered as near recent. Assuming that the dated shell represents the correct sediment age, the recent sedimentation rates in this area are then very high. The total average for the last approximate 10,000 years is 5.4 cm/ky since 10,390 y.B.P., which is lower than in the two cores discussed above, 82-225 and 82-137. Thus considerable variation in sedimentation rates may be undetected due to undersampling. Core 84-11, further east and away from the coast (Fig. 34), has a sedimentation rate of 12.0 cm/ky back to 1,270 y.B.P. at the 10 cm level. Variations corresponding to the high rates during recent times in core 82-321 are therefore unlikely to have occurred in this region.

Considering the location in the vicinity of a surging glacier, it may be justified to relate variations in sedimentation rate to oscillatory glacier behaviour. Increased input from the Bråsvellbreen drainage area to central parts of the basin, which also receive sediment from other sources, should result in a carbonate increase. The upper 40 cm of 82-321 was analyzed at intervals of 2–3 cm (Fig. 32). Both calcite and dolomite fall from relatively high values in the top to a minimum between 16 and 27 cm before they rise between 27 and 36 cm and then drop down a little to 40 cm. The high values in the upper part correspond well with the increased sedimentation rate calculated for this interval. The curves are smooth, and no feature indicative of single surge

events can be identified. However, mixing through bioturbation will most likely mask separate signals. It is therefore probable that surges or periods of increased surge activity are marked by intervals of higher carbonate, such as the increase below 27 cm. Similar down-core distributions of carbonates are also recognized in other cores (Fig. 32), although not as distinctly for both calcite and dolomite as in 82-321. Most of the other cores have a less dense sampling interval.

In summary, surge activity may have a significant effect on sedimentation rates over short time intervals. The resulting sediment layers are relatively thin, however, due to the short time intervals involved. Averaging over longer periods, for instance the Holocene, the effect in the case of Bråsvellbreen seems restricted but could be significant if there were periods of more frequent surging. A likely scenario could be that most of the deposition off Bråsvellbreen took place during the surge periods, with significantly lower rates in other periods.

Extrapolating the mean sedimentation rates downwards from the oldest dated interval in core 81-137 gives an age of 12,500 y.B.P. for the top of the firm, pebbly material (Fig. 34) of acoustic Unit 5, interpreted to be the Late Weichselian till. This implies deglaciation of the region at this time. Core 82-321, on the other hand, has at least 1.2 m of soft, pebbly mud below the oldest dated interval of 9,950 y.B.P. Possible explanations for this are:

- a) The area was not covered by grounded ice during the Late Weichselian.
- b) Sedimentation rates were higher than in the area of core 81-137.
- c) The thickness of soft, pebbly mud is due to down-slope mass movement.
- d) The date in 82-321 is erroneous, due to mixed ages of the dated foraminifer tests.

Based on previous discussions on the existence of a Late Weichselian Barents Sea ice sheet (e.g. Elverhøi & Solheim 1983), a) seems unlikely. b) appears more likely and could be caused by winnowing/non-deposition in shallow regions and enhanced deposition in deeper regions. A short time-lag in deglaciation of the two locations is also likely due to the differences in water depth. A glacier front situated on the shallow shoulder in the proximity of 82-321 could supply relatively large sediment volumes in a short time interval,

as is reported from other ice-proximal areas (e.g. Elverhøi et al. 1983). However, although no slump indications have been observed in the vicinity of 82-321, neither c) nor d) can be excluded until more dates are obtained from this region.

Consolidation

The main process taking place in the surge zone during post surge stagnation is that of gravity loading as the ice comes to rest. The two main effects of this are the formation of the local topography through redistribution of mobile sediments by subglacial pressure gradients and compaction of the subglacial sediments. Loading by the surged glacier is a likely cause of the wide range of shear strengths measured in the sediments above the assumed Late Weichselian till surface, despite a relatively short time interval. To investigate the consolidation characteristics of the material, oedometer tests were carried out (Fig. 35) on two samples, one from the surge zone (station 82-232.1, at the 10 cm level) and one from the area outside the surge moraine (82-237, 30 cm level).

At station 82-232, overconsolidated material was encountered at the sea floor, and only the core cutter and catcher of the vibrocorer recovered any sample. Sample disturbance can not be excluded, but the firm ($S_u = 77$ kPa) and apparently cohesive material did not appear disturbed. Pre-consolidation stress (P_c') was calculated using Casagrande's (1936) method. Due to a weakly defined deflection point on the curve (Fig. 35A), P_c' cannot be defined exactly, but falls in the range 300–400 kPa.

The ice thickness over station 82-232 immediately after the surge is uncertain, but based on the present-day glacier surface profile a thickness above sea level in the order of 50–70 m is likely. As the water depth in this region is nearly 100 m, the ice exerting a net load on the substratum would have a thickness of 40–60 m. The load would then be 350–530 kPa. When uncertainties both in the calculation of P_c' and the estimation of ice load are taken into account, the P_c' found from the oedometer test may clearly result from the ice load.

The Terzaghi consolidation theory, as outlined in e.g. Atkinson & Bransby (1978) and Lambe & Whitman (1979), can be used to estimate the time

necessary to consolidate the present sediment by a given load. In this respect the most important parameter obtained from the consolidation tests is the coefficient of consolidation (C_v), which is expressed as

$$C_v = kM/g$$

where k is the permeability, M the constrained modulus and G the unit weight of water. C_v is a material constant, but may increase with vertical stress in the virgin compression zone as a response to the decrease in permeability and increase in modulus as the sample is compacted.

Two dimensionless variables are introduced in calculating the compaction:

$$Z = z/H \text{ and } T = C_v t/H^2$$

where z is the sample depth and H the total drainage distance (i.e. the total sediment thickness down to impermeable base). T is termed the time factor and t is the time. The sediment behaviour is given by

$$\partial u^2/\partial Z^2 = \partial u/\partial T$$

where u is the excess pore pressure. Initially, the entire load is carried by the excess pore pressure. The excess pore pressure at the sediment surface is assumed to dissipate instantaneously, and the boundary condition for all t is $u = 0$ for $Z = 0$. Fig. 36 shows solutions for a homogeneous (constant C_v) sedimentary column. The consolidation ratio U_z is defined as $1 - u/u_0$, where $u_0 = u$ for $t = 0$. Consolidation will never be mathematically complete, but for all practical purposes a complete compaction (i.e. complete dissipation of excess pore pressure) can be assumed when $T = 1$. The time for "complete" consolidation is therefore given by

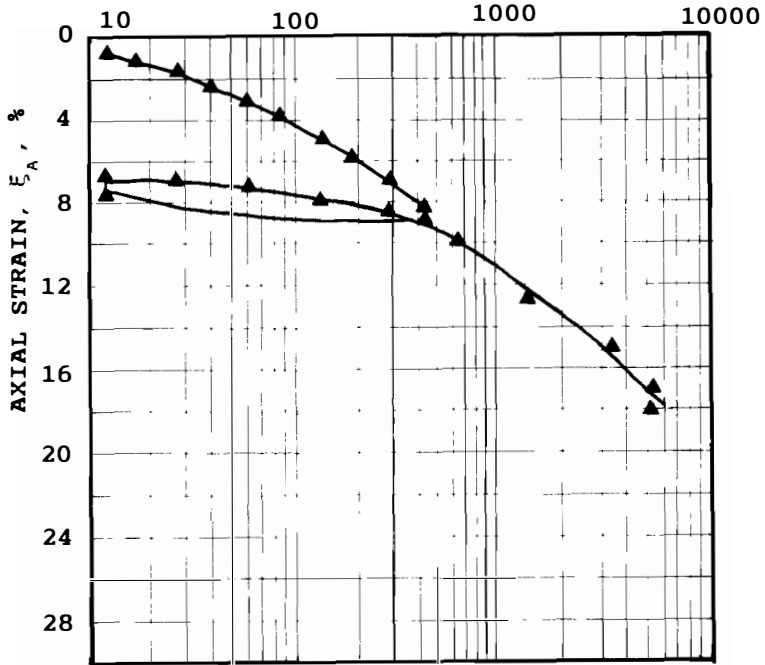
$$t = H^2/C_v$$

The time is independent of load. For values of T less than 0.05, the base of the sedimentary column is not compacted, while the top is fully compacted (Fig. 36).

Use of a C_v of 2.5 m²/year found from the consolidation test of the sample at station 82-232 will give a time for full consolidation of the entire 5 m sedimentary column of 10 years, which is well within the time available for compaction by the surged glacier after the 1938 surge. The tested sample at 10 cm depth is in this respect nearly at the sediment surface and would consolidate almost instantaneously.

82-232, 10cm

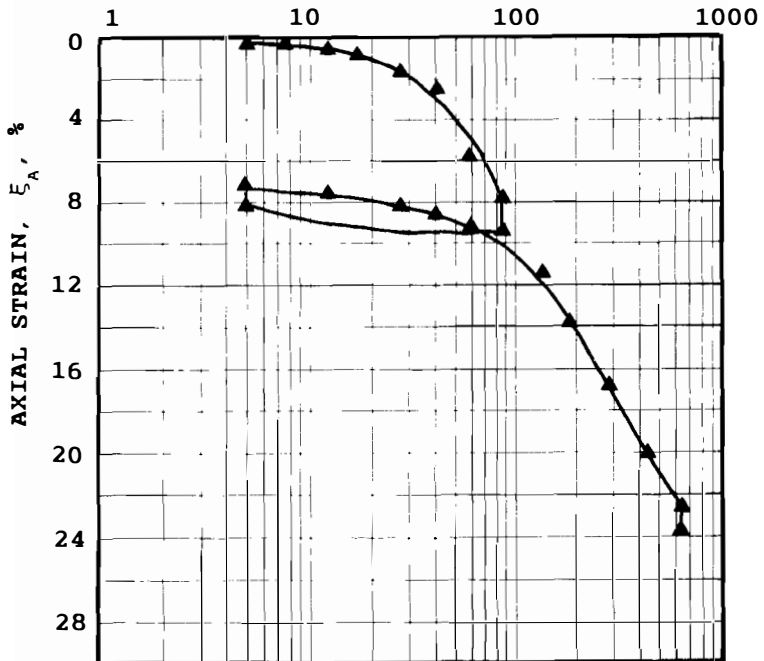
EFFECTIVE AXIAL STRESS, σ'_A (kPa)



A

82-237, 30cm

EFFECTIVE AXIAL STRESS, σ'_A (kPa)



B

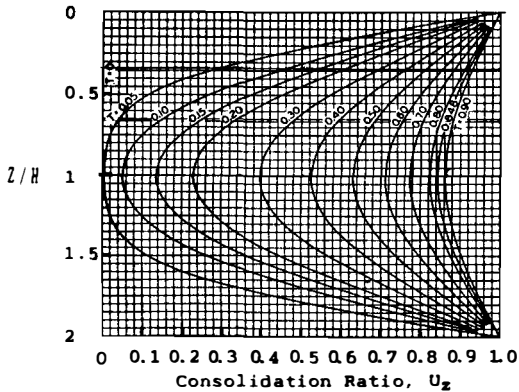


Fig. 36. Consolidation as a function of depth and time factor. From Taylor (1942). z = depth to sample. H = total drainage distance.

The consolidation test of core 82-237, outside the end moraine is of particular interest because the fine-grained mud of this sample apparently corresponds to the overconsolidated mud found in cores 83-31 and 83-32. Hence, obtaining consolidation characteristics of 82-237 may provide valuable information that can be applied on the overcompacted samples.

Calculation of a P_c' (Casagrande 1936) of 40–50 kPa shows that the sample has experienced a slight load. A possible cause for this may be the action of icebergs. In any case, the pre-consolidation of 82-237 must result from processes normal to this environment, and it is most likely that the muds in cores 83-31 and 83-32 experienced similar processes prior to loading by the surging glacier. Considering the glacier loading of the samples in the surge zone, the mud in core 82-237 may therefore correspond to the initial state of these sediments.

In the following, core 83-31, level 75 cm (Fig. 18D), will be used. The deformation can be found by

$$\varepsilon = e_0 - e/1 + e_0$$

where e_0 is the initial void ratio and e the void ratio of the considered sample. e is found by

$$e = w\rho_s/\rho_w$$

where w is water content and ρ_s and ρ_w are densities of grains and water respectively. Using a grain density of 2.7 g/cm³ and water content of

30% for the overconsolidated mud of core 83-31, gives $e_{31} = 0.81$.

The deformation involved in compacting the mud of 82-237 into the overconsolidated mud of 83-31 is therefore

$$\varepsilon = e_{237} - e_{31}/1 + e_{237}$$

With $e_{237} = 1.377$, this gives a deformation $\varepsilon = 0.24$.

Assumed maximum ice thickness above sea level immediately after the surge is 70 m, resulting in a load of 620 kPa. From the consolidation curve of sample 82-237, this corresponds to a deformation of approximately 0.22. Taking all uncertainties in parameter estimation into account, these values (0.24 and 0.22) are sufficiently similar to state that the assumed ice load is capable of consolidating muds of the type found in core 82-237 to the state found in the overconsolidated samples 82-31 (and also 82-32).

In using the consolidation test of core 82-237 to find the time required to obtain this degree of consolidation, the same approach as for 82-232 can be used. With a C_v of 2.0 m²/year for the mud of 82-237, and still using a total sediment thickness of 5 m, the entire sedimentary column will consolidate in 12.5 years, still well within the time the sediment at 83-31 had experienced the glacier load.

Andresen et al. (1979) obtained empirical relationships between S_u , P_0' , overconsolidation ratio (OCR) and plasticity index PI. Ten samples were tested for P_c' using Andresen et al. (1979) curves. P_c' values estimated with this method fall within the range of 300–570 kPa, corresponding with ice thicknesses of 34–65 m. This further supports the consolidation effect of the surging glacier. Since maximum consolidation seems to occur relatively rapidly in these sediments, only the first surge cycle will have a consolidating effect. Unless they are larger, any later surges will leave the preconsolidated sediments unaffected in terms of consolidation.

Post-surge deposition

The retreat phase will expose subglacial sediment and morphological features and subsequently form new features (push-moraines), as discussed

Fig. 35. Consolidation curves (oedometer test) for two samples outside Bräsvellbreen. A. In the surge zone. B. In the surge-distal zone. Note that only the core cutter and catcher recovered sediment in 82-232.

previously. Meltwater discharge will probably rapidly decrease to non-surge values and again be channeled through concentrated outlets. As meltwater activity decreases, deposition through subglacial melt-out most likely also decreases, although some material may still be deposited through this process subglacially or at the front. The most important mode of sediment output and

deposition is now through the main meltwater outlets (Pfirman 1985). Both field observations (Larsen 1982) and remote sensing techniques (Dowdeswell 1984) show major sediment plumes in surface waters outside the main outlets. Sea floor morphology and sedimentation outside the major outlet at the east side of Bråsvellbreen have been discussed separately (Pfirman 1985; Pfirman

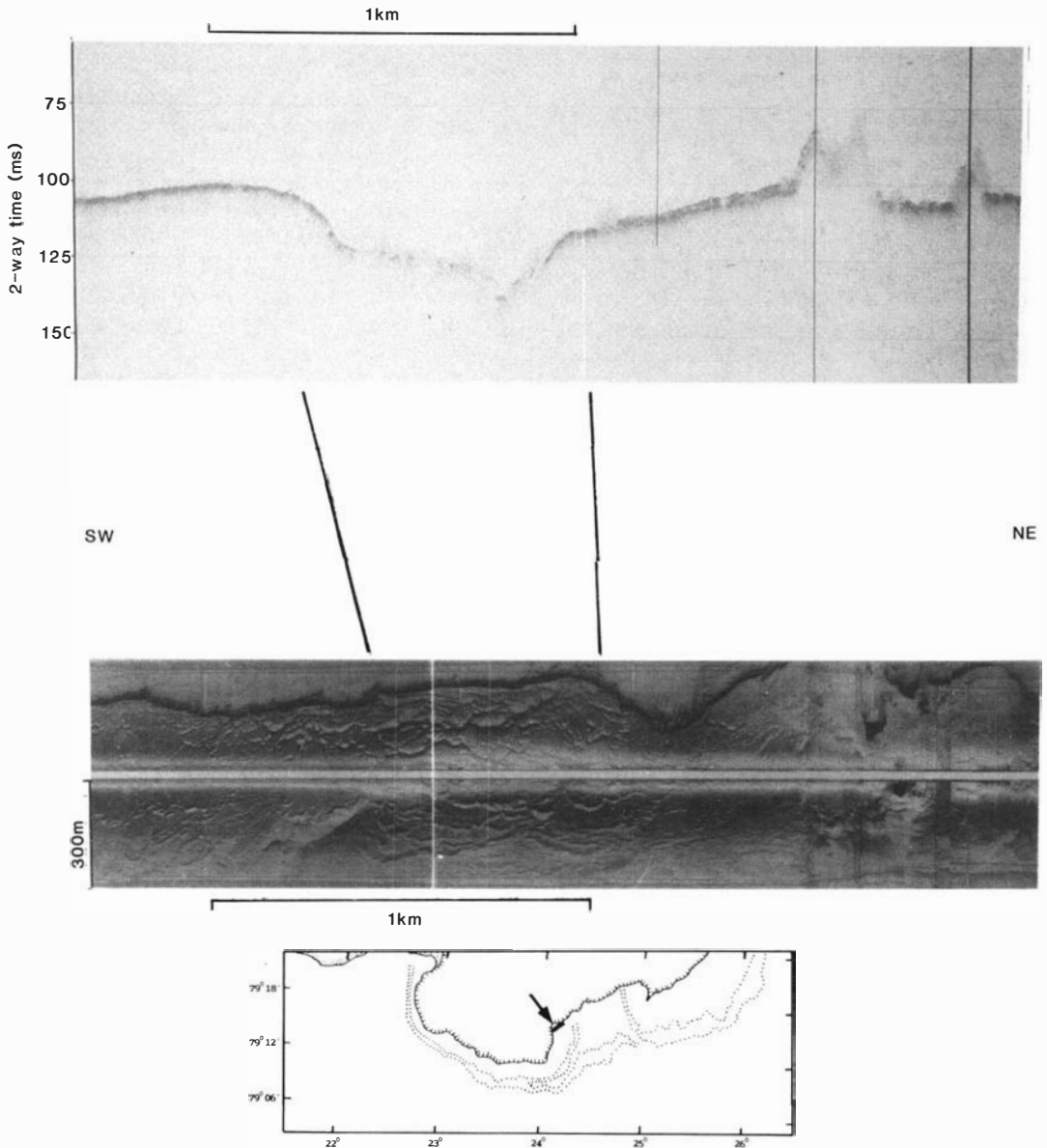


Fig. 37. 3.5 kHz record (upper) and side-scan sonograph (lower) across the main Bråsvellbreen meltwater outlet (arrow). (Modified from Pfirman & Solheim 1989).

& Solheim 1989) and only the main conclusions are included here. Water samples obtained in 1981, from the upper 10 m within 300 m of the main meltwater outlets, contained up to 28 mg/l of particulate material, as opposed to 2 mg/l in the ambient coastal water. The turbid plume is entrained in the coastal current and the bulk of the suspended sediment is deposited within 20 km off the glacier front. Concentrations drop to less than 5 mg/l within 5 km of the outflow. The relatively low concentrations imply low depositional rates, and given the short time-interval the outlet has been stable after the surge, the deposits are in general not detectable by conventional acoustic means. However, in the vicinity of the main eastern Bråsvellbreen outlet, there are thicker acoustically transparent deposits thought to result from rapid ice proximal deposition from meltwater. These include an 8–10 ms thick lense in a depression outside the outflow, a 3 ms drape off the edges of the depression and some (2–4) larger mounds with up to 35 ms of sediment (Fig. 37). The former sediment is formed into annual push moraines similar to other areas close to the ice front, while the latter mounds are interpreted as beaded esker deposits in accordance with the model proposed by Banerjee & McDonald (1973). These are rapidly formed where sediment-laden meltwater encounters sea water, possibly at some distance behind the ice front proper.

Increased iceberg production

Another important effect of glacier surges is the increased number of icebergs delivered both during the surge (Fig. 4B) and during retreat. According to seal-hunters, the abundance of icebergs may have been as much as one order of magnitude higher in 1937 than during normal years (Vinje 1985). From the side-scan sonar records in the regions of recent iceberg ploughing (Fig. 13A), there seems to be almost complete reworking of the uppermost sediments. This will usually lead to a depletion of fines, and Vorren et al. (1983) introduced the term “iceberg turbate” for this type of sediment. Due to the intense fracturing of the surging ice, the majority of the icebergs are probably of intermediate to small size (Dowdeswell 1989), causing the largest effect in the shallowest regions, most likely above 100 m water depth off Bråsvellbreen. The enhanced ploughing may contribute to increased redistribution of sediments with redeposition of

fine-grained material in deeper regions during surge.

Erosion by the latest Bråsvellbreen surge

Glacier surges are short-term, catastrophic events and may not be representative for glacial erosion in general. However, as material obviously is transported and delivered to the surge moraine and as the suspension load to the surge-distal area is increased, there is an effect, which, if repeated, may be of importance for the total erosion.

There is no control of the amount of material brought in from behind the pre-surge position of the ice front. A situation is therefore considered below where the total amount of material delivered to the surge moraine and the region outside is eroded from the new area covered by the glacier. Since some of the material most certainly is brought in from other parts of the drainage area, this situation should give maximum values of erosion. The following figures are important for this consideration:

- New area covered by the glacier after the surge: 460 km².
- Volume of surge moraine ridge, only the inner ridge in the easternmost part: approximately 0.5 km³
- Area that received material deposited from suspension, tentatively taken as a zone reaching 35 km from the ice front at maximum extent: 4,100 km².
- Average thickness of sediment deposited from suspension in the above area: tentatively 2 cm.
- Volume of material deposited from suspension: approximately 0.08 km³.

As the surge moraine configuration clearly shows that the western part of the ridge was formed during at least two surges, half the volume of this part of the ridge can be removed, which leaves approximately 0.35 km³ material in the youngest surge moraine. Based on these values, 0.42 km³ of material has been delivered by the surging glacier. Given a source area of 460 km², this implies a maximum average erosion of approximately 1.0 m. As both end members are un lithified sediments, no sediment bulk densities are considered in these calculations. Considering the entire Bråsvellbreen drainage area, including the surge zone, as source area, the total erosion is

0.35 m. With more information on the amount of sediment brought in from the entire drainage area, the figure for erosion may be further reduced. Furthermore, the possibility that the surge moraine ridge is formed through more than two surges can not be ruled out. Although much reduced, the calculated erosion per time-unit will remain considerably greater than what is usually calculated for ice sheets and presently glaciated areas (Larsen & Mangerud 1981; Laine 1980; Elverhøi et al. 1983; Elverhøi 1984). It should be kept in mind, however, that the surging Bråsvellbreen glacier eroded soft sediments with a high-frequency small-scale topography similar to that found in the region today, and that the effects discussed here took place during a very short time-interval compared to the periods generally considered when discussing glacial erosion.

Ice volumes and surge frequencies

The present data, combined with results from recent radio-echo soundings over Austfonna (Dowdeswell 1984; Dowdeswell et al. 1986), provide a basis for volumetric estimates and hence estimates of surge frequencies for Bråsvellbreen and Basin 3 (Table 1). A very simplified model is used, consisting of two elements: a) the amount of ice in the "new" part of the glacier, taken as the "surged ice", built out past the pre-surge ice front, and b) total net annual accumulation. a)/b) gives an estimate of the surge interval. The most uncertain factors for the calculations are as follows:

1. Position of the pre-surge glacier front (Fig. 4). For Bråsvellbreen, the 1936 front published by Glen (1937) has been modified to align the present coastline with the sides of the glacier proper, while in the case of Basin 3, the pre-surge ice front was assumed to form a smooth continuation of the coastline on either side of the glacier.
2. Mass balance and position of the equilibrium line. A mass balance curve for Midtre Lovénbreen in western Spitsbergen (Liestøl 1984) has been used, but with its position shifted with a change in the height of the equilibrium line (Fig. 38). Variations in precipitation and mean temperature will result in shifts of the equilibrium line rather than the shape of the curve (O. Liestøl, pers. comm. 1987). Only sparse
3. The boundary between the source and receiving areas during surge. The boundary between the source and receiving areas during surge is probably situated below the equilibrium line proper. The equilibrium line on Hessbreen, western Spitsbergen, is situated at approximately 350 m whereas the thickening of the snout as the result of a surge in 1973–74 starts at 250 m. A similar effect is demonstrated at Usherbreen, Svalbard (Hagen 1987). However, the surface profile did not change sig-

information exists on the mass balance of Austfonna. Schytt (1964) measured accumulation rates at a number of points near the summit of the inner part of Bråsvellbreen for the 1957–58 season. These values match well with the mass balance curve for Midtre Lovénbreen, shifted to correspond with an equilibrium line at 300 m a.s.l. Kristiansen & Sollid (1986) present equilibrium line heights of approximately 350 and 300 m a.s.l. for Bråsvellbreen and Basin 3, respectively. Dowdeswell & Drewry (1989) present recent data from Basin 5, northeast of Basin 3, indicating an equilibrium line at 300–350 m a.s.l. for this basin. Based on the above information, the equilibrium line is here placed at 300 m a.s.l. for both Bråsvellbreen and Basin 3, and the shifted mass balance curve for Midtre Lovénbreen (Fig. 38) used for estimation of net annual accumulation.

information exists on the mass balance of Austfonna. Schytt (1964) measured accumulation rates at a number of points near the summit of the inner part of Bråsvellbreen for the 1957–58 season. These values match well with the mass balance curve for Midtre Lovénbreen, shifted to correspond with an equilibrium line at 300 m a.s.l. Kristiansen & Sollid (1986) present equilibrium line heights of approximately 350 and 300 m a.s.l. for Bråsvellbreen and Basin 3, respectively. Dowdeswell & Drewry (1989) present recent data from Basin 5, northeast of Basin 3, indicating an equilibrium line at 300–350 m a.s.l. for this basin. Based on the above information, the equilibrium line is here placed at 300 m a.s.l. for both Bråsvellbreen and Basin 3, and the shifted mass balance curve for Midtre Lovénbreen (Fig. 38) used for estimation of net annual accumulation.

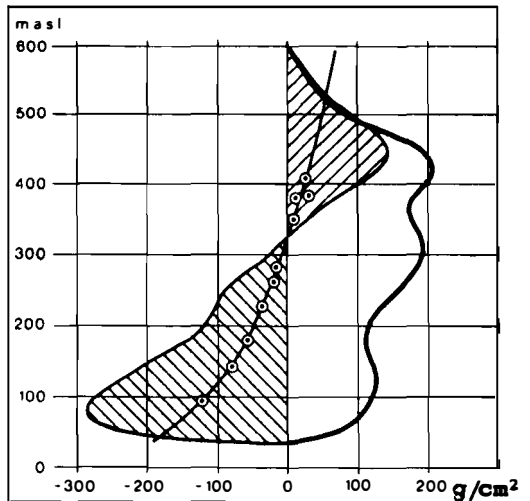


Fig. 38. Mass balance curve for Midtre Lovénbreen, western Spitsbergen (from Liestøl 1983). For the Austfonna calculations, the equilibrium line was placed at 300 m a.s.l., and the curve was parallel shifted.

nificantly between 250 m and 350 m (Liestøl 1974). At Austfonna, surface profiles immediately after the surge have been estimated by modifying present surface profiles from the equilibrium line to reach the maximum position, with the same height of the ice front above sea level as today. Although the exact shape of the glacier snout in maximum position probably was somewhat flatter than today since ablation tends to steepen the profile of a glacier, the error introduced with this simplification is minor compared to 1. and 2.

4. Annual loss from the accumulation area. Dowdeswell & Drewry (1989) measured ice velocities up to 47 m/year near the equilibrium line of Basin 5. Velocities of both Bråsvellbreen and Basin 3 are, however, likely to be much less and probably not more than 10 m/year (J.A. Dowdeswell, pers. comm. 1988). That there must be a difference is also indicated by the difference in glacier surface shape (Fig. 3). The annual push moraines and some fractures along the front indicate that there is a slight movement, but the exact amount is unknown. Calculations of annual surplus accumulation and hence a surge interval have been made with both zero transport and with a velocity of 10 m/year (Table 1), as these values present a reasonable ice velocity bracket for Bråsvellbreen and Basin 3.

Net accumulation averages for 100 m intervals in the accumulation area are summed to give

the total net accumulation. All ice volumes are transformed to mass of water in tons, using an ice density of 0.9 g/cm³.

The calculated surge interval for Bråsvellbreen supports Schytt's (1969) postulated estimate of "considerably more than 200 years," based partly on glacier outline from published maps. At present, the surface profile and calculated driving stress (Dowdeswell 1984, 1986a) indicate that both Bråsvellbreen and Basin 3 are in a quiescent phase and most likely quite far from a new surge. The calculated surge interval for Basin 3 does not correspond with a surge during Nordenskiöld's (1875) expedition in 1873. This may result from a) the observations not being from a surge, b) inaccurate positioning on a different basin, c) glaciological and climatic changes through time, d) large sources of error in the present calculations, or combinations of these. An unreported surge of these significant dimensions after 1900 seems unlikely. The calculated time interval may therefore be too short. This demonstrates the difficulties in these types of calculations. In that respect c) and d) above are key points. In particular for Bråsvellbreen, variations in ice velocity and the position of the equilibrium line will have a significant effect on the calculated values. A shift in the equilibrium line to 350 m a.s.l. will increase the calculated surge interval to 620 and 1,120 years for the 0 and 10 m/year ice velocity, respectively. When periods of several hundred years are considered, climatic fluctuations may also be important. A possibility that should be

Table 1. Calculations of surge volumes and frequencies.

		Bråsvellbreen		Basin 3	
Total area of glacier		1,115 km ²		1,250 km ²	
Accumulation area		504 km ²		878 km ²	
Ablation area		611 km ²		372 km ²	
Surged amount of ice		96 km ³	87*10 ⁹ t	91 km ³	82*10 ⁹ t
Net annual accumulation		238*10 ⁶ t		638*10 ⁶ t	
Annual loss from the accum. area	0 m/year	0	0	0	0
	10 m/year	0.075 km ³	68*10 ⁶ t	0.063 km ³	57*10 ⁶ t
Surplus accumulation		238 - 170*10 ⁶ t		638 - 581*10 ⁶ t	
Surge interval		≈ 370 - 510 years		≈ 130-140 years	

kept open is that surges may partly have been a result of climatic deterioration during the little ice age, and that new surges, for instance of Bråsvellbreen, are unlikely under the present climatic conditions.

Although the calculations are uncertain, some main trends are noticeable:

- Large volumes of ice (> 90 km³) are involved in the surges.
- The ratio of accumulation area to ablation area at present is approximately 1:1 for Bråsvellbreen and 2:1 for Basin 3, leading to a correspondingly higher total net annual accumulation in Basin 3.
- The surge interval of Bråsvellbreen seems to be long, compared to most reported surging glaciers (Meier & Post 1969).
- The calculated surge interval of Basin 3 is significantly shorter than that of the somewhat smaller Bråsvellbreen. This demonstrates the effect of the size of accumulation area, although a steeper profile and narrower drainage area also most likely have an effect.
- Surging tidewater glaciers leave a distinct suite of sea floor morphological features. The most prominent is a terminal ridge, here termed surge moraine, marking the maximum surge extent, and a system of discontinuous ridges in the area inside the moraine, here termed the surge zone. The latter ridges form a pattern which is related to the topography of the glacier base during surge and is formed through squeeze-up of mobile sediment during and immediately after surge.
- Bråsvellbreen has undergone at least two surges. The fossil trace of a previous surge, either considerably larger than the last surge or with a different direction of motion, is manifested as an outer surge moraine that almost merges with the Basin 3 moraine.
- Sediments in the surge zone and surge moraine are predominantly acoustically homogeneous gravel and pebble-rich diamictons formed by the reworking of pre-surge sediments mixed with allochthonous material brought in by meltwater or directly carried by the surging ice. In the surge moraine there is a tendency towards finer grades in the distal direction. Patches of pre-surge sediments can be found relatively undisturbed, embedded in the diamictons. These are overcompacted by the glacier but show a character distinctly different from the surrounding material. Local meltwater activity during retreat forms patches of clean, well-sorted sands.
- The most important process for formation of the surge moraine is ice push, but high loads of suspended sediment are also discharged by meltwater at the glacier front during the surge. The material is then subsequently reworked and pushed by the rapidly advancing glacier.
- Slumping and gravity flowing of the rapidly deposited material modify the surge moraine, particularly the distal slope.
- The squeeze-up ridges in the surge zone are preserved through post-surge stagnation of the ice and retreat through calving. However, after a time period dependent on glacier characteristics, the glacier returns to normal activity. Hence, Bråsvellbreen is presently forming annual push moraines. That surging glaciers are not completely stagnant despite their many quiescent phases is also documented from other Svalbard glaciers (Liestøl 1984).
- An important effect of tidewater glacier surges is a massive increase in the output of icebergs

Summary and conclusions: facies distribution off marine, surging glaciers

The following is a summary of the results obtained off Austfonna. Although some of the results and interpretations are site specific, a number of the points listed below may also have a more general significance for surging tidewater glaciers. This is exemplified in the facies model of Fig. 39.

- The Austfonna ice cap has several surging drainage basins. Of these, Bråsvellbreen and Basin 3 are the largest. The last Bråsvellbreen surge was documented by aerial photography in 1938. Basin 3, on the other hand, is interpreted to have surged, based on comparison with results from Bråsvellbreen in combination with glaciological information (Dowdeswell 1984, 1986a,b).
- Calculated surge frequencies show that Bråsvellbreen has a tendency to surge less frequently than Basin 3, demonstrating the importance of the size of the accumulation area relative to the ablation area, height of equilibrium line and overall glacier shape.

- that both carry sediments and cause increased reworking of the sea floor sediments through gouging. Modern iceberg gouging in the study area is depth limited to 120–130 m, but the bulk of the surge-produced bergs were smaller. Local topography may shelter areas shallower than 120 m from scouring. During quiescent periods, the production of icebergs is low.
- With the exception of the modern iceberg plough marks, the region outside the surge moraines, here termed the surge-distal zone, is characterized by features “normal” to the high latitude shelf environment: fossil iceberg plough marks, pockmarks and patches of sediment waves, most likely related to tidal currents.
 - Surge-distal deposits are mainly glaciomarine muds. Zones of increased pebble content may result from increased iceberg rafting during glacier surges. Increased iceberg gouging will also rework sediment into an iceberg turbate (Vorren et al. 1983), depleted in fines.
 - Five acoustic units can be identified off Bråsvellbreen if the surge moraine is taken as a separate unit (Unit 2). Unit 1 covers all surge zone diamictons above the Late Weichselian till. Changes are too frequent and local within this material to be detected by conventional acoustic surveys using a near surface source and receiver configuration. In the surge-distal zone the upper acoustic Unit 3 is only found in deep water and represents fine-grained sediments, while the underlying Unit 4 has a higher coarse component. Unit 5 underlies the entire study area and mostly represents the Late Weichselian till or, locally, upper bedrock if till is absent.
 - Physical properties of the sediments are largely dependent upon lithology. A median grain size of 0.016 mm appears to mark an important change in water content, total carbon, and total organic carbon contents. The surge zone shows large variation in all parameters due to the unsorted character of the material and various degree of compaction – from the soft top sediment, through different degrees of compaction caused by the surge, to the underlying basal till of presumably Late Weichselian age. The surge moraine has less sample coverage, but shows values not significantly different from the surge zone sediments, with the exception of the most overconsolidated material in the latter zone. The more muddy deposits in the surge-distal zone in general show properties characteristic for a higher proportion of finer material and lack of overcompaction. However, the action of icebergs may have had a compacting effect.
 - Compressional wave velocity and acoustic impedance show good correlation with other physical parameters, in particular with water content and plasticity index. Hence, acoustic measurements can be used as a reconnaissance tool for obtaining other properties in this type of environment.
 - The most important depositional event is emplacement of the surge moraine. Although of a local character, this feature constitutes an important sediment accumulation in an environment of generally slow deposition. If surges are frequent, the formation of surge moraines may involve large sediment volumes that are moved further offshore. As they constitute relatively significant positive topographic features, these accumulations will also be more susceptible than their surroundings to erosion by other processes such as waves, currents and icebergs.
 - In the surge-distal region, the increase in sedimentation rate from individual surges may be large, but as the time intervals are short, the resulting sediment layer is probably less than 2–3 cm thick. However, if there are periods of more frequent surges, e.g. due to climatic variations, this may have a significant effect on the overall sedimentation rate over a longer time-interval, for example through the Holocene. Off Bråsvellbreen most of the post-glacial sediments may have been supplied during surges.
 - The major increase in sedimentation during a surge appears to be surprisingly local, concentrated to the surge moraine. This is demonstrated by the abrupt distal termination of the surge moraine, and the fact that iceberg plough marks immediately outside the moraine are not filled in with sediment.
 - Although a surge is of short duration, surging glaciers are capable of consolidating fine-grained sea floor sediments. Consolidation, however, is laterally variable, probably due to the heterogeneous and crevassed character of the surging ice proper.
- In summary, surging glaciers do not produce sedimentological characteristics that are unique to this environment. Similar sediments can be found in most ice proximal (term essentially used in accordance with Powell (1984)) environments. However, the combination of lithology, mor-

phology (particularly important), physical properties and sedimentation rates may be diagnostic; these parameters may therefore be integrated in a facies model (Fig. 39), where the area is divided in a proximal zone (including the surge moraine) and a distal zone. Although documentary evidence for surging exists in the case of Bråsvellbreen, at least the morphological part of the facies model seems to also be applicable for Basin 3 of the Austfonna ice cap. When interpreting older sequences and formerly glaciated regions, the whole system of features should be considered, and, if possible, both proximal and distal regions should be identified.

Acknowledgements

A large number of individuals and organisations have been involved in various parts of this study. Most of the data could not have been collected without the valuable assistance and enthusiasm of the crew on board the R/V Lance. The Norwegian Hydrographic Survey (NSKV) is acknowledged for making it possible for us to take part in their hydrographic cruises in 1984 and 1985. Olav T. Egderød and Thomas Martinsen are both thanked for carrying out field operations during these cruises. Anders Elverhøy, Yngve Kristoffersen, Stephanie Pfirman, Jørn Thiede, Olav Liestøl, Jon O. Hagen, Bjørn Andersen, Julian Dowdeswell, Michael Hambrey, Tor Løken and Toralf Berre have all given valuable, constructive criticism to various parts of the manuscript. Espen Kopperud, Donald Tumasonis and Petter Antonsen did the final drafting of the figures. A part of the study was carried out while the author was funded by the Office of Naval Research (ONR), grant no. N 00014-81-G-0001 to Y. Kristoffersen. ARCO Norway Inc. is acknowledged for providing funds for parts of the geotechnical analyses. The Norwegian Petroleum Directorate (NPD) sponsored and participated in the 1980 and 1983 cruises. Funds for meetings with J. A. Dowdeswell and colleagues at the University College of Wales, Aberystwyth, to integrate geological and glaciological data were provided by NATO grant no. 0747/87.

References

- Aagaard, K., Foldvik, A., Gammelsrød, T. & Vinje, T. 1983: One-year records of current and bottom pressure in the strait between Nordaustlandet and Kvitøya, Svalbard, 1980–81. *Polar Research 1 n.s.*, 107–113.
- Ahlmann, H. W. 1933: Scientific results of the Swedish-Norwegian Arctic Expedition in the summer of 1931. Part VIII. Glaciology. *Geografiska Annaler 15*, 161–216, 261–295.
- Akal, T. 1972: The relationships between the physical properties of underwater sediments that affect bottom reflection. *Marine Geology 13*, 251–266.
- Alley, R. B., Blankenship, D. D., Rooney, S. T. & Bentley, C. R. 1989: Sedimentation beneath ice shelves – the view from ice stream B. *Marine Geology 85*, 101–120.
- American Society for Testing and Materials (ASTM) 1983: Standard test method for pulse velocity through concrete. Designation: C597-83, 376–379.
- Andersen, J. L. & Sollid, J. L. 1971: Glacial chronology and glacial geomorphology in the marginal zones of the glaciers Midtdalsbreen and Nigardsbreen, South Norway. *Norsk Geografisk Tidsskrift 25*, 1–38.
- Andresen, A., Berre, T., Kleven, A. & Lunne, T. 1979: Procedures used to obtain soil parameters for foundation engineering in the North Sea. *Norwegian Geotec. Inst., Publ. 129*, 1–18.
- Andrews, J. T. 1973: The Wisconsin Laurentide ice sheet: dispersal centers, problems of rates of retreat, and climatic implications. *Arctic and Alpine Research 5*, 185–199.
- Atkinson, J. H. & Bransby, P. L. 1978: *The mechanics of soils, an introduction to critical state soil mechanics*. McGraw-Hill, London.
- Banerjee, I. & McDonald, B. C. 1973: Nature of esker sedimentation. Pp. 132–154 in Jopling, A. V. & McDonald, B. C. (eds): *Glaciofluvial and glaciolacustrine sedimentation. Soc. Econ. Paleont. Mineral. Spec. Publ. 23*.
- Baranowski, S. 1977: The subpolar glaciers of Spitsbergen seen against the climate of this region. *Results of investigations of the Polish scientific Spitsbergen expeditions, III*, 93 pp.
- Bennett, R. H. & Nelsen, T. A. 1983: Scaffloor characteristics and dynamics affecting geotechnical properties at shelf-breaks. *SEPM Spec. Publ. 33*, 333–355.
- Bjørklund, G. 1985: Parallel ridges at the former ice-divide zone in Dalarna, Sweden – possible crevasse-fillings. *Geografiska Annaler 67A*, 129–131.
- Blake, W. Jr. 1962: *Geomorphology and glacial geology in Nordaustlandet, Spitsbergen*. Unpubl. Ph.D thesis, Ohio State University.
- Boulton, G. S. 1970: On the origin and transport of englacial debris in Svalbard glaciers. *J. Glaciol. 9*, 213–229.
- Boulton, G. S. 1972: The role of thermal regime in glacial sedimentation. Pp. 1–19 in Price, R. J. & Sugden, D. E. (eds.): *Polar geomorphology. Inst. Br. Geogr. Spec. Publ. 4*.
- Boulton, G. S. 1975: Processes and patterns of sub-glacial sedimentation: a theoretical approach. Pp. 7–42 in Wright, A. E. and Mosely, F. (eds.): *Ice ages: Ancient and modern*. Seel House Press, Liverpool.
- Boulton, G. S. 1976: The development of geotechnical properties in glacial tills. Pp. 292–303 in Leggat, R. F. (ed.): *Glacial till. The Royal Society of Canada, Spec. Publ. 12*.
- Boulton, G. S. 1986: Push-moraines and glacier-contact fans in marine and terrestrial environments. *Sedimentology 33*, 677–698.
- Boulton, G. S. & Jones, A. S. 1979: Stability of temperate ice caps and ice sheets resting on beds of deformable sediment. *J. Glaciol. 24*, 29–43.
- Boulton, G. S. & Paul, M. A. 1976: The influence of genetic processes on some geotechnical properties of glacial tills. *Q. J. Eng. Geol. 9*, 159–194.
- Bryan, G. M. 1980: The hydrophone-pinger experiment. *J. Acoust. Soc. Am. 68*, 1403–1408.
- Buchan, S., McCann, D. M. & Taylor Smith D. 1972: Relations between the acoustic and geotechnical properties of marine sediments. *Q. J. Eng. Geol. 5*, 265–284.
- Budd, W. F. 1975: A first simple model for periodically self-surging glaciers. *J. of Glaciol. 14*, 3–21.
- Bugge, T. 1980: Shallow geology on the continental shelf off Møre and Trøndelag, Norway. *IKU Publ. 104*, 44 pp.
- Casagrande, A. 1936: The determination of the pre-con-

- solidation load and its practical significance. *Proc. 1st Int. Conf. Soil Mech Found. End.*, Cambridge, Mass. 60.
- Casagrande, A. 1948: Classification and identification of soils. *Trans Am. Soc. Civ. Eng.* 113, 901-930.
- Clapperton, C. M. 1975: The debris content of surging glaciers in Svalbard and Iceland. *J. Glaciol.* 14, 395-406.
- Clarke, G. K. C. 1976: Thermal regulation of glacier surging. *J. Glaciol.* 16, 231-250.
- Clarke, G. K. C., Collins, S. G. & Thompson, D. E. 1984: Flow, thermal structure and subglacial conditions of a surge-type glacier. *Can J. Earth Sci.* 21, 232-240.
- Clarke, G. K. C., Schmok, J. P., Ommaney, S. L. & Collins, S. G. 1986: Characteristics of surge-type glaciers. *J. Geophys. Res.* 91, 7165-7180.
- Clukey, E. C., Nelson, H. & Newby, J. E. 1978: Geotechnical properties of northern Bering Sea sediment. *U.S. Geological Survey. Open-file report 78-408.* 27 pp.
- Dege, W. 1948: Das nordostland von Spitsbergen. *Polarforschung* 2, 72-83, 152-163.
- Dege, W. 1949: Meinc umseglung des Nordostlandes von Spitzbergen. *Festschrift zum 70. Geburtstag des Ord. Professors der Geographie, Dr. L. Mecking., Bremen-Horn.* 79-96.
- Denton, G. H. & Hughes, T. J. 1981: The Arctic ice sheet: An outrageous hypothesis. Pp 437-467 in Denton, G. H. & Hughes, T. J. (eds.): *The last great ice sheets.* John Wiley & Sons.
- Dolgushin, L. D. & Osipova, G. B. 1974: Surging glaciers. *Priroda* 2, 85-99.
- Dowdeswell, J. A. 1984: Remote sensing studies of Svalbard glaciers. Unpubl. Ph.D thesis, University of Cambridge 250 pp.
- Dowdeswell, J. A. 1986a: Drainage basin characteristics of the Nordaustlandet ice caps. Svalbard. *J. Glaciol.* 32, 31-38.
- Dowdeswell, J. A. 1986b: Remote sensing of ice cap outlet glacier fluctuations on Nordaustlandet, Svalbard. *Polar Research* 4 n.s., 25-32.
- Dowdeswell, J. A. 1989: On the nature of Svalbard icebergs. *Journal of Glaciology* 35, 224-234.
- Dowdeswell, J. A. & Drewry, D. J. 1985: Place names on the Nordaustlandet ice caps. Svalbard. *Polar Record* 22, 519-539.
- Dowdeswell, J. A. & Dewry, D. J. 1989: The dynamics of Austlonna, Nordaustlandet, Svalbard: Surface velocities, mass balance and subglacial meltwater. *Annals Glaciol.* 12, 37-45.
- Dowdeswell, J. A., Drewry, D. J., Leistøl, O. & Orheim, O. 1984a: Airborne radio-echo sounding of sub-polar glaciers in Spitsbergen. *Norsk Polarinst. Skr.* 182, 41 pp.
- Dowdeswell, J. A., Drewry, D. J., Leistøl, O. & Orheim, O. 1984b: Radio-echo sounding of Spitsbergen glaciers: problems in the interpretation of layer and bottom returns. *J. Glaciol.* 30, 16-21.
- Dowdeswell, J. A., Drewry, D. J., Cooper, A. P. R. & Gorman, M. R. 1986: Digital mapping of the Nordaustlandet ice caps from airborne geophysical investigations. *Annals Glaciol.* 8, 51-58.
- Dreimanis, A. & Vagners, U. J. 1971: Bimodal distribution of rock and minimal fragments in basal tills. Pp. 237-250 in Goldthwait, R. P. (ed.): *Tilla symposium.* Ohio State Univ. Press.
- Drewry, D. J. 1986: *Glacial geologic processes.* Edward Arnold Publishers, Ltd. 276 pp.
- Drewry, D. J. & Liestøl, O. 1985: Glaciological investigations of surging ice caps in Nordaustlandet, Svalbard. 1983. *Polar Record* 22, 357-378.
- Dyke, A. S. & Prest, V. K. 1987: Later Wisconsinan and Holocene history of the Laurentide ice sheet. *Abstracts from the 16th Arctic Workshop.* Edmonton, Canada, 1987, p. 18.
- Eide, O. 1974: Marine soil mechanics, applications to North Sea offshore structures. *Norwegian geotechnical Institute Publication 103.* 20 pp.
- Ekman, S. R. 1971: Seismic investigations on the Nordaustlandet ice caps. *Geografiska Annaler* 53A, 1-13.
- Elverhøi, A. 1984: Erosjon og sedimenttransport fra bredekte områder. *Norsk Polarinstutt Rapportserie* 17, 43-82.
- Elverhøi, A. & Solheim, A. 1983: The Barents Sea ice sheet - a sedimentological discussion. *Polar Research* 1 n.s., 23-42.
- Elverhøi, A., Lønne, Ø. & Seland, R. 1983: Glaciomarine sedimentation in a modern fjord environment, Spitsbergen. *Polar Research* 1 n.s., 127-149.
- Elverhøi, A., Pirman, S. L., Solheim, A. & Larsen, B. B. 1989: Glaciomarine sedimentation and processes on high Arctic epicontinental seas - exemplified by the northern Barents sea. *Marine geology* 85, 225-250.
- Elverhøi, A., Nyland Berg, M., Russwurm, L. & Solheim, A. 1990: Late Weichselian ice recession in the central Barents Sea. Pp. 289-307 in Bleil, U. & Thiede, J. (eds.): *Geologic history of the polar oceans: Arctic versus Antarctic.* Kluwer Academic Publ., The Netherlands.
- Forsberg, C. F. 1983: *Sedimentation and early diagenesis of Late Quaternary deposits in central parts of the Barents Sea.* Unpubl. Cand. scient. thesis, University of Oslo. 120 pp.
- Glen, A. R. 1937: The Oxford University Arctic Expedition North East Land, 1935-36. *Geographical Journal* 90, 193-222, 289-314.
- Glen, A. R. 1941: A sub-arctic glacier cap: the West Ice of North East Land. *Geographical Journal* 98, 65-76, 135-146.
- Gravenor, C. P. & Kupsch, W. O. 1959: Ice-disintegration features in western Canada. *Journal of Geology* 67, 48-64.
- Hagen, J. O. 1987: Glacier surge at Usherbreen, Svalbard. *Polar Research* 5 n.s., 239-252.
- Hagen, J. O., Licstøl, O., Sollid, J. L., Wold, B. & Østrem, G. 1986: Subglasiale undersøkelser ved Bondhusbreen, Folgefonna. *Meddelelser fra Geografisk Institutt, Universitetet i Oslo, Naturgeografisk serie, Rapport no. 4.* 82 pp.
- Hambrey, M. J. & Muller, F. 1978: Structures and ice deformation in the White Glacier, Axel Heiberg Island, Northwest Territories, Canada. *Journal of Glaciology* 20, 41-66.
- Hamilton, E. L. 1974: Prediction of deep-sea sediment properties: state-of-the-art. Pp. 1-44 in Inderbitzen, A. L. (ed.): *Deep Sea Sediments.* Plenum Publ. Co.
- Hamilton, E. L. 1980: Geoacoustic modelling of the sea floor. *J. Acoust. Soc.* 68, 1313-1340.
- Hare, F. K. 1976: Late Pleistocene and Holocene climates: some persistent problems. *Quaternary Research* 6, 507-517.
- Harland, W. B. & Hollin, J. T. 1953: Oxford and Cambridge Spitsbergen Expedition 1951. *Polar Record* 6, 800-803.
- Hartog, J. M. 1950: Oxford University Expedition to Nordaustlandet (North East Land) 1949. *Polar Record*, 5, 613-619.
- Hartog, J. M. & Thompson, H. R. 1950: Oxford University Expedition to North East Land, 1949. *Oxford University Exploration Club Bulletin* 3, 5-10.
- Herron, S. & Langway, C. C. Jr. 1979: The debris-laden ice at the bottom of the Greenland ice sheet. *Journal of Glaciology* 23, 193-207.
- Hollin, J. T. 1956: Oxford University Expedition of Nordaustlandet, 1955. *Polar Record* 8, 28.

- Hoppe, G. 1952: Hummocky moraine regions, with special reference to the interior of Norrbotten. *Geografiska Annaler* 34, 1–72.
- Horn, D. R., Horn, B. M. & Delach, M. N. 1968: Correlation between acoustical and other physical properties of deep-sea cores. *J. Geophys. Res.* 73, 1939–1957.
- Horvath, E. V. & Field, W. O. 1969: References to glacier surges in North America. *Can. J. Earth Sci.* 6, 845–851.
- Hovland, M. 1983: Elongated depressions associated with pockmarks in the western slope of the Norwegian Trench. *Marine Geology* 51, 35–46.
- Hovland, M. & Judd, A. G. 1988: *Seabed pockmarks and seipages. Impact on Geology, Biology and the Marine Environment.* Graham & Trotman Ltd., London. 293 pp.
- Hughes, T. J. 1974: Study of unstable Ross Sea glacial episodes. *ISCAP Bulletin 3: Orono, Me., Institute for Quaternary Studies, University of Maine.* 93 pp.
- Humphrey, N., Raymond, C. & Harrison, W. 1986: Discharges of turbid water during mini-surges of Variegated Glacier, Alaska, U.S.A. *J. Glaciol.* 32, 195–207.
- Johnson, H. D. 1981: Shallow siliclastic seas. Pp. 207–258 in Reading, H. G. (ed.): *Sedimentary environments and facies.* Blackwell Scientific Publications.
- Johnson, P. G. 1975: Recent crevasse fillings at the terminus of the Donjek Glacier, St. Elias Mountains, Yukon Territory. *Quaestiones Geographicae* 2, 53–59.
- Josephans, H. W., Zevenhuizen, J. & Klassen, R. A. 1986: The Quaternary geology of the Labrador shelf. *Can. J. Earth Sci.* 23, 1190–1213.
- Kamb, B. 1987: Glacier surge mechanism based on linked cavity configuration of the basal water conduit system. *J. Geophys. Res.* 92 (B9), 9083–9100.
- Kamb, B., Raymond, C. F., Harrison, W. D., Engelhardt, H., Echelmeyer, K. A., Humphrey, N., Brugman, M. M. & Pfeffer, T. 1985: Glacier surge mechanism: 1982–1983 surge of Variegated Glacier, Alaska. *Science* 227, 469–479.
- King, L. H. & MacLean, B. 1970: Pockmarks on the Scotian shelf. *Geol. Soc. Am. Bull.* 81, 3141–3148.
- Kristiansen, K. L. & Sollid, J. L. 1986: Svalbard, glacial-geologisk- og geomorfologisk kart, 1:1000 000. *Nasjonalatlas for Norge.* Geografisk Institutt, Universitetet i Oslo.
- Lagally, M. 1932: Zur Thermodynamik der Gletscher. *Zeitschrift für Gletscherkunde* 20, 199–214.
- Laine, E. P. 1980: New evidence from beneath the western North Atlantic for the depth of glacial erosion in Greenland and North America. *Quaternary Research* 14, 69–96.
- Lamb, H. H. 1977: *Climate: present, past and future. Vol. 1, Fundamentals and climate now.* Methuen, London. 835 pp.
- Lambe, T. W. & Whitman, R. V. 1979: *Soil mechanics, SI version.* John Wiley & Sons, New York. 553 pp.
- Larsen, E. & Mangerud, J. 1981: Erosion rate of a Younger Dryas cirque glacier at Kråkenes, western Norway. *Annals of Glaciology* 2, 153–158.
- Larsen, E., Klakegg, O. & Longva, O. 1988: Brattvåg and Ona. Quaternary geological maps 1220 III and 1220 IV – scale 1:50,000 with description. *Norges Geologiske Undersøkelse, Skrifter* 85, 1–41.
- Larsen, T. 1982: Rapport fra Norsk Polarinstittutts tokt med 'Lance' til Svalbard 6/8–2/9, 1982 (Tokt II). *Norsk Polarinst. Rapportserie* 10. 160 pp.
- Lauritzen, Ø. & Ohta, Y. 1984: Geological map, Svalbard, 1:500 000, Sheet 4G, Nordaustlandet. *Norsk Polarinst. Skr.* 154D. 14 pp.
- Lawson, D. E. 1979: Sedimentological analysis of the western terminus of the Matanuska Glacier, Alaska. *U.S. Army, Corps of Engineers, Cold Regions Research and Engineering Laboratory, Report* 79-9, 112 pp.
- Lewis, C. F. M., Blasco, S. M., Bornhold, B. D., Hunter, J. A. M., Judge, A. S., Kerr, J. W., McLarsen, P. & Pelletier, B. R. 1977: Marine geological and geophysical activities in Lancaster Sound and adjacent fjords. *Geological survey of Canada, Paper* 77-1A. 495–506.
- Liestøl, O. 1969: Glacier surges in west Spitsbergen. *Can. J. Earth Sci.* 6, 895–897.
- Liestøl, O. 1974: Glaciological work in 1972. *Norsk Polarinst. Årbok* 1972. 125–135.
- Liestøl, O. 1976: Årsmørene foran Nathorstbreen? *Norsk Polarinst. Årbok* 1976, 361–363.
- Liestøl, O. 1984: Glaciological work in 1983. *Norsk Polarinst. Årbok* 1983. 35–45.
- Liestøl, O. 1985: Glaciers of Svalbard, Norway. In Williams, R. S. Jr. (ed.): *Satellite image atlas of glaciers. U.S. Geological Survey Professional Paper, Chapter 5: Europe.*
- Løken, T. 1976: Geology of superficial sediments in the northern North Sea. *Norwegian Geotechnical Institute, Publ. no.* 114, 45–60.
- Martinsen, T. 1985: *Rapport for lett-seismiske undersøkelser og geologisk prøvetaking 1985, utført i tilknytning til Norges Sjøkartverks opplodding i Barentshavet.* Unpubl. report, Norsk Polarinstittutt. 13 pp.
- Meier, M. F. & Post, A. 1969: What are glacier surges? *Can. J. Earth Sci.* 6, 807–817.
- Molnia, B. F. 1983: Subarctic glacial-marine sedimentation; a model. Pp. 95–144 in Molnia, B. F. (ed.): *Glacial marine sedimentation.* Plenum Press, New York and London.
- Moum, J., 1966: Falling drop used for grain-size analysis of fine-grained materials. *Norwegian Geotechnical Institute, Publ. no.* 70.
- Nordenskiöld, A. E. 1875: Den Svenska Polarexpeditionen, 1872–1873. *K. Svenska Vetenskapsakademiets Handlingar* 2 (18). 132 pp.
- Norish, K. & Taylor, R. M. 1962: Quantitative analysis by X-ray diffraction. *Clay Mineralogy Bull.* 5, 98–104.
- Nyland Berg, M. 1991: Sedimentologiske og geofysiske undersøkelser av sen-kenozoiske sedimenter på sydøstskråningen av Spitsbergenbanken, det nordlige Barentshav. Unpubl. thesis, Univ. of Oslo. 203 pp.
- Palosuo, E. & Schytt, V. 1960: Til Nordostlandet med den Svenska glaciologiska expeditionen. *Terra* 72, 11–19.
- Paterson, W. S. B. 1981: *The physics of glaciers.* 2nd. edition. Pergamon Press, Oxford. 380 pp.
- Paul, M. A. & Jobson, L. M. 1987: *On the acoustic and geotechnical properties of soft sediments from the Witch Ground basin, central North sea.* Unpubl. report, Department of Civil Engineering, Heriot-Watt University, Edinburgh, Scotland.
- Pessl, F. & Frederick, J. E. 1981: Sediment source for meltwater deposits. *Annals of Glaciology* 2, 92–96.
- Pfirman, S. 1985: *Input, dispersal and deposition of suspended sediments from glacial meltwater.* Ph.D. thesis, Woods Hole Oceanographic Institution, WHOI-85-4. 284 pp.
- Pfirman, S. L. & Solheim, A. 1989: Subglacial meltwater discharge in the open-marine tidewater glacier environment: Observations from Nordaustlandet, Svalbard archipelago. *Marine Geology* 86, 265–281.
- Powell, R. D. 1984: Glacimarine processes and inductive lithofacies modelling of ice shelf and tidewater glacier sediments based on Quaternary samples. *Marine Geology* 57, 1–52.
- Powell, R. D. 1985: Iceberg calving and its influence on ice-proximal subaqueous glacial facies lithofacies. *14th Arctic Workshop; Land-Sea interaction, Halifax 1985, Abstract.* 101–103.

- Prest, V. K. 1969: Retreat of Wisconsin and recent ice in North America. *Geological Survey of Canada, Map 1257 A*.
- Price, R. J. 1970: Moraines at Fjallsjökull, Iceland. *Arctic and Alpine Research* 2, 27–42.
- Raymond, C. F. 1987: How do glaciers surge? A review. *J. Geophys. Res.* 92 (B9), 9121–9134.
- Rey, F., Skoldal, H. R. & Slagstad, D. 1987: Primary production in relation to climatic changes in the Barents Sea. Pp. 29–46 in Loeng, H. (ed.): *The effect of oceanographic conditions on the distribution and population dynamics of commercial fish stock in the Barents Sea*. Proceedings of the third Soviet-Norwegian symposium, Murmansk 1986.
- Richards, A. F., Palmer, H. D. & Perlow, M. Jr. 1975: Review of continental shelf marine geotechnics: Distribution of soils, measurement of properties, and environmental hazards. *Marine Geotechnology* 1, 33–67.
- Robin, G. de Q. & Weertman, J. 1973: Cyclic surging of glaciers. *J. Glaciol.* 12, 3–18.
- Rokoengen, K., Gunleiksrud, T., Lien, R. L., Løfaldi, M., Risc, L., Sindre, E. & Vigran, J. O. 1980: Shallow geology on the continental shelf off Møre and Romsdal. Description of 1:250 000 Quaternary geology map 6203. *IKU Publ. no. 105*. 49 pp.
- Ruddiman, W. F. & Duplessy, J.-C. 1985: Conference on the last deglaciation: Timing and mechanism. *Quaternary Research* 23, 1–17.
- Ruddiman, W. F. & McIntyre, A. 1981: The mode and mechanism of the last deglaciation: Oceanic evidence. *Quaternary Research* 16, 125–134.
- Russwurm, L. 1990: Sedimentologiske og geofysiske undersøkelser av sen-kvartære sedimenter, nordlige Barentshav. Unpubl. thesis. Univ. of Oslo. 182 pp.
- Salvigsen, O. 1978: Holocene emergence and finds of pumice, whalebones and driftwood at Svartknausflya, Nordaustlandet. *Norsk Polarinst. Årbok 1977*, 217–228.
- Salvigsen, O. 1981: Radiocarbon dated raised beaches in Kong Karls Land, Svalbard, and their consequences for the glacial history of the Barents Sea area. *Geografiska Annaler* 63A, 283–291.
- Salvigsen, O. & Nydal, R. 1981: The Weichselian glaciation in Svalbard before 15 000 B.P. *Boreas* 10, 433–446.
- Schwab, W. C. & Lee, H. J. 1983: Geotechnical analyses of submarine landslides in glacial-marine sediment, northeast Gulf of Alaska. Pp. 145–184 in Molnia, B. F. (ed.): *Glacial-marine sedimentation*. Plenum Press, New York and London.
- Schytt, V. 1964: Scientific results of the Swedish glaciological expedition to Nordaustlandet, Spitsbergen, 1957 and 1958. Parts I and II. *Geografiska Annaler* 46, 243–281.
- Schytt, V. 1969: Some comments on glacier surges in eastern Svalbard. *Can. J. Earth Sci.* 6, 867–873.
- Sharp, M. 1984: Annual moraine ridges at Skalfellsjökull, south east Iceland. *J. Glaciol.* 30, 82–93.
- Sharp, M. 1985: "Crevasse-fill" ridges – a land form type characteristic of surging glaciers? *Geografiska Annaler* 67A, 213–220.
- Smith, R. A. 1976: The application of fracture mechanics to the problem of crevasse penetration. *J. Glaciol.* 17, 223–228.
- Solheim, A. 1986: Submarine evidence of glacier surges. *Polar Research n.s.*, 91–95.
- Solheim, A. & Elverhøi, A. 1985: A poekmark field in the central Barents Sea: gas from a petrogenic source? *Polar Research* 3 n.s., 11–19.
- Solheim, A. & Kristoffersen, Y. 1984: The physical environment, western Barents Sea. 1:1500000, sheet B: Sediments above the upper regional unconformity: thickness, seismic stratigraphy and outline of the glacial history. *Norsk Polarinst. Skr.* 179 B, 26 pp.
- Solheim, A. & Pfirman, S. L. 1985: Sea-floor morphology outside a grounded, surging glacier; Bråsvellbreen, Svalbard. *Marine Geology* 65, 127–143.
- Solheim, A., Russwurm, L., Elverhøi, A. & Nyland Berg, M. 1990: Glacial geomorphic features in the northern Barents Sea: direct evidence for grounded ice and implications for the pattern of deglaciation and late glacial sedimentation. Pp. 253–268 in Dowdeswell, J. A. & Scourse, J. D. (eds.): *Glacimarine environments: Processes and sediments. Geological Society Special Publication no. 53*.
- Sollid, J. L. & Carlson, A. B. 1984: DeGeer moraines and eskers in Pasvik, North Norway. *Striae* 20, 55–61.
- Stuiver, M., Denton, G. H., Hughes, T. J. & Fastook, J. L. 1981: History of the marine ice sheet in West Antarctica during the last glaciation: A working hypothesis. Pp. 319–436 in Denton, G. H. & Hughes, T. J. (eds.): *The last great ice sheets*. John Wiley & Sons, 319–436.
- Taylor Smith, D. 1975: Geophysical assessment of sea-floor properties. *Oceanology International* 75, 320–328.
- Thompson, H. R. 1953: Oxford Expeditions to Nordaustlandet (North East Land), Spitsbergen. *Arctic* 6, 213–222.
- Thorarinsson, S. 1969: Glacier surges in Iceland, with special reference to the surges of Bruarjökull. *Can. J. Earth Sci.* 6, 875–882.
- Vagners, U. J., 1969: *Mineral distribution in tills, south-central Ontario*. Ph.D. dissertation, Univ. West Ontario, London, Canada. 270 pp.
- Vinje, T. 1985: The physical environment, western Barents Sea: Drift, composition, morphology and distribution of sea ice fields in the Barents Sea. *Norsk Polarinst. Skr.* 179C, 26 pp.
- Vorren, T., Hald, M., Edvardsen, M. & Lind-Hansen, O. W. 1983: Glacigenic sediments and sedimentary environments on continental shelves: general principles with a case study from the Norwegian shelf. Pp. 61–63 in Ehlers, J. (ed.): *Glacial deposits in north-west Europe*. A. A. Balkema, Rotterdam.
- Vorren, T. & Kristoffersen, Y. 1986: Late Quaternary glaciation in the south-western Barents sea. *Boreas* 15, 51–59.
- Wensaas, L. 1986: *En sedimentologisk og mineralogisk undersøkelse av bunnsedimenter (< 63 µm) fra det nordlige Barentshavet*. Unpubl. Cand. scient. thesis, University of Oslo. 178 pp.
- Weertman, J. 1969: Water lubrication mechanism of glacier surges. *Can. J. Earth Sci.* 6, 929–942.
- Weertman, J. 1973: Can a water-filled crevasse reach the bottom surface of a glacier? *Union Geodesique et Geophysique Internationale. Association Internationale d'Hydrologie Scientifique. Commission de neiges et Glaces. Symposium on the hydrology of glaciers*. Cambridge, 1969, 139–145.
- Weertman, J. 1976: Milankovitch and solar radiation variations and ice age ice sheet sizes. *Science* 261, 17–20.
- Worsley, D. & Aga, O. J. 1986: *The geological history of Svalbard: Evolution of an arctic archipelago*. Statoil, Stavanger, Norway. 121 pp.
- Østerholm, H. 1978: The movement of the Weichselian ice sheet over northern Nordaustlandet, Svalbard. *Geografiska Annaler* 60A, 189–208.

Appendix 1. Sediment samples in the study area. (Legend at the end).

1981

Position North East		Station Ident./Num. of Samples	Water Depth (m)	Sample Type	Bottom Photo	Core Length (m)
79.136	23.579	NP81-136/2	109	1		1.0
79.150	23.580	NP81-137/3	112	1		1.2
79.136	23.511	NP81-138/3	107	1		1.6
79.183	23.554	NP81-140/2	86	1		0.2
79.194	23.560	NP81-141	94	1		0.2
79.187	22.928	NP81-216/2	81	1		0.6

1982

Position North East		Station Ident./Num. of Samples	Water Depth	Sample Type	Bottom Photo	Core Length (m)
79.307	22.633	NP82-224	21	2	X	0.1
79.304	22.581	NP82-225	36	1		0.8
79.308	22.589	NP82-226	36	2		
79.153	22.962	NP82-229	55	1	X	0.5
79.211	23.124	NP82-230	81	1	X	0.5
79.223	23.089	NP82-231/4	83	1/2	X	0.4
79.194	23.785	NP82-232/2	82	1	X	0.3
79.178	23.787	NP82-233	101	1	X	0.3
79.162	23.732	NP82-234/2	79	1	X	1.7
79.150	23.620	NP82-235	106	1		1.1
79.040	23.548	NP82-237	105	1		1.1
79.164	23.914	NP82-239	87	1	X	0.4
79.220	22.892	NP82-241	57	2		0.5
78.924	25.769	NP82-317	142	1	X	1.3
78.899	24.525	NP82-319/2	215	1		1.67
79.008	23.076	NP82-321	99	1	X	1.8
79.254	22.754	NP82-323/2	39	2		1.1
79.242	22.797	NP82-324	43	2		0.6
79.245	22.804	NP82-326	45	2		1.7
79.253	22.737	NP82-327	44	2		0.5

1983

Position North East		Station Ident./Num. of Samples	Water Depth (m)	Sample Type	Bottom Photo	Core Length (m)
79.181	23.980	NP83-27	75	2	X	0.4
79.168	23.948	NP83-28	73	2	X	3.0
79.141	23.966	NP83-29	91	2	X	1.2
79.193	23.375	NP83-31	92	2		1.0
79.216	23.138	NP83-32	54	2		0.5
79.208	23.103	NP83-34	78	2		3.2
79.195	23.060	NP83-35	96	2		1.0
79.228	23.053	NP83-36	78	2		0.8
79.200	23.213	NP83-37/2	57	2		0.7
79.240	22.815	NP83-38	42	2		2.7

Appendix 1—continued

1984

Position		Station Ident./Num. of Samples	Water Depth (m)	Sample Type	Bottom Photo	Core Length (m)
North	East					
78.921	26.351	NP84-1	102	6	X	
78.916	26.144	NP84-2	110	6	X	
79.015	26.224	NP84-3	168	6	X	
78.997	25.969	NP84-4	172	6	X	
78.969	25.641	NP84-5	182	6	X	
79.067	25.491	NP84-6	219	6	X	
79.121	25.764	NP84-7	220	6	X	
79.102	26.347	NP84-8	232	6	X	
79.123	26.339	NP84-9	246	6	X	
79.112	26.342	NP84-10	260	6	X	
79.065	25.972	NP84-11	225	1	X	0.60
79.086	25.968	NP84-12	236	1	X	0.85
79.144	25.952	NP84-13	248	1	X	1.30
79.151	26.212	NP84-14	266	6	X	
79.232	26.203	NP84-15	212	6	X	
79.255	25.465	NP84-16	124	6	X	
79.309	25.607	NP84-17	112	6	X	
79.377	25.936	NP84-18	128	6	X	
79.293	25.935	NP84-19	90	6	X	
79.411	26.182	NP84-20	68	6	X	

Appendix 1—continued

1985

Position		Station Ident./Num. of Samples	Water Depth (m)	Sample Type	Bottom Photo	Core Length (m)
North	East					
78.819	21.870	NP85-1	50	6	X	
78.827	21.938	NP85-2	60	6		
78.833	22.070	NP85-3	71	6	X	
78.840	22.138	NP85-4	90	6		
78.848	22.266	NP85-5	110	6	X	
78.865	22.522	NP85-6	125	6		
78.885	22.905	NP85-7	141	6	X	
78.915	23.458	NP85-8	155	6	X	
78.922	23.630	NP85-9	170	6	X	
78.954	24.178	NP85-10	185	6	X	
78.962	24.329	NP85-11	200	6	X	
78.971	24.525	NP85-12	215	6	X	
79.183	23.468	NP85-13	91	6		
79.135	23.535	NP85-14	109	6	X	
79.050	23.602	NP85-15	105	6	X	
78.993	23.667	NP85-16	134	6	X	
78.856	23.848	NP85-17	178	6	X	
78.860	24.219	NP85-18	168	6	X	
78.865	24.834	NP85-19	164	6		
79.001	24.891	NP85-20	216	6		
79.056	24.430	NP85-21	158	6	X	
79.082	24.886	NP85-22	180	6		
79.212	24.667	NP85-23	134	6		
79.250	24.742	NP85-24	80	6	X	
79.308	24.874	NP85-25	52	6	X	
78.848	23.507	NP85-26	153	1		1.46
78.933	24.378	NP85-27	202	1		0.00
79.017	25.083	NP85-28	218	1		0.47
79.143	24.843	NP85-29	157	1		1.25

Legend:

Sample type: 1: Gravity corer
 2: Vibrocorer
 6: Grab

Bottom photo: X: yes

Appendix 2. Grain size distributions.

Station	Water Depth (m)	Level (cm)	Clay	Silt	%		>16 mm (g)
					Sand	Gravel	
81-136,1	109	0-5	21	40	10	27	136,7
		47-50	26	67	7	1	0,0
		90-93	52	48	1	0	0,0
81-137,1	112	59-62	37	45	13	5	0,0
		70-75	18	22	28	30	5,25
81-137,3	112	42-47	34	62	4	1	0,0
		50-55	10	14	31	45	38,0
81-138,1	107	20-23	22	36	22	19	0,0
		54-57	18	33	26	23	4,4
		82-85	19	34	22	22	0,0
81-138,3	107	95-97	18	35	26	21	0,0
81-140,1	86	16-19	21	34	22	23	12,0
81-186	320	45-50	57	43	1	0	0,0
		107-110	2	6	90	0	0,0
		120-125	24	31	42	3	0,0
		135-140	13	25	60	1	0,0
		150-153	24	26	48	3	0,0
81-216,1	81	0-3	10	24	36	30	18,1
		3-6	11	25	37	27	13,0
		30-33	9	35	35	22	42,5
		37-40	16	35	25	24	24,85
82-224	26	0-20	15	28	34	22	0,0
82-225,2	36	0-5	22	43	12	22	150,35
		68-72	25	53	16	6	0,0
82-226	36	0-20	17	21	33	29	0,0
82-229,1	56	0-5	13	20	22	45	7,2
		18-22	16	33	22	28	12,9
		40-50	14	36	23	28	29,45
82-230,2	71	0-5	18	34	28	20	0,0
		30-35	22	42	21	16	0,0
		50-55	30	53	11	5	0,0
82-231	83	8-13	22	32	24	22	32,0
		23-28	20	29	32	19	30,44
		30-35	28	43	15	15	0,0
82-232,2	82	0-5	14	25	32	28	0,0
		35-40	20	34	27	20	0,0
82-233,1	97	0-3	12	17	29	42	0,0
82-234,1	83	0-3	23	28	16	34	35,43
		125-130	22	32	26	20	15,57
		160-168	20	29	27	24	0,0
82-234,2	83	0-5	22	36	16	24	3,29
		100-103	21	31	25	24	9,95
82-235,1	106	0-5	15	17	9	59	68,0
		57-61	40	53	6	1	0,0
		87-90	34	59	6	0	0,0
		103-107	27	32	15	26	38,09
82-237	106	0-3	26	37	10	27	0,0
		43-47	32	63	4	1	0,0
		95-100	17	30	19	36	28,5

Appendix 2--continued

Station	Water Depth (m)	Level (cm)	Clay	Silt	%		>16 mm (g)
					Sand	Gravel	
82-239,1	81	0-5	27	32	21	20	0,0
		30-35	22	36	22	19	5,0
82-239,2	81	25-30	14	20	35	32	15,32
82-241,1	56	0-5	29	29	21	19	25,0
		18-23	28	35	21	16	0,0
82-321	99	0-5	31	41	14	14	0,0
		20-23	45	27	13	13	0,0
		55-58	28	44	11	18	0,0
		105-108	42	28	16	12	0,0
		150-153	22	50	19	8	40,18
82-323,1	39	173-176	25	44	19	12	35,73
		0-4	14	18	28	40	8,32
		22-26	15	22	28	35	21,04
		63-68	20	26	31	22	18,22
		86-94	20	25	24	31	0,0
82-323,2	39	95-100	20	23	29	28	17,3
		0-5	29	40	29	2	0,0
		58-62	20	25	32	23	0,0
		90-95	21	24	29	26	0,0
		98-103	20	30	27	24	0,0
82-324,1	43	0-4	23	32	21	24	0,0
		50-53	22	25	27	26	6,73
		58-63	21	24	27	28	19,1
82-326,1	45	0-3	16	21	29	34	0,0
		15-18	11	12	28	48	12,28
		30-33	22	26	38	14	5,65
		55-58	6	10	38	47	9,8
		83-86	23	24	41	13	0,0
		105-109	20	24	42	14	6,3
		124-128	12	18	42	28	0,0
82-327,1	44	167-172	14	15	44	28	0,0
		0-5	22	27	28	22	2,9
		31-36	18	21	28	33	47,3
		39-42	17	26	26	31	0,0
		45-48	14	19	28	39	8,5
83-26	70	0-3	3	24	72	1	0,0
		15-17	1	3	90	5	0,0
		30-33	1	3	46	48	0,0
		60-65	19	24	25	33	35,68
83-27	75	0-5	2	11	66	22	0,0
83-28	73	0-5	34	41	19	7	29,29
		100-105	23	27	23	26	0,0
		250-255	24	31	26	19	5,67
83-29	91	0-6	28	29	11	33	0,0
		40-45	32	56	12	1	0,0
		60-65	22	28	22	28	0,0
		100-105	23	29	19	28	42,45
83-30	76	10-15	2	5	86	8	0,0
83-31	92	0-5	2	3	88	7	0,0
		30-35	24	33	24	19	11,49
		50-80	20	72	5	3	0,0

Appendix 2—continued

Station	Water Depth (m)	Level (cm)	Clay	Silt	%		Gravel	>16 mm (g)
					Sand	Gravel		
83-32	54	65–70	27	41	23	9	0,0	
83-34	78	0–5	34	42	21	3	0,0	
		50–55	19	32	26	22	10,54	
		250–255	17	30	29	24	0,0	
83-35	96	0–5	43	47	6	4	0,0	
		22–27	48	44	7	2	0,0	
		85–90	34	46	7	13	9,26	
83-38	42	0–5	17	30	22	32	82,92	
		100–105	16	25	23	35	0,0	
		217–222	26	40	22	11	5,24	
		240–245	19	22	23	37	0,0	
83-39	43	0–5	4	9	86	2	0,0	
		60–65	—1—		16	84	14,67	
84-11	225	0–5	57	31	8	4	0,0	
		20–25	51	34	14	1	0,0	
		33–36	36	39	19	6	0,0	
84-13	248	0–4	59	40	1	0	0,0	
		10–13	63	34	2	1	0,0	
		30–33	32	42	18	8	0,0	
		45–48	60	35	4	1	0,0	
		51–54	42	31	18	8	0,0	
		61–64	30	41	22	7	0,0	
85-26	153	0–4	49	47	3	1	0,0	
		10–13	55	41	3	1	0,0	
		20–25	54	36	6	4	0,0	
		33–36	66	24	3	6	0,0	
		46–50	54	30	12	5	0,0	
		60–63	27	40	24	9	0,0	
		80–85	23	29	32	16	0,0	
		120–123	29	35	29	7	0,0	
85-28	218	0–4	61	35	4	0	0,0	
		15–18	51	42	5	2	0,0	
		40–44	36	34	20	10	0,0	
85-29	157	0–3	51	32	11	6	0,0	
		18–22	54	41	4	●	0,0	
		33–37	52	46	1	0	0,0	
		60–64	53	40	6	1	0,0	
		80–85	21	34	23	22	0,0	
		100–105	26	31	16	28	0,0	

Appendix 3. Physical properties
A. The surge zone

STA	LE	Dw	Su	BD	Vp	TC	TOC	GR	SA	SI	CL	MED	W1	W2	W _i	W _p	PI	IMP
81-140.1	17	86						23	22	34	21	4.6	40	41				
81-141.1	10	94	33.0					30	36	24	10	1.3						
81-216	2	81						27	37	25	11	1.9	16					
81-216	5	81																
81-216	20	81						22	35	35	9	2.7	18					
81-216	32	81						24	25	35	16	4.1	12	14				
81-216	38	81	160.0					19	28	34	18	4.3	27	29				
81-216	50	81						16	21	42	22	5.4	23					
82-230.2	3	69	12.0			6.2	0.69	6	11	54	30	6.8	27	29				
82-230.2	32	69	60.0		1660			19	28	34	18	4.3	13	19	28.8	18.7	10.1	
82-230.2	53	69			1840	6.3	0.65	6	11	54	30	6.8	27	29				
82-231.3	3	82	20.0		1940			19	32	29	20	3.8	13	19				
82-231.3	17	82	80.0		2130	6.6	0.61	14	14	43	28	6.6	13	19				
82-231.3	37	82	100.0		2600	6.5	0.57	14	14	43	28	6.6	13	19				
82-232.1	10	84	77.0	1.99				28	33	25	14		22					
82-232.2	5	84	42.0			6.3	0.39	20	27	34	20	4.4	15	19	26.9	17.8	9.1	
82-232.2	40	84	52.0		1900	5.6	0.67	20	27	34	20	4.4	20					
82-232.2	50	84				5.9	0.52	42	29	17	12	0.4	18	24				
82-233.1	3	97						20	21	32	27	6.4	20	26				
82-233.1	27	97						19	22	36	22	1.5	21					
82-239.1	2	83	12.0			5.6	0.56	20	21	32	27	6.4	28					
82-239.1	20	83	35.0			6.1	0.43	19	22	36	22	1.5	20	26	28.0	17.6	10.4	
82-239.1	35	83				6.0	0.62	40	28	18	14	0.8	28					
82-323.1	3	35				3.1	0.55	35	28	22	15	1.8	20					
82-323.1	24	35			2100	6.8	0.27	22	31	26	20	3.3	16					
82-323.1	60	35			2190	5.3	0.99	28	29	23	20	3.0	16	26				
82-323.1	95	35			1780			2	29	40	29	6.5	19					
82-323.2	3	35	10.0					23	32	25	20	3.0	19	28				
82-323.2	15	35	20.0		1690			26	29	24	21	3.3	16					
82-323.2	60	35			1890			24	27	30	20	4.0	17	25				
82-323.2	90	35	63.0		2020			26	27	25	22	3.4	14	21				
82-323.1	105	35						34	29	21	16	2.2	14	21				
82-324.1	10	39	145.0		1780	6.2	0.55	48	28	12	11	-0.9	14	23				
82-324.1	55	39			2000	6.2	0.60	14	38	26	22	3.7	12	23				
82-326.1	2	42						47	38	10	6	-0.6	15	21				
82-326.1	17	42						13	41	24	23	3.5	15	21				
82-326.1	30	42			2100			14	38	26	22	3.7	14	23				
82-326.1	60	42			2100			47	38	10	6	-0.6	15	21				
82-326.1	80	42						13	41	24	23	3.5	15	21				
82-326.1	105	42			2050			14	42	24	20	3.1	15	21				

Appendix 3—continued
A. The surge zone—continued

STA	LE	Dw	Su	BD	Vp	TC	TOC	GR	SA	SI	CL	MED	W1	W2	W1	Wp	PI	IMP
82-326.1	128	42						28	42	18	12	1.5						
82-326.1	170	40			2150			28	44	15	14	1.3						
82-327.1	3	40				6.3	0.62	22	28	27	22	3.9	20	26				
82-327.1	30	40				6.2	0.74	33	28	21	18	1.6						
82-327.1	45	40				6.0	0.75	31	26	26	17	2.6						
82-327.1	52	40				5.2	0.96	39	28	19	14	0.3	14	24				
83-27.1	15	75		2.47	2400								12	16	27.7	16.1	11.6	5.93
83-27.1	30	75		2.12	2200			19	24	33	24	5.3	17	24				
83-31	33	97																
83-31	45	97	5.0															
83-31	55	97	100.0		1573													
83-31	75	97	93.0	1.94	1570	4.0	1.74	3	5	72	20	6.9	30	30	54.1	22.2	31.9	3.05
83-31	81	97	80.0	1.76	1570								32	32	45.8	21.3	24.5	2.76
83-32	15	54	40.0															
83-32	26	54	60.0															
83-32	57	54	40.0															
83-32	67	54	70.0	1.75		4.8	1.53	9	23	41	27	6.4	34		65.2	25.4	39.8	
83-32	50	54	50.0															
83-32	65	54	78.0															
83-36	10	78	5.6	2.46														
83-36	35	78	83.0	2.19	1890								19	27	38.9	20.0	18.9	4.14
83-36	48	78	90.0	2.03	1890								15	21				
83-36	75	78	56.0										14	21	40.4	19.5	20.9	3.84
83-37.1	5	57	5.0															
83-37.1	25	57	23.0	2.09									17	28				
83-37.1	38	57	45.0															
83-37.1	65	57	100.0	2.38														
83-37.2	43	57		2.26														
83-38	33	42		2.31														
83-38	90	42	50.0	2.21	1592								8	17	40.5	18.9	21.6	
83-38	120	42		2.16									12	25	64.3	19.6	44.7	
83-38	120	42		2.16									14	28	47.0	21.3	25.7	3.52
83-38	218	42	125.0	1.82	1690			35	23	25	16	5.8	15	29	44.9	22.1	22.8	
83-38								11	22	40	26		19	21				3.08

STA	LE	Dw	Su	BD	Vp	TC	TOC	GR	SA	SI	CL	MED	W1	W2	W ₁	W _p	PI	IMP
82-319.2	100	215	1.4															
82-319.2	133	215	2.0										30	35				
82-319.2	158	215	3.1										30	35				
82-321.1	16	100	0.9				13	13	27	45		7.9	34	39				
82-321.1	30	100	1.6				18	11	44	28		6.6						
82-321.1	45	100	5.1															
82-321.1	85	100	3.8				12	16	28	42		8.3	25	30				
82-321.1	115	100	5.5				8	19	50	22		6.2	24	30				
82-321.1	140	100	4.7				12	19	44	25		6.3	50	52				
82-321.1	170	100	4.7										24	30				
82-321.2	15	100	6.3										50	52				
82-321.2	35	100	6.9	1481									24	30				
83-29	10	91	6.9															
83-29	25	91	7.2	1.96	1470								49	51	57.7	22.8	34.9	2.88
83-29	40	91	7.8				1	12	56	32		7.1						
83-29	60	91	4.4	2.14	2000		28	22	28	22		3.8	16	26	32.0	15.1	16.9	4.28
83-29	110	91			1504		28	19	29	23		4.5	12	17	27.2	15.3	11.9	
83-29	90	91			1750													
83-29	110	91			2160													
83-35	10	96	10.0	1.74														
83-35	20	96	12.5															
83-35	30	96	8.0				2	7	44	48		8.7	53	55	63.3	23.9	39.4	2.62
83-35	73	96	9.0		1504								73		77.0	28.2	48.8	2.41

Legend.

- STA Station nr.
- LE Level in core (cm)
- Dw Water depth (m)
- Su Undrained shear strength (kPa)
- BD Bulk density (g/cm³)
- TC Total carbon (%)
- TOC Total organic carbon (%)
- GR Gravel (%)
- SA Sand (%)
- SI Silt (%)
- CL Clay (%)
- MED Median diameter (phi)
- W1 Water content, uncorrected
- W2 Water content, corrected for fractions > 0.5 mm
- W₁ Liquid limit (%)
- W_p Plastic limit (%)
- PI Plasticity index (%)
- IMP Acoustic impedance (10⁶ kg/m²s)

Appendix 4. Mineralogy from XRD

CA: Calcite

DO: Dolomite

NC: 14, 10 & 7 Å minerals + quartz and feldspar (non-carbonates)

Station	Level	Fraction: <63 µm			Fraction: <2 µm			Fraction: <4 µm			Comments
		CA	DO	NC	CA	DO	NC	CA	DO	NC	
81-216	0-3	64	17	19							
	50-55	74	6	20							
82-230	0-5	51	27	22							
	30-35	68	17	15							
82-231	50-55	52	23	25	38	10	52				
	0-5				32	8	60				
82-232	35-40	62	21	17							
	0-5	59	18	23							
82-233	46-51	51	19	30	50	7	43				
	0-3	70	16	14							
82-239	0-5	51	25	24							
	30-35	60	21	19	45	8	47				
82-323	0-5	73	11	16							
	58-62	86	4	10							
	90-95	49	22	29							
	100-105	38	19	43							
82-327	0-5	71	8	21							
	46-51	57	12	31							
83-31	50-80							2	6	92	
83-32	65-70							8	5	87	
84-17	0-5							3	5	92	
84-18	0-5							5	5	90	
82-224	0-20	66	12	22	58	2	40				
82-234	0-3	55	20	25							
80-37	0-2							0	5	95	
	15-17							0	6	94	
	55-56							0	4	96	
	87-88							0	3	97	
81-136	47-50	0	18	82							
82-225	0-5	66	14	20							
	68-72	42	22	36							
82-226	0-20	76	10	14							
82-229	0-5	38	23	39	29	8	63				
	18-22	20	23	57	7	6	87				
	40-49	9	53	38							
		5	39	56							
		4	28	68							
82-237		0	21	79							
		8	15	77							
		0	0	100							
	0-3	35	19	46							
	43-47	5	22	73	0	5	95				
	95-100	9	19	72	9	0	91				

Appendix 4—continued

Station	Level	Fraction: <63 μm			Fraction: <2 μm			Fraction: <4 μm			Comments	
		CA	DO	NC	CA	DO	NC	CA	DO	NC		
83-321	0-2							17	8	75		
	6-7							9	7	84		
	8-9							7	7	86		
	10-11							5	6	89		
	12-13							4	3	93		
	14-15							3	3	94		
	16-17							2	2	96		
	20-21							2	2	96		
	23-24							2	2	96		
	26-27							2	2	96		
	29-30							3	2	95		
	32-33							4	3	93		
	36-37							6	4	90		
	39-40							4	3	93		
83-29	0-6							34	8	58		
	40-45							4	7	89		
	60-65							34	5	61		
84-11	100-105							73	4	23		
	0-5							0	3	97		
84-13	20-25							0	0	100		
	33-36							2	0	98		
	0-4							0	0	100		
	10-13							0	0	100		
	30-33							3	0	97		
	45-48							6	2	92		
84-16	51-54							0	0	100		
	61-64							3	0	97		
	0-5							4	5	91		
	7-8							0	3	97		
85-26	10-13							0	3	97		
	17-18							2	2	96		
	20-21							0	0	100		
	23-24							3	3	94		
	27-28							1	2	97		
	33-36							3	3	94		
	40-41							2	2	96		
	46-50							3	0	97		
	60-63							6	0	94		
	80-85							12	0	88		
	120-123							12	0	88		
	85-28	0-4							0	5	95	
		15-18							0	0	100	
		40-44							3	0	97	
85-29	0-3							5	6	89		
	18-22							0	5	95		
	33-37							0	3	97		
	60-64							0	2	98		
	100-105							9	2	89		

